UNIVERSITÀ DEGLI STUDI DI MILANO

Facoltà di Medicina e Chirurgia

Scuola di Dottorato in Scienze Biomediche Cliniche e Sperimentali
Medicina sperimentale e biotecnologie mediche

Dipartimento di Biotecnologie Mediche e Medicina Traslazionale
(BIOMETRA)

Dottorato di Ricerca in
PATOLOGIA E NEUROPATOLOGIA SPERIMENTALI
(XXVII CICLO)

TESI DI DOTTORATO DI RICERCA
(MED 03/04/05)

"A step-by-step process to generate functional osteoclasts from site specific gene-corrected induced pluripotent stem cells: an autologous cell therapy approach to treat autosomal recessive osteopetrosis"

Sharon Muggeo

Matr. R09816

Coordinatore del dottorato: **Prof. Massimo Locati**

Relatore: **Dr.ssa Anna Villa**

Correlatore: **Dr.ssa Francesca Ficara**

Anno accademico 2013/2014

Index

1 Introduction

1.1 Embryonic stem cells

Embryogenesis is the first process at the early stage of an individual formation and development. The female ovum is fertilized by a spermatozoon, with the consequent formation of a zygote, a single diploid cell. It undergoes several mitotic divisions and cellular differentiation, arriving at the stage of morula, composed by sixteen cells. Then a fluid-filled cavity forms inside the morula, which becomes a blastocyst. Cells initiate to specialize and divide their competencies: the external layer is called trophoblast and do not contribute to the proper embryo, forming the fetal part of the placenta, umbilical cord and associated structures. Cells remaining inside the cavity form the inner cell mass which gives rise to the whole embryo tissues. Cells isolated and put in culture from the inner cell mass are pluripotent cells called embryonic stem (ES) cells. Mouse ES cells were derived for the first time in 1981 by Evans and Kaufman (Evans and Kaufman, 1981), whereas human ES cell lines were established in 1998 by Thomson (Thomson et al, 1998). They have self-renewal ability and capacity to differentiate in a variety of cellular populations belonging to the primary germ layers: ectoderm, endoderm and mesoderm. They have a high proliferation rate and can be kept in culture with unlimited capacity of expansion (Fig.1).

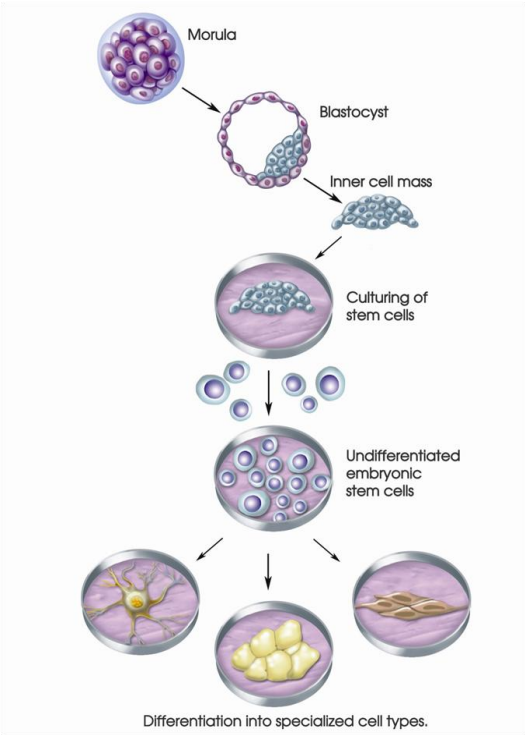

Fig.1. Embryonic stem cells. ES cells derived from the inner cell mass of a blastocyst. When they are put in culture, they are able to differentiate into specialized cell types belonging to all three germ layers (from Understanding Stem Cells: An Overview of the Science and Issues from the National Academies).

ES cells can be used to study stemness, pluripotency and differentiation processes and to generate different cellular lineages (Cowan et al, 2004). Affected ES lines or genetically modified ES lines can be established in culture and injected into blastocysts to generate chimeric mice, fundamental for pathogenesis study (Bradley et al, 1984). Moreover, ES cells have been proposed as a therapeutic tool in regenerative medicine. Since cells have several critical issues such as genetically instability in culture, easiness to generate teratomas (tumors composed of tissue from the three germ layers) and risk of immune rejection upon transplantation in allogenic recipients (Swijnenburg et al, 2008), the first report of human ES cells usage in the clinic is very recent (Schwartz et al, 2012). In this trial the authors treated macular degeneration observing no detrimental effects or rejection. This is a still debated point, since ES cells should be an immune-privileged population, usually not subjected to rejection due to a down-regulation of the host immune response (Fändrich et al, 2002).
Finally, the use of human ES cells raises strong ethical questions since their collection leads to the destruction of the embryo preventing its further development, whereas once implanted in uterus it could produce a human being (Sugarman, 2008).

1.2 Induced pluripotent stem cells

To overcome some of the raised issues, alternative lines of study have been developed to obtain pluripotent cells starting from adult differentiated cells.
The somatic cell nuclear transfer (SCNT), for instance, uses the cytoplasm of an enucleated oocyte to de-differentiate the nucleus of a somatic cell. The result is the development of a blastocyst by which is possible the ES cells collection (Gurdon, 1962). Dolly the Sheep was the first successfully cloned mammal using this process (Wilmut et al, 1997). However, this technique is difficult to perform, has low efficiency and low probability to successfully obtain normal ES cells. Moreover, maternal mitochondria present in oocyte cytoplasm remain (Inoue et al, 2004) and, in a human setting, ethical questions are not resolved at all, since lots of oocytes from donor females are necessary to perform the technique (Fig.2).

Recently, an alternative approach has been developed with the generation of induced pluripotent stem cells (iPSc). They are pluripotent stem cells derived from the reprogramming of somatic cells, described for the first time by Takahashi and Yamanaka (Takahashi and Yamanaka, 2006). They over-expressed in murine fibroblasts defined transcription factors specific for inducing and maintaining stemness characteristics. They found four genes sufficient for the reprogramming procedure: POU class 5 homeobox 1 (POU5F1) gene (Oct4), Sex determining region Y (SRY)-box

2 gene (Sox2), Kruppel-like factor 4 gene (Klf4) and v-myc myelocytomatosis viral oncogene homolog gene (c-Myc).

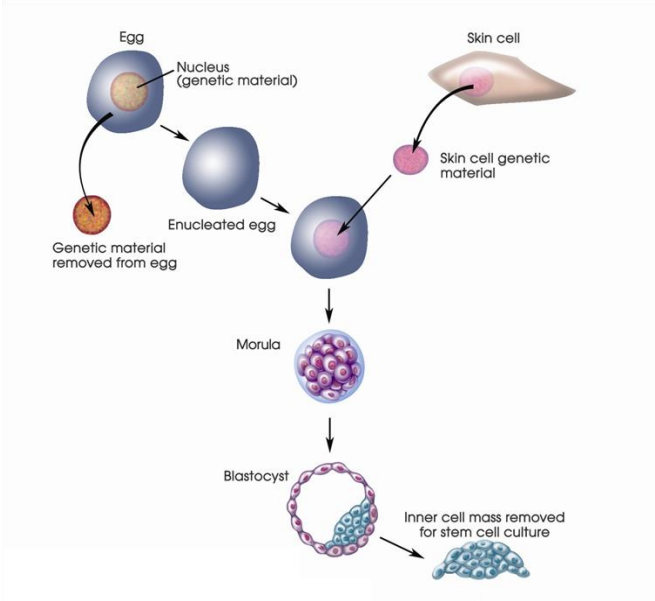

Fig.2. Somatic cell nuclear transfer. ES cells can derive from a blastocyst generated *in vitro*. The nucleus from an adult cell (for example a skin cell) is inserted into an egg without the nucleus (from Understanding Stem Cells: An Overview of the Science and Issues from the National Academies).

iPSc are similar to ES cells for morphology, stemness markers expression, self-renewal and *in vitro* and *in vivo* differentiation ability. Later on, human iPSc were also generated (Takahashi et al, 2007). During time, the combination of employed transcriptional factors changed in various ways, diminishing or replacing involved genes. For instance, Sox2 can be substituted by Sox1; Klf4 by Klf2 and Klf5; c-Myc by N-Myc and L-Myc (Nakagawa et al, 2008, Nagamatsu et al, 2013). Furthermore, since over-expression of c-Myc could lead to tumorigenesis because of its role in cell cycle progression, apoptosis and cellular transformation, some groups tried to eliminate it from the reprogramming cocktail demonstrating that it can be dispensable (Okita et al, 2007, Wernig et al, 2008). Other reprogramming factors were also tested, such as Lin-28 homolog A gene (Lin28) (Yu et al, 2007), Nanog homeobox gene (Nanog) (Park et al, 2008), Glis1 family zinc finger 1 (Glis) (Maekawa et al, 2011), BMI1 polycomb ring finger oncogene (Bmi1) (Moon et al, 2011), oestrogen-related receptor beta (Esrrb) (Zhang et al, 2008) and Wnt ligands (Wnt3, Wnt6, Wnt8a and Wnt10a) (Kim et al, 2010). Reprogramming with only two factors is also possible using Oct4 and Klf4 (Shi et al, 2008) or Oct4 and Sox2 (Huangfu et al, 2008). Oct4 is found to be the indispensable factor for the reprogramming procedure (Kim et al, 2009).

The first induction protocol used to generate iPSc employed a retroviral vector to deliver the

selected genes. It was an integrating vector in which the majority of viral genes were replaced by the desired ones and the backbone was engineered to avoid the replication of the native virus and its spread to other cells without any control (Dull et al, 1998). Retroviral vectors show a preference for integrating in promoter and enhancer regions of transcriptionally active genes, so their integration can influence the expression of adjacent genes (Nienhuis et al, 2006). This situation is determined by the structure of the virus, in which its long-terminal repeats (LTRs) contain enhancers and promoters and a strong splice donor site.

Therefore, other systems were developed, such as the engineering of a subclass of retroviral virus: lentivirus. They present several advantages over the retroviral system showing a safer integration profile (Montini et al, 2006). In particular, the self-inactivating (SIN) setting further improves the biosafety of these vectors, lowering the risk of adjacent genes activation by deleting transcriptional control elements of the LTRs and by the use of an independent weak-to-moderate internal promoter to guide transgenes expression (Zufferey et al, 1998). Then, the insertional mutagenesis safe issue was approached by developing vectors that can be excised from the host genome after the reprogramming activity, for example by placing loxP or Flp recognition target (FRT) sequences in the LTRs to guide the recombination activity mediated by Cre or Flp recombinase, respectively (Russ et al, 1996, Ludwig et al, 1996).

To avoid completely integration-derived risks, other delivery methods were developed. Plasmids (Okita et al, 2008), adenoviral vectors (Stadtfeld et al, 2008) or non-integrating viral vectors, for example Sendai virus (Ban et al, 2011), carrying the reprogramming genes are unable to integrate in the host DNA and remain episomic with only a transient expression of the transgenes. Alternative strategies are represented by transposones, such as PiggyBac, that allow the translocation of reprogramming genes into the genome (Woltjen et al, 2009).

Then, small molecules can replace one or two reprogramming factors, such as valproic acid (Shi et al, 2008), p53 and retinoblastoma inhibitors (Zhao et al, 2008) or ascorbic acid and a GSK3-β inhibitor (Bar-Nur et al, 2014). Finally, recombinant proteins (Zhou et al, 2009), synthetic mRNAs (Warren et al, 2010) and microRNAs (Anokye-Danso et al, 2011) were employed, developing systems that facilitate their translocation into the target cells.

1.3 Application of iPSc

iPSc represent a promising tool for different applications (Fig.3). The most applied and successful use is represented by the *in vitro* disease modelling, since iPSc can be derived from accessible cells of patients and differentiated into the affected cellular type, giving the chance to observe their characteristics and molecular mechanisms. This procedure allows to avoid invasive procedures to

obtain the desired cell types and at the same time to study their development and differentiation stages. iPSc were generated from patients affected by amyotrophic lateral sclerosis (Dimos et al, 2008), spinal muscular atrophy (Ebert et al, 2009), Parkinson's disease (Soldner et al, 2009), cardiovascular diseases (Narsinh et al, 2011), Down syndrome (Park et al, 2008), polycystic kidney disease (Freedman et al, 2013), and many more. As a result, the more they recapitulate the diseased phenotype, the more efficiently they can be employed as a toxicity and drug screening platform (Guo et al, 2011, Matsa et al, 2011, Egawa et al, 2012). The international StemBANCC project was formed in 2012 to create and store iPS lines for drug screening (www.stembancc.org).

Murine iPSc injected into blastocysts can also generate germline-competent chimera mice to perform *in vivo* study of diseases (Okita et al, 2007).

Furthermore, iPSc represent a hope for the personalized medicine, in the regenerative medicine field. iPSc can be obtained from specific individuals and used after gene correction for cell replacement in an autologous setting. As proof of principle of the feasibility of the technique, various attempts were made in mice, such as treatment of sickle cell anemia (Hanna et al, 2007), Parkinson's disease (Wernig et al, 2008), platelet deficiency (Takayama et al, 2010), diabetes (Alipio et al, 2010), and spinal cord injury (Tsuji et al, 2010). The first clinical trial using autologous iPSc started in Japan in 2013 for the treatment of age-related wet-macular degeneration (Cyranoski, 2013).

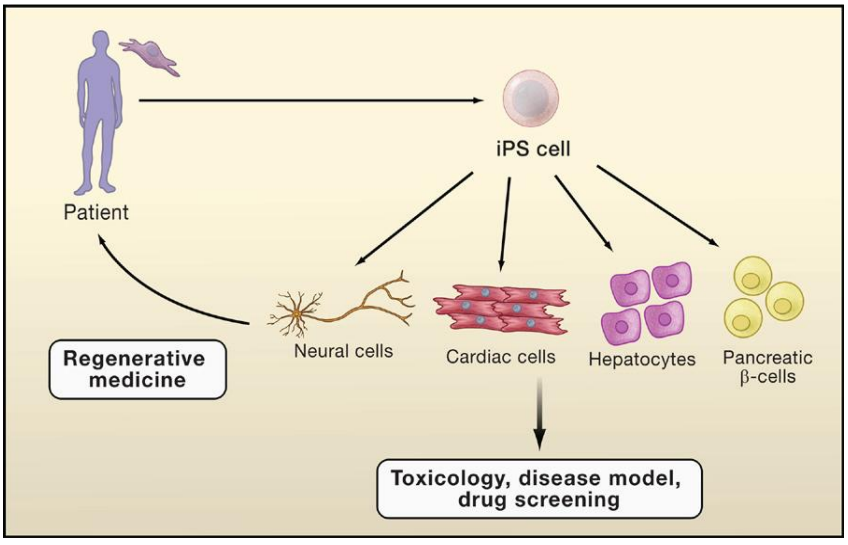

Fig.3. Application of induced pluripotent stem cells. iPSc could be employed to create disease models, to screen effective and safe drugs and as a tool of regenerative medicine, to treat patients through cell transplantation therapy (from Yamanaka, 2009).

1.4 Gene therapy

Gene therapy consists in restoring the functionality of a defective gene. *Ex vivo* approaches have the advantage to select the target cells and if necessary expand or differentiate them and transplant them back, avoiding the exposure of the patient to the gene transfer vector. Hematopoietic stem cells (HSCs) are easily accessible and HSC transplant is a conventional technique, but it requires a human leukocyte antigen (HLA)-compatible donor. This need limits the number of patients that can benefit from transplantation and forces the use of mismatched donors, with the consequence of increasing the intensity of conditioning regiments and post-transplant immunosuppression in order to avoid graft rejection and graft versus host disease (GvHD).

Autologous HSCs gene therapy represents an emerging therapeutic opportunity for several monogenic diseases of the blood, to circumvent problems linked to the requirement of compatible donors and to the side effects of conditioning, reducing the morbidity and mortality of the transplant procedure. Hurdles are related to the requirement of *ex vivo* culture of HSCs, which are particularly vulnerable to prolonged *in vitro* manipulation and to the gene transfer efficiency, which can decrease the long-term reconstitution potential of the infused cells.

Various efforts have been made to identify the best vector to transfer a wild type (wt) gene in the appropriate cell type. Vector-related insertional mutagenic events and unregulated transgene expression can lead to oncogenesis, toxicity or elimination of the gene-modified cells. The design of low risk integrating systems that can achieve stable expression of corrective genes is fundamental. Homologous recombination is the best way to avoid insertional mutagenesis maintaining a stable and appropriate gene expression. The defective copy of the target gene is replaced by the correct one in the physiological position into the genome, due to a recombination procedure mediated by homologous flanking regions included up- and down-stream of the gene into the targeting system (Capecchi, 1989). The larger homology sequences are included in the vector, the best efficiency of homologous recombination is reached, even if it remains quite low.

To reach the goal of site-specific gene correction, also other methods have been developed based on artificial nucleases, such as zinc finger nucleases (ZFN) (Sebastiano et al, 2011), transcription activator-like effector nucleases (TALEN) (Sakuma et al, 2013), and RNA-guided nucleases (CRISPR/Cas) (Horii et al, 2013). They provoke DNA double-strand breaks to a pre-selected genomic site and, providing a DNA template, the endogenous repair process seals the break including the exogenous sequence. The risks are the disruption or the editing of the original sequence with a non-homologous end joining and off-target breaks that can lead to structural genome rearrangements, in addition to the very low efficiency. For these reasons their use is still under investigation. Moreover, they can correct only small mutations into the genome, because of

their intrinsic characteristics, while in a lot of genetic diseases the problems reside in large deletion of the DNA sequence. Hence, bacterial artificial chromosomes (BAC) that have been used since 1992 to carry large portions of DNA (Shizuya et al, 1992), presently represent the best tool to obtain homologous recombination in pluripotent cells (Howden et al, 2011).

iPSc could be an alternative source of cells for production and gene correction of hematopoietic cells. iPSc have an easily accessible cell source, obtainable without invasive procedures and can be expanded indefinitely providing an unlimited supply of immunologically matched cells. They allow overcoming problems of primary cells gene targeting, in fact the feasibility to perform gene targeting is greater for their tolerance to homologous recombination. They are continuously proliferating and easily transfected and can be selected and expanded to obtain a homogeneous population in which 100% of the cells are genome edited. The proof of principle of the feasibility of the clinical application was provided by the successful treatment of sickle cell anemia in a mouse model by transplantation of gene-corrected iPSc (Hanna et al, 2007).
One of the main issues is the need of a correct cellular differentiation into the desired cell type that must be efficient, reproducible and safe.

1.5 Development of the murine hematopoietic system

1.5.1 The hematopoietic system

Hematopoiesis is the process by which all the different blood cellular populations are generated and continuously maintained. It is a hierarchical system at the top of which are rare stem cells (less than one out of 10^5 bone marrow cells) preserving self-renewal ability and multipotent differentiation capacity (Orkin and Zon, 2008, Weissman and Shizuru, 2008). Through various cell divisions they give rise to multipotent progenitors, which have lost self-renewal ability, and then to oligopotent lineage committed progenitors increasingly restricted in a stepwise manner, which produce all terminally differentiated cells (Fig.4) (Spangrude et al, 1998).This classification was subsequently refined with newly identified intermediate populations and modifications in the branching scheme.
The definition of HSCs is functional: they are endowed with the ability to reconstitute the entire blood system of a lethally irradiated recipient (long-term repopulating assay), thus showing *in vivo* their self-renewal and multipotency capacity (Coulombel, 2004). *In vitro* assays demonstrate the differentiation ability of the progenitors, but do not measure HSCs activity. To isolate these cells different strategies were developed, mostly based on cell surface marker cytofluorimetric analysis, even if different laboratories often use slightly different combination of markers for their definition

(Purton and Scadden, 2007). Hematopoiesis has been characterized in the mouse, which is considered as a model for human development (Tavian and Peault, 2005).

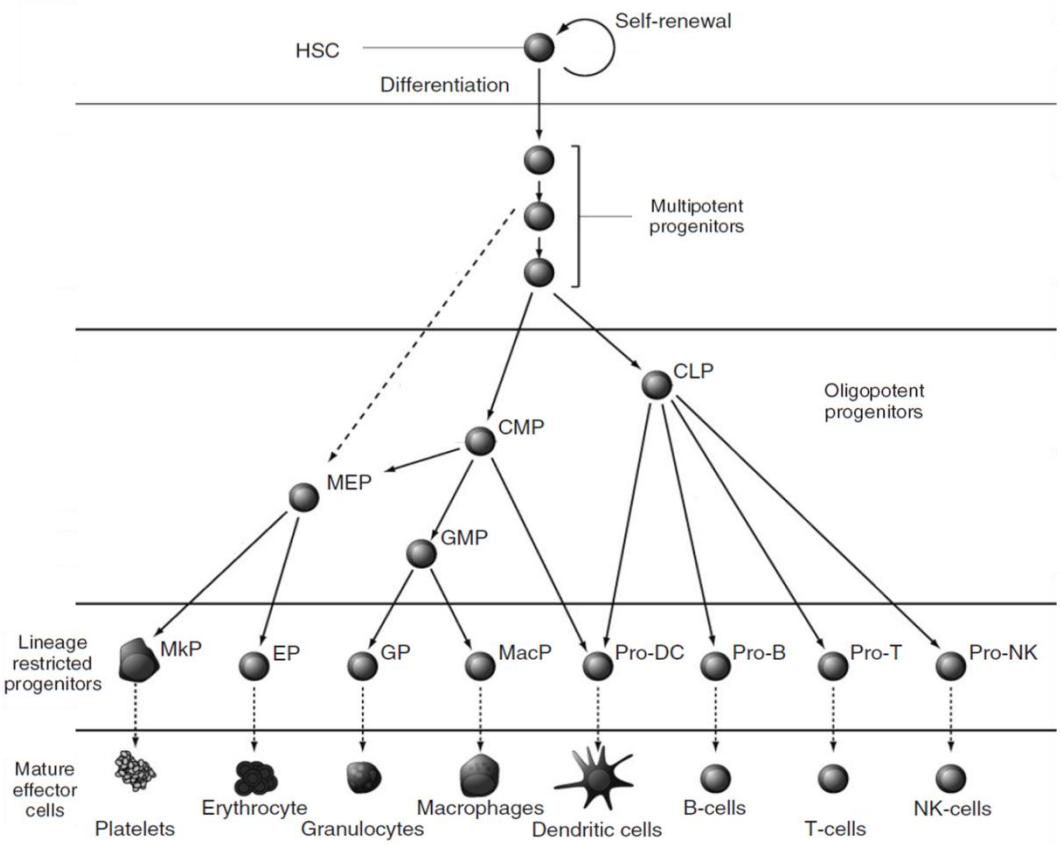

Fig.4. The hierarchical model of hematopoiesis. HSC has a long-term capacity to self-renew and to differentiate into all the hematopoietic lineages. HSCs originate multipotent progenitors which in turn branch in two lineages: lymphoid and myeloid. Common myeloid progenitors (CMP) produce megakaryocyte-erythrocyte progenitors (MEP), which generate platelets and erythrocytes, and granulocyte-monocyte progenitors (GMP), which provide granulocytes and macrophages. CMP also produce myeloid-derived dendritic cells. Multipotent progenitors can also give rise to MEP in a direct way. B, T, NK cells and plasmacytoid dendritic cells are obtained from common lymphoid progenitors (CLP). DC, dendritic cell; EP, erythrocyte progenitor; GP, granulocyte progenitor; MacP, macrophage progenitor; MkP, megakaryocyte progenitor; NK, natural killer (adapted from Seita and Weissman, 2010).

HSCs, as other stem cells, are negative for markers typical of the various differentiated lineage (Lin^-) and express the markers Kit oncogene (c-Kit) and Stem cell antigen 1 (Sca1), defining the expression LKS. Going deeper in the classification, they lack the expression of CD34 (Osawa et al, 1996) and CD135 (Flk2) (Adolfsson et al, 2001), while multipotent progenitors acquire expression of CD34 and multipotent progenitors further downstream in the hematopoietic tree express both markers (Yang et al, 2005). Of note, CD34 assumes differential expression according also to the age of mice, as it is expressed by HSCs in mice younger than 8 weeks (Matsuoka et al, 2001). To further identify HSCs there is also a combination of markers called signalling lymphocyte activation molecule (SLAM): $CD150^+$, signaling lymphocytic activation molecule family member 1 (Slamf1), natural killer cell receptor 2B4 ($CD244^-$) and $CD48^-$, (Kiel et al, 2005). Subsequently it

has been reported that $CD150^+$ $CD48^-$ signature is sufficient. At last, due to their common developmental origin, endothelial cells and HSCs co-express CD31, prominin-A (CD133), cadherin 5, type 2 (VE-cadherin) (Taoudi et al, 2005), vascular endothelial growth factor (VEGF) receptor and Tie2 (Rafii et al, 2002). As for the surface markers that characterize HSCs during the embryonic development, integrin, alpha 2b (CD41) is a temporal restricted marker of nascent HSCs (Fig.5) (Robin et al, 2011). It is only re-expressed in some lineage-committed progenitors and megakaryocytes (Bertrand et al, 2005). Emerging HSCs do not express the pan-hematopoietic marker Protein tyrosine phosphatase, receptor type C (CD45), but it is acquired during time and characterizes all the adult hematopoietic cells (Mikkola et al, 2003, Medvinsky et al, 2011).

At the onset of the hematopoietic system there are two proliferative waves: primitive and definitive. The first provides short-lived transitory populations of red blood cells to the developing embryo, to satisfy the short need of the embryonic growth when definitive specialized niches have not yet developed. The second wave, partially overlapping in time of origin, develops from permanent HSCs having the adult characteristics and being capable of long-term multilineage repopulation (de Bruijn et al, 2000, Dzierzak and Speck, 2008).

1.5.2 Primitive hematopoiesis

Hematopoiesis develops in multiple sites of the embryo depending on its stage of development (Fig.5). During the first phase of gestation, cells of the embryo undergo an epithelial-to-mesenchymal transition, giving rise to mesoderm and definitive endoderm. Then mesodermal precursors called hemangioblasts commit to blood cells. They are rare common progenitors of primitive erythrocytes and endothelial cells, identified by the fetal liver kinase 1 (Flk1) marker. They colonize the first hematopoietic organ, the yolk sac, which belongs to the associated structures of the embryo, deriving from trophoblast together with placenta and umbilical cord and it is formed of extra-embryonic endoderm and mesoderm (Kinder et al, 1999, Medvinsky et al, 2011). Hemangioblasts migrate there around day 7 after fertilization, in murine gestation, and produce the first primitive hematopoietic cells, which express low levels of CD41 and lack expression of CD43 and CD45 which are expressed later during maturation (Moore and Metcalf, 1970, Moore et al, 1994, Lessard et al, 2004). They are lineage-restricted and give rise to primitive erythroid precursors expressing embryonic globins and, once established the circulatory system, to myeloerythroid progenitors (Palis et al, 1999).

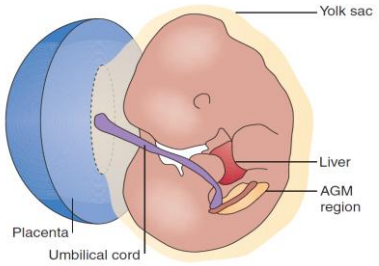

Fig.5. Hematopoietic sites. Representation of all hematopoietic sites in embryo at 11.5 days after fertilization (Medvinsky et al, 2011).

1.5.3 Definitive hematopoiesis

Definitive HSCs, the only ones able to reconstitute an irradiated host, arise at day 10.5 from the aorta-gonad-mesonephros region (AGM) (Medvinsky and Dzierzak, 1996, Dzierzak and Speck 2008). This embryonic organ originates at day 9.5 from the para-aortic splanchnopleura, located at the caudal portion of the embryo deriving from the combination of the lateral plate mesoderm with the adjacent endoderm layer. AGM comprises dorsal aorta, genital ridges and mesonephros (Medvinsky et al, 1993, Cumano et al, 1996). Hematopoietic cells are found on the ventral wall of the dorsal aorta where aortic endothelial cells convert into hematopoietic cells, and blood flow contributes to the signals necessary for their development (de Bruijn et al, 2002, North et al, 2009, Rybtsov et al, 2011). This endothelial-to-hematopoietic transition occurs from hemogenic endothelium giving rise to distinct clusters of hematopoietic cells (Antas et al, 2013).

Long-term reconstituting cells from AGM express c-Kit, CD31 and CD34, with low levels of CD45 and Mac-1 (CD11b) (Sanchez et al, 1996). Definitive HSCs expand upon the expression of sonic hedgehog (Shh), VEGF and bone morphogenetic protein 4 (BMP4), essential to regulate the generation of hematopoietic lineage, but not for the endothelial one (Damert et al, 2002, Hochman et al, 2006, Walmsley et al, 2008). At day 12.5 AGM diminishes the capacity to generate stem cells. At day 11 definitive HSCs are found in extra-embryonic arteries (de Brujin et al, 2000, Gordon-Keylock et al, 2013). Also yolk sac has definitive hematopoietic stem/progenitors which can mature into adult HSCs, but, since the circulation is established in the meanwhile, it is possible that they are derived from the AGM and then migrate into the yolk sac: their real origin and their site of maturation remain elusive (Yoder et al, 1997, McGrath et al, 2003). Subsequently these cells migrate towards placenta around day 11, another hematopoietic site (Ottersbach and Dzierzak, 2005). Placenta derives at day 8.5 from the fusion of the chorionic ectoderm with the allantois, mesodermal tissue that emerges at day 7.5 from the posterior end of the embryo (Rossant and Cross, 2001). Then, HSCs move to fetal liver from day 11.5 through 14.5, and undergo a rapid and

massive expansion losing the expression of CD41 marker (Takeuchi et al, 2002, Robin et al, 2011). The liver remains a hematopoietic site for up to two weeks after birth (Kamps and Cooper, 1982). At day 18 cells from fetal liver colonize the adult hematopoietic sites: bone marrow, spleen, thymus and lymph nodes, although bone marrow represents the primary niche of the stem cell compartment. The functional properties of HSCs (multilineage potential, self-renewal and engraftability) appear gradually during development and the surface markers used to identify them are not consistent with the embryonic ones (Cumano and Godin, 2007).

Adult HSCs reside in the bone marrow medulla within an organized structure composed by different type of cells, which sustain the HSC characteristics. This niche is formed by an osteoblastic and a vascular part. The first is a specialized stromal microenvironment located near the endosteum and composed of osteoblasts, bone forming cells derived from mesenchymal stem cells, with the task to maintain HSCs quiescence and their correct number (Calvi et al, 2003, Zhang et al, 2003). The inactive state is maintained through numerous signaling pathways and adhesion molecules like the membrane bound Stem Cell Factor (mbSCF) on osteoblasts which connect to the c-Kit receptor on HSCs (Czechowicz et al, 2007, Thorén et al, 2008). HSCs emerge from the hemogenic endothelium and the early hematopoietic microenvironment is composed of endothelial cells. This association is maintained also into the adult bone marrow, since the niche is formed also by a vascular part with sinusoidal endothelial cells (Kiel et al, 2005, Medvinsky et al, 2011).

1.5.4 *In vitro* differentiation

The idea of setting the correct culture conditions to obtain HSCs *in vitro* dates back three decades ago. The first attempts were made to generate cystic multilayered structures called embryoid bodies (EBs) that recapitulate the early embryo (Doetschman et al, 1985). Upon culturing ES cells in suspension, they aggregate in spheroid containing all the three primary germ layers and can be forced to differentiate to the hematopoietic lineage upon specific stimulation of the mesoderm at the expense of the other two layers. EBs can give rise to colony forming cells (CFC) containing c-Kit$^+$, CD45$^+$ and CD41$^+$ cells by adding cytokines in various combinations such as stem cell factor (SCF), fms-related tyrosine kinase 3 ligand (Flt-3 ligand), interleukin 3 (IL-3), interleukin 6 (IL-6), granulocyte colony stimulating factor (G-CSF), and thrombopoietin (TPO) (Wiles and Keller, 1991). BMP4 increased the clonogenic efficiency and the multilineage potential (Mitjavila-Garcia et al, 2002, Chadwick et al, 2003). Attempts of transplantation into irradiated hosts were done with the resulting cells and they contributed to both the myeloid and lymphoid lineages, even if without

being so fully differentiated to HSCs to home correctly to the bone marrow and give rise to long-term engraftment (Burt et al, 2004).

Another method to obtain hematopoietic lineages from pluripotent cells without the EBs step is the co-colture with different stromal cell lines, such as ST-1 (Tsai et al, 1986) or osteopetrotic 9 (OP9) (Nakano et al, 1994). The first is a fibroblastoid cell line which derived from a long-term liquid culture of human fetal liver cells and it was demonstrated to support hematopoiesis *in vitro* by producing macrophage colony stimulating factor (M-CSF) and IL-6 and, upon treatment with IL-1, also producing granulocyte-macrophage colony stimulating factor (GM-CSF) and G-CSF. The second line was established from bone marrow stromal cells of an osteopetrotic mouse, *op/op* mutant, which is deficient in M-CSF expression. These cells were chosen because high amount of M-CSF inhibits the differentiation to other hematopoietic lineages than myeloid (Choi et al, 2012). With this culture system $Flk1^+$ cells can be obtained and then erythrocytes, B-lymphocytes, megakaryocytes, natural killer and dendritic cells in presence of erythropoietin (EPO) (Nakano et al, 1994), IL-7 and Flt3L (Cho et al, 1999; Vandekerckhove et al, 2011). To obtain T lymphocytes are necessary OP9 cells expressing delta-like ligand 1 (OP9-DL1), a ligand of Notch (Schmitt et al, 2004). Other stromal cell lines were chosen among the ones which sustain hematopoiesis *in vivo* and modulate the hematopoietic lineage progression. For instance, supporting cells derived from the AGM maintain HSCs in culture (Kusadasi et al, 2002), fetal liver-derived stromal cells favour the generation of hematopoietic cells with increased homing capacity (Qiu et al, 2005) and primary endothelial cells promote the hematopoietic differentiation of pluripotent stem cells towards the hemogenic endothelium expressing pro-angiogenic factors and extracellular matrix components involved in specification and maintenance of hemato-endothelial identity (Rafii et al, 2013).

However, despite all extensive efforts made, *in vitro* efficient differentiation of transplantable HSCs from pluripotent stem cells (ES or iPSc) is still a great challenge. The reason resides in both technical and knowledge deficiencies: we lack a complete understanding of the physiological pathways that regulates HSCs emergence and development, and we cannot reproduce completely the steps and the microenvironments involved in these processes. More likely is to obtain progenitor cells or primitive hematopoiesis, which emerge first, dominate the culture and may inhibit the development of definitive hematopoiesis. Multistep protocols more closely reproduce the *in vivo* developmental conditions, with culture conditions changing at particular time points.

The only way described until now, in fact, provides strong manipulation of the cells by over-expressing transcriptional factors. The first example is the use of homeobox transcription factor 4 (Hoxb4), followed by its partner caudal type homeobox 4 (Cdx4), because of its implication in self-renewal of definitive HSCs (Kyba et al, 2002, Wang et al, 2005). It was delivered by a retroviral

vector into ES derived EBs cultured on OP9 cells. The authors employed an inducible construct in order to avoid undesirable effects on hematopoietic differentiation upon the constitutive expression of the transgene. They obtained *in vitro* and *in vivo* hematopoiesis, including engraftment and multilineage differentiation in irradiated recipients.

Alternative genes were also tested, such as LIM-homeobox transcription factor 2 (Lhx2) (Kitajima et al, 2011), or the combination of GATA binding protein 2 (Gata2), Growth Factor Independent 1B (Gfi1b), FBJ murine osteosarcoma viral oncogene homolog (cFos), and Ets variant 6 (Etv6) (Pereira et al, 2013) that induce hematopoietic cells through endothelial precursors. The next goal should be the transgene-free differentiation to avoid all related safety issues and afford a more physiological differentiation pathway, characteristics required for clinical applications.

1.6 Osteopetrosis disease

Osteopetrosis is a severe inherited disorder leading to an increased bone mass caused by defects in the resorbing activity of osteoclasts. HSC transplantation is the only therapeutic option for this rare bone disorder. Few patients have access to a HLA-identical donor, therefore they could significantly benefit from the use of autologous corrected cells able to reconstitute the hematopoietic system. For this reason, the transplant of autologous gene-corrected iPSc differentiated into HSCs could be an alternative strategy.

1.6.1 Bone organization

Bone is a highly specialized tissue forming the skeleton in association with cartilage. It is divided into an organic phase made mostly of type I collagen and an inorganic phase containing ions in the form of hydroxyapatite (Boskey, 1989). Throughout life, bones undergo a constant renewal through a coordinated balanced work of destruction and reconstruction, by osteoclast and osteoblast cells respectively, known as bone remodeling. This is a dynamic physiological process, which allows the maintenance of the bone architecture, quality and strength (Teitelbaum and Ross, 2003).

Osteoclasts are giant fused multinucleated cells containing 3 to about 30 nuclei per cell. They have pleomorphic mitochondria, great number of vacuoles and lysosomes and well developed membranes of the Golgi apparatus. The region of attachment to the bone, the sealing zone, is made of F-actin cytoskeletal filaments disposed in a ring oriented perpendicular to the bone surface, forming podosomes or focal contacts. The part responsible for the resorption activity, which forms within this sealing zone in close contact with the bone matrix, is the ruffled border, a cell membrane with numerous interdigitations, which increase the surface area facing the space of resorption, the resorption lacuna (Fig.6) (Martin and Sims, 2005).

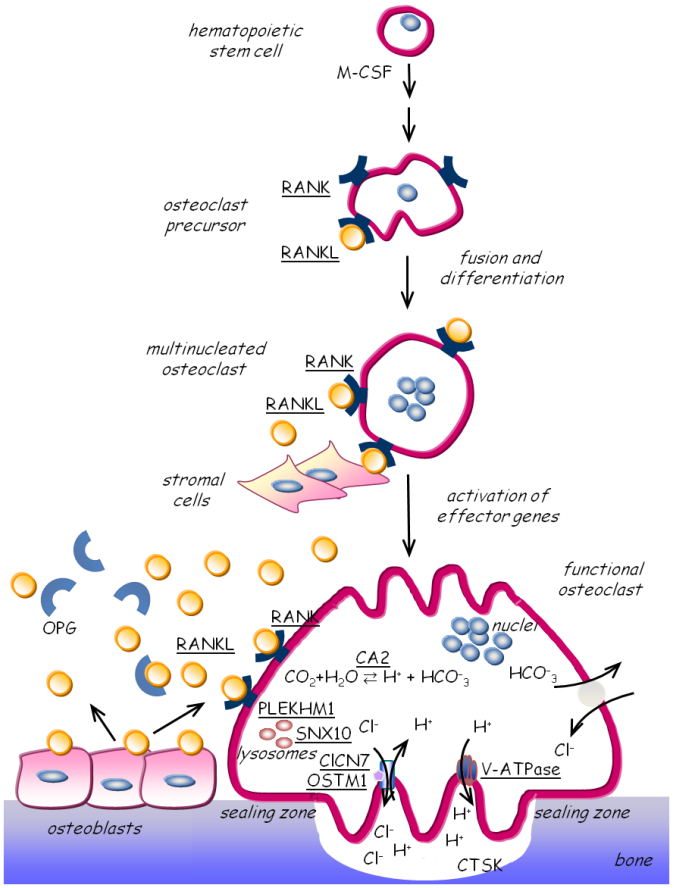

Fig.6. Osteoclast differentiation and structure. Schematic representation of osteoclast differentiation from HSCs, and its principal structures (modified from Pangrazio et al, 2011).

Osteoclasts activity consists in proteolytic enzymes secretion and activation of a large number of vacuolar proton pumps that secrete HCl, resulting in the low pH required for dissolution of the mineralized matrix (Roodman et al, 1991). Lysosomal enzymes, such as tartrate-resistant acid phosphatase (TRAP) and β glucuronidase, or not-lysosomal enzymes, such as cysteine proteinase cathepsin K (CTSK) and metal-matrix proteinase 9 (MMP9) cut the organic phase (Drake et al, 1996). They are active at low pH and carbonic anhydrase II (CAII) is the enzyme responsible to produce the protons that acidify the environment. It catalyzes the conversion of CO_2 and H_2O to H_2CO_3, which then dissociates into H^+ and HCO_3^- (Kenny, 1985). The H^+ ions are carried to the resorption lacuna by the vacuolar H^+ ATPase proton pump, while the HCO_3^- ions are extruded via exchange with Cl^- ions, transported there by chloride channels ClC7, a pump that dissipates the membrane potential generated (Fig.6) (Schlesinger et al, 1997). Parathyroid hormone (PTH) and prostaglandin E2 (PGE2) increase the acid secretion, while calcitonin decreases it. Osteoclasts remove the degraded material through transcytosis and disrupt it through lysosomes (Suda et al, 1992).

A complete cycle of remodeling in humans lasts four months, with 20-30 days for resorption and three months to bone formation. Osteoblasts are mononuclear cells responsible for bone reconstruction, have cuboidal shape with wide Golgi apparatus and endoplasmic reticulum, characteristics, indicating high levels of protein synthesis. They secrete type I collagen, osteocalcin, osteopontin, osteonectin and large amounts of calcium and phosphate. After the reconstruction activity, they die by apoptosis or differentiate into osteocytes (Manolagas, 2000).

Osteoblasts originate from mesenchymal stem cells, which differentiate into osteoprogenitors, then into pre-osteoblasts and finally into osteoblasts (Ducy et al, 2000), while osteoclasts derive from myeloid precursors belonging to the hematopoietic lineage (Martin and Sims, 2005). Osteoclast differentiation is supported by bone marrow stromal cells, early cells of the osteoblastic lineage (Rodan and Martin, 1981). Osteoblasts express receptor activator of nuclear factor kappa-B (NF-kB) ligand (RANKL) which bounds to the RANK receptor on the membrane of myeloid cells. This binding induces the expression of NF-kB and the production of M-CSF which stimulates the monocyte specification and is involved in the survival of mature osteoclasts by preventing apoptosis and increasing cell mobility (Fuller et al, 1993). Moreover, the axis RANKL-RANK is able to initiate the formation, fusion, activation and polarization, as well as resorbing activity of osteoclasts (Woo et al, 2000). RANKL is the necessary and sufficient factor for osteoclastogenesis induction. Osteoblasts secrete osteoprotegerin (OPG), a receptor decoy for RANKL, which acts as inhibitor of the osteoclasts fusion and differentiation (Fig.6) (Lacey et al, 1998).

1.6.2 Different forms of osteopetrosis

Osteopetrosis is a heterogeneous group of rare genetic bone conditions of increased bone mass, which is caused by defects in the balanced activity of bone remodeling. They are genetically and phenotypically heterogeneous, presenting as autosomal dominant osteopetrosis (ADO), intermediate autosomal osteopetrosis (IAO) and autosomal recessive osteopetrosis (ARO). ADO, known as Albers-Schönberg disease, is usually the most benign form of adult-onset, characterized by the occurrence of multiple fractures and osteomyelitis, IAO presents with some bone abnormalities, visual and hearing impairment associated with mild anemia, and ARO, also called infantile malignant osteopetrosis, shows the most severe phenotype presenting soon after birth (Stark and Savarirayan, 2009). We have addressed our studies to the severe recessive form.

ARO has an incidence of 1:250,000 in the general population, however has a considerably higher incidence in specific geographic regions (Fasth, 2009). It is a life-threatening disease caused by a

defect in the resorbing activity of osteoclasts, which results in defective bone resorption and excess of bone mineralization. The generalized increased bone density leads to decreased bone strength, with the risk of multiple fractures causing deformities and inflammation, because of their difficulty to heal. Patients show growth retardation, macrocephaly, eye protrusion, dental abnormalities with delayed tooth eruption, hypocalcemia and secondary hyperparathyroidism (da Silva Santos et al, 2009). Bone sclerosis leads to neurological defects due to inappropriate cranial foramina formation. As a result, patients experience compression of nerves and spinal cord leading to progressive blindness and deafness, increased intracranial pressure and hydrocephalus (Steward, 2003). In addition, the lack of bone resorption causes progressive narrowing of the medullary cavity, resulting into anemia, thrombocytopenia and compensatory extramedullary hematopoiesis in spleen and liver, with consequent hepatosplenomegaly and recurrent infections usually in infancy (Gerritsen et al, 1994). The onset of ARO is perinatal and without treatment the prognosis is severe (Villa et al, 2009).

Osteopetrotic patients can be distinguished in "osteoclast-rich" cases characterized by the presence of normal or increased number of multinucleated osteoclasts unable to resorb bone and "osteoclast-poor" forms in which osteoclasts are absent (Villa et al, 2009). The "osteoclast- poor" forms are due to defects in differentiation of osteoclasts, as examples for mutations in RANK (Guerrini et al, 2008) or in its ligand RANKL (Sobacchi et al, 2007). On the contrary, the "osteoclast-rich" forms are due to defect in the acidification of the resorption lacuna or in the formation of the ruffled border, disrupting indispensable elements for the osteoclasts functionality (Venta et al, 1991).

1.6.3 Genetics of ARO

Genetic analysis of human ARO started in 2000 and a variety of mutations in seven different genes were found during years, describing approximately 80% of patients (Fig.7) (Villa et al, 2009).

The most frequently mutated gene is TCIRG1 (T cell immune regulator 1), encoding for the a3 subunit of the vacuolar-type proton transporting ATPase pump (V-ATPase) (Frattini et al, 2000). A variety of mutations have been reported, including deletions, insertions, nonsense, missense, and splice-site mutations, also in the 5' untranslated region (UTR) (Sobacchi et al, 2001, Pangrazio et al, 2012). The V-ATPase pump is a multimeric protein composed by a V1 complex and a membrane-spanning V0 domain. V1 subunit is involved in ATP hydrolysis, while the V0 part is responsible for proton pumping (Qin et al, 2012). TCIRG1 encodes for the a3 subunit, the major component of the V0 complex, one of the four tissue-specific a subunits, also called 116-kDa subunits. The a3 is highly expressed in late endosomes, lysosomes and in the plasma membrane during osteoclasts differentiation. In bone-resorbing osteoclasts, it is responsible for H^+ production (Toyomura et al,

2003). V-ATPase interacts with actin during ruffled-border formation, probably with a bound mediated by a3 subunit (Lee et al, 1999).

Another frequently mutated gene is CLCN7 (chloride channel 7) that encodes for the Cl^-/H^+ exchanger Chloride Channel 7 (CLC7). The mutations are missense or nonsense and cause a wide spectrum of phenotypes, from severe to mild form. Primary neurological symptoms, like retinal degeneration and cerebral atrophy, can also appear (Graves et al, 2008).

CLC7 is stabilized on the lysosomal membranes by CLC7-osteopetrosis-associated transmembrane protein 1 (OSTM1) complexes. OSTM1 is a type I transmembrane protein with ubiquitin binding activity (Leisle et al, 2011). Mutations in this gene prevent ruffled-border formation causing osteopetrosis "osteoclast-rich" (Chalhoub et al, 2003) and lysosomal pathology (Pressey et al, 2010). This form of ARO is extremely severe because of the dramatic degeneration of central nervous system. Patients suffer from neurodegeneration, optic atrophy, microcephaly, cortical atrophy (Pangrazio et al, 2006).

Another molecule, pleckstrin homology domain-containing family M member 1 (PLEKHM1) protein, localized on lysosomes is implicated in vesicular trafficking. Mutations cause protein loss of function provoking a mild form of osteopetrosis (Van Wesenbeeck et al, 2007).

Mutations in sorting nexin-10 (SNX10) have been associated with an "osteoclast-rich" ARO that closely resembles the one caused by TCIRG1 mutations (Aker et al, 2012). In fact, PX domain of SNX10 interacts with the V1 subunit of V-ATPase (Chen et al, 2012).

The last two genes identified as responsible for ARO are associated to "osteoclasts-poor" forms: tumor necrosis factor (TNF) ligand superfamily member 11 (TNFSF11), also known as RANKL, and TNF receptor superfamily member 11A (TNFRSF11A), known as RANK. They encode for the osteoclastogenic cytokine and its receptor, respectively (Nakagawa et al, 1998, Takayanagi 2012).

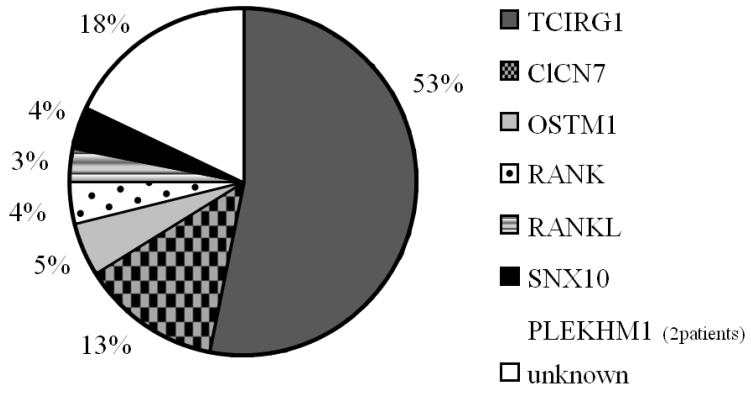

Fig.7. Distribution of molecular defects in ARO patients. All the seven genes identified as responsible for ARO are represented with the percentages of patients affected (Sobacchi, personal communication).

Molecular diagnosis is fundamental for the classification and has important clinical implications for the treatment of the disease.

1.6.4 Treatment of osteopetrosis

The only available treatment for osteopetrosis is HSC transplantation, a technique performed since the early 1980s, due to the hematopoietic origin of osteoclasts (Coccia et al, 1980). This approach has important limitations, discovered during years of clinical practice. Patients affected by ADO do not usually undergo to HSC transplantation because of the high risk of conditioning. Moreover, "osteoclast-poor" ARO due to RANKL mutations cannot be cured by HSC transplantation, as this protein is expressed by osteoblasts and stromal cells (Guerrini et al, 2008). For this disease, the treatment option tested in a preclinical study is the pharmacological administration of a synthetic form of the soluble cytokine RANKL (Lo Iacono et al, 2012).

For the "osteoclasts-rich" osteopetrosis, transplantation leads to the prevention and reversion of symptoms such as osteosclerosis and extramedullary hematopoiesis if performed as early as possible before the onset of the clinical signs. Irreversible defects, such as progressive neurodegeneration typical of CLCN7 and OSTM1 osteopetrosis, or hearing and visual impairment due to intracranial nerve compression, can be prevented but not reversed once they have occurred (Steward, 2003).

The success of transplantation depends on good engraftment of donor cells, which is strongly limited by the need for a compatible donor. In fact the main complications in the allogenic HSC transplantation are rejection and GvHD, occurring when donor T cells recognise and attack host cells. These severe complications depend on the degree of HLA mismatch, donor and recipient sex and age disparity, cell source and conditioning regimen intensity (Ferrara, 1995). A decade ago, using HLA-identical donors the success percentage was about 73%, while with HLA-related donors was about 43% (Driessen et al, 2003). During the years the technique has greatly improved. With HLA-identical donors the 5-year disease-free survival rate is now estimated at 88%, while with HLA-matched unrelated donors is at 80%. Nevertheless, this rate is evaluated only at 66% for patients transplanted with HLA-haploidentical donor. Moreover, engraftment complications are the most frequent cause of death and increase with the patient's age, in fact patients treated after the age of 10 months frequently undergo to serious complications (Schulz, 2013).

Severe complications were also frequently observed when alternative stem cell sources are used, such as T cell depleted HSCs from HLA-haploidentical donors or cord blood from unrelated donors (Schulz et al, 2002). Complications include rejection, delayed hematopoietic reconstitution, venous occlusive disease, pulmonary hypertension and hypercalcemic crisis (Steward et al, 2004).

The earlier the patients undergo HSC transplantation, the better is their outcome, with significant improvement in the quality of life. To this end, a different approach had been proposed in an osteopetrosis mouse model, in which HSC transplantation is performed directly into the uterus, the earliest time-point in which the administration of hematopoietic cells can prevent the clinical manifestation. This approach prevents the onset of rejection, GvHD and osteopetrotic disease before birth (Frattini et al, 2005, Tondelli et al, 2009). Therefore the same method should be taken into consideration also for patient's treatment. A prenatal diagnosis of osteopetrosis could open the possibility to perform HSC transplantation before birth, as already reported for other genetic diseases (Wengler et al, 1996, Pirovano et al, 2004).

1.6.5 Osteopetrosis murine models

Several murine models have been used to study the ARO disease, both spontaneous mutant mice and engineered knockout mouse models. They reproduce the osteoclast defects observed in human ARO, involving the same mutated genes.

The ones which mimic the "osteoclasts-rich" osteopetrosis are the engineered complete knockout for *Tcirg1* gene (Li et al, 1999), the spontaneous *oc/oc* model (osteosclerotic), carrying a deletion of the first three exons of *Tcirg1* (Scimeca et al, 2000); the complete knockout of *Clcn7* gene showing bone and neurological defects (Kornak et al, 2001); the spontaneous *gl/gl* (grey lethal) mutant carrying a mutation in *Ostm1* gene showing severe osteopetrosis together with primary retinal and neuronal degeneration, as reported in patients (Chalhoub et al, 2003); and the rat *ia/ia* (incisor-absent) model having a truncating mutation in *Plekhm1* gene (Van Wesenbeeck et al, 2007).

The mouse models recapitulating the "osteoclasts-poor" osteopetrosis are the complete knockout of RANKL (Kong et al, 1999), the engineered *tles/tles* (toothless) mouse bearing a point mutation in RANKL (Douni et al, 2012), and the complete knockout of RANK (Li et al, 2000), all well mimicking the corresponding form of osteopetrosis observed in human.

In the present work, we have addressed our studies on the spontaneous *oc/oc* mouse model presenting severe growth retardation, thickened bones and reduced medullary cavity. Due to the lack of a3 protein, V-ATPase pump is present on endosomal compartment, but it is absent at the level of plasma membrane, causing a defect in the acidification of the resorption lacuna. Affected mice show severe osteopetrosis with typical radiologic and histological characteristics and die two to three weeks after birth (Fig.8) (Scimeca et al, 2000). The hematopoiesis is altered, with increased myelomonocytic differentiation in bone marrow, liver and spleen and blocked B-lymphoid

differentiation. As patients, they experience high susceptibility to infections, probably due to immunological alterations (Blin-Wakkach et al, 2004).

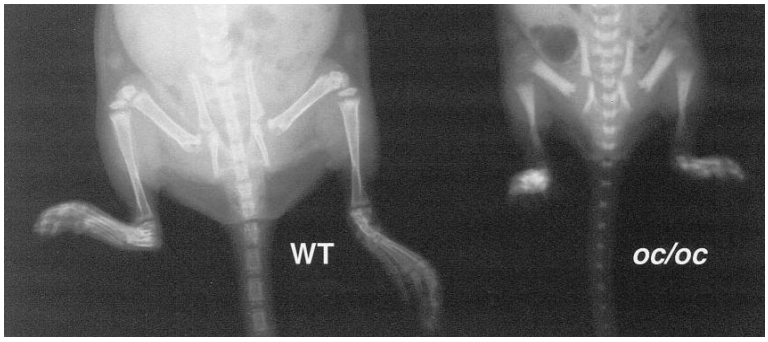

Fig.8. Osteosclerotic bone in *oc/oc* mouse model. Radiographic images of a normal mouse (wt, on the left) and an osteosclerotic one (*oc/oc*, on the right) (Scimeca et al, 2000).

The *oc/oc* mutant mouse represents a good model to a deeper understanding of the cellular basis of the ARO disease and as a tool to evaluate new therapeutic approaches to be applied in future to the human clinical setting.

2 Aim of the project

ARO is a severe inherited disorder leading to an increased bone mass caused by defects in the resorbing activity of osteoclasts. Among the heterogeneous group of osteopetrosis, ARO shows the most severe phenotype, leading to death early in life if not treated. The mouse model *oc/oc* well recapitulates the disease features. HSC transplantation is the only treatment so far available to cure the disease, however its success is limited to the restricted number of available matched donors. Thus, the transplant of autologous corrected hematopoietic cells represents an attractive alternative therapeutic strategy to exploit. In particular, due to the limitations in performing gene correction of primary cells, the generation of iPSc from patients who do not have access to a HLA-identical donor could allow site-specific genetic correction by homologous recombination followed by differentiation towards hematopoietic progenitors and autologous transplantation.

In the present thesis, I have exploited iPSc as a potential source of cells able to *in vitro* and *in vivo* differentiate into functional osteoclasts resorbing bone. To this end, I have performed the following strategy: (a) generation of iPSc from murine wt and *oc/oc* fibroblasts; (b) correction of *oc/oc* iPSc replacing the mutated gene through homologous recombination, by using a BAC engineered vector with a genomic region encompassing the entire *Tcirg1* gene coding sequence and its flanking regulatory sequences; (c) set up a protocol for the differentiation of wt, uncorrected and corrected *oc/oc* iPSc into hematopoietic precursors; (d) further differentiation of obtained myeloid precursors into very specialized cells such as osteoclasts, demonstrating their rescued resorbing activity upon gene-correction. The process is aimed at generating transplantable hematopoietic cells, including osteoclast precursors, with the final goal of transplanting them in the ARO mouse model *oc/oc* to revert the phenotype, thus providing a proof of principle for an autologous cell therapy approach to treat ARO.

3 Methods

3.1 Reagents

- *DMEM:* Dulbecco's Modified Eagle Medium (DMEM, Sigma-Aldrich), 20% fetal bovine serum (FBS, BioWithttaker), 100 U/ml penicillin and streptomycin (P/S, 10000 U/ml penicillin and 10000 U/ml streptomycin, Lonza), 2 mM L-glutamine (200 mM in 0.85% NaCl solution, Lonza);
- *ES medium:* Knock out Dulbecco's Modified Eagle Medium (KO-DMEM, Gibco), 20% embryonic stem cell fetal bovine serum (ES-FBS, Gibco), 100 U/ml P/S, 2 mM L-glutamine, β-mercaptoethanol (Gibco), 1X non-essential amino acids (100X, Gibco);
- *Freezing medium:* 10% dimethyl sulfoxide (DMSO, Sigma-Aldrich), 90% FBS;
- *MACS buffer:* 0.5 % bovine serum albumine (BSA, Merck), 2 mM ethylenediaminetetraacetic acid (EDTA, Fluxa) in 1X phosphate buffered saline (PBS, EuroClone);
- *PBS FACS:* 2 % FBS, 1 mM EDTA in 1X PBS;
- *Carnoy's fixative:* methanol (Merck):glacial acetic acid (Merck) 3:1;
- *TBST:* 20 mM Tris(hydroxymethyl)aminomethane hydrochloride (Tris-HCl, Fluxa) pH 7.4, 0.15 M NaCl (Merck), 0.05 % Tween-20 (Sigma-Aldrich);
- *Washing buffer:* 0.2% BSA, 0.05% Tween in 1X PBS;
- *Perm buffer:* 5% FBS, 0.5% Triton (Sigma-Aldrich) in 1X PBS;
- *TLB solution*: 1M Tris pH 8.3, 0.5 M EDTA, 20%SDS, 5M NaCl;
- *TE buffer:* 10 mM Tris pH 8.0, 1 mM EDTA.

3.2 Procedures

3.2.1 Mice

wt C57BL/6 CD45.1 mice, B6C3Fe a/a-Tcirg1oc/J CD45.2 (*oc/oc*) mice and non-obese diabetic-scid IL2rγ(null) (NSG) mice were purchased from Charles River or Jackson Lab. *oc/oc* CD45.1 mice were obtained after crossing of congenic CD45.1 with *oc/oc* animals. Animal care and experimental procedures were performed in accordance with ethical rules by the institutional review board.

3.2.2 Cells culture

3.2.2.1 Mouse embryonic fibroblasts isolation

Mouse embryonic fibroblasts (MEFs) were derived from wt C57BL/6 CD45.1 E13.5 embryos. They were collected in a 100-mm tissue culture dish containing PBS and sterilized with P/S diluted

in PBS. Using sterile scissors, the placenta, heads and intra-abdominal organs were discarded. Remaining tissues were washed in PBS, minced with dissecting scissors and suspended in 0.5 ml Trypsin-EDTA (200 mg/L Versene (EDTA), 170000 U/L trypsin, Lonza) per embryo. The suspension was transferred into 50 ml conical tube and incubated in 37°C water bath for 10 minutes. Cell aggregates were dissociated by vigorous pipetting. Trypsin-EDTA was inactivated with DMEM and the suspension was filtered using a 40 µm membrane filter. After a centrifugation at 1500 rpm for 5 minutes, pellet was resuspended in 1 ml DMEM per embryo and plated into 100-mm tissue culture dishes containing 7 ml DMEM. Cells were incubated at 37°C, 5% CO_2 until confluence. Next, they were transferred into 150-mm tissue culture dishes. After cells were trypsinized and centrifuged at 1200 rpm for 10 minutes, pellet was resuspended in 1 ml freezing medium per cryovial.

3.2.2.2 Feeder layer preparation

MEFs were used as feeder cells for iPSc after they were inactivated by 10 µg/ml Mitomycin C (Sigma-Aldrich) for 3 hours. Tissue culture plates were prepared by coating them with gelatin solution 0.1% (Gelatin Type B from bovine skin, Sigma-Aldrich). Gelatin solution was obtained by adding 500 mg of gelatin to 500 ml of distilled water and sterilizing it by filtration using a 0.22 µm membrane filter. Gelatin solution was warmed before use, plated and immediately aspirated. Plates were left open to dry up completely. After 3 hours MEFs cells were washed twice with PBS and incubated with Trypsin-EDTA for 5 to 10 minutes, collected by gentle pipetting, centrifuged at 1200 rpm for 10 minutes and seeded on gelatin-coated tissue culture plates (2500 cell/cm^2). Plates were incubated overnight at 37 °C, 5% CO_2 before plating iPSc.

3.2.2.3 Murine fibroblasts isolation

oc/oc fibroblasts were obtained from tale biopsy. The latter was sterilized with P/S diluted in PBS and transferred into a plate where it was minced with dissecting scissors. They were collected with 1.5 ml DMEM and plated in a 35-mm tissue culture dish. When fibroblasts grew, pieces were discarded and cells were cultured until 80% confluency. At this point they were transferred by Trypsin-EDTA into 100-mm tissue culture dish as described before (§3.2.2.1).

3.2.3 Transduction

Cells were collected and counted. $2x10^5$ cells were plated into a 6-well plate and incubated for 6 hours. Lentiviral vector carrying reprogramming genes (provided by Dr. Luigi Naldini's group) was added to plate at 1 multiplicity of infection (MOI) with 4 ng/ml polybrene (Sigma-Aldrich). Cells

were incubated overnight. The following day the medium was replaced and after 48 hours cells were collected and seeded onto MEFs feeder layer. Murine cells were plated with ES medium supplemented with 10^3 U/ml leukemia inhibitor factor (LIF, Millipore) added fresh every time. Half of the medium was changed every other day.

3.2.4 iPSc picking

iPS-like colonies were detected 4 weeks later and individually picked. 50 µl Trypsin-EDTA was distributed in 96-well plate and a pipet tip set at 5 µl was wet with Trypsin-EDTA. Using this tip, colonies were picked from the fibroblast layer and transferred into plate. After 10 minutes, cells in the colonies were dissociated by pipetting up and down and cell suspension was transferred on MEFs feeder layer into 24-well plates with ES medium supplemented with LIF. Half of the medium was changed every other day. Then they were transferred into gelatin-coated 6-well plates with mitomycin-inactivated MEFs and then into 100-mm plates until the stabilization of the line. Cells were frozen as previously described with freezing medium (§3.2.2.1).

3.2.5 Lipofection

$2x10^5$ cells were plated into a gelatin-coated 6-well plate with mitomycin-inactivated MEFs in 2 ml ES medium without P/S but supplemented with LIF and were incubated for 4 hours. Two 1.5 ml microcentrifuge tubes were prepared with 100 µl Opti-MEM Reduced Serum Medium (Invitrogen) without P/S and serum. In one tube 2 µg plasmid DNA carrying Cre recombinase cDNA (Dr. Luigi Naldini's group) was added, while in the other tube 6 µg Lipofectamine 2000 (Invitrogen) was added in a 1:3 ratio (pDNA:Lipofectamine 2000). Reagents were incubated 5 minutes at RT, then were mixed and incubated 20 minutes at RT. The suspension was added to cells. After an overnight incubation at 37°C and 5% CO_2, medium was replaced with ES medium supplemented with LIF. After a week, iPSc were sub-cloned at a limiting dilution. To separate iPSc from feeder layer cells, they were trypsinized and left 10 minutes in a low attachment Petri dish with 8 ml ES medium. MEFs adhered more rapidly than iPSc and when medium was collected they remained into the Petri. Then cells were put in a 15 ml collection tube for 10 minutes and MEF, which were bigger, precipitated. 7 ml was transferred in a new tube and centrifuged at 1200 rpm for 10 minutes. Cells were plated at the limiting dilution of 0.3 cell per well into 5 gelatin-coated 96-well plates with mitomycin-inactivated MEFs with 50 µl ES medium supplemented with LIF. The following day 50 µl ES medium supplemented with LIF was added and then medium was changed every other day. When colonies grew they were transferred into different plates according to the numbers of cells.

3.2.6 Alkaline phosphatase staining

iPSc were cultured into a gelatin-coated 6-well plate with mitomycin-inactivated MEFs. Medium was aspirated and cells were fixed with 4% paraformaldehyde (PFA, Sigma-Aldrich) for 2 minutes. Cells were washed with TBST. Reagents from Leucocyte Alkaline Phosphatase Kit (Sigma-Aldrich) were mixed: Fast Red Violet (FRV) with Naphthol AS-BI phosphate solution and water in a 2:1:1 ratio (FRV:Naphthol:water). 1 ml obtained solution was added to cells and incubated into the dark for 15 minutes at RT. 1 ml TBST was added to wash cells and then was replaced with PBS.

3.2.7 Karyotype

iPSc were cultured into a 100-mm tissue culture dish and incubated with 0.1 µg/ml colchicine (KaryoMAX colcemid solution, Life Technologies) for 2 hours at 37°C, 5% CO_2. Cells were washed with 2 ml PBS and treated with 2 ml Trypsin-EDTA. Medium, PBS and Trypsin-EDTA were collected in a 15 ml conical tube, which was centrifuged at 1200 rpm for 10 minutes. Supernatant was discarded gently using a pipet tip set at 1000 µl and pellet was resuspended in the remaining volume. Then, 1 ml of a solution containing 75 mM KCl (Fluxa) pre-warmed at 37°C was added drop by drop. During 5 minutes and 30 seconds 7 ml KCl was added drop by drop and then cells were centrifuged at 1200 rpm for 10 minutes. Supernatant was discarded gently and 1 ml Carnoy's fixative (prepared fresh every time and frozen at -20°C) was added drop by drop. Pellet was resuspended vigorously and 7 ml Carnoy's fixative was added drop by drop. Cell suspension was stored for 45 minutes at -20°C and then centrifuged at 1200 rpm for 10 minutes. Supernatant was discarded gently and 8 ml fixative was added drop by drop. Cell suspension was stored for 30 minutes at -20°C and then centrifuged at 1200 rpm for 10 minutes. Cells were washed twice with fixative and pellet was resuspended in an adequate volume of fixative. 20 µl suspension was dropped on a Histo-bound charged slide (Marienfeld) into 2 spots and slide was exposed to water vapor for 5 seconds. Slide was aged overnight at room temperature and the following day was mounted by using Vectashield mounting medium with 4,6-diamidino-2-phenylindone (DAPI) (Vector Laboratories) for G-banding. Slide was scored under an Olympus BX61 Research Microscope equipped with a cooled CCD camera. Images were captured and analysed with Applied Imaging Software CytoVision (CytoVision Master System with Karyotyping & FISH).

3.2.8 Immunofluorescence

iPSc were cultured on MEFs cells plated onto 0.1% gelatin-coated round cover slides put in 24-well tissue culture plates until they reached the desired confluence. Then, cells were washed with PBS and fixed with 500 µl 4% PFA in PBS for 15 minutes into the dark. After 2 washes with 500 µl

washing buffer, cells were permeabilized and blocked with 500 µl perm buffer for 1 hour at RT. Then, cells were washed with 500 µl washing buffer and primary antibodies were added overnight at 4°C (or 1 hour at room temperature) at the described dilutions listed in Tab.1. The following day cells were washed 3 times with 500 µl washing buffer. Secondary antibodies at the concentration reported in Tab.1 were added for 1 hour at RT into the dark. Cells were washed four times with 500 µl washing buffer. DAPI, 1:50000 diluted in water, was added for 5 minutes at RT into the dark. Cells were washed with water and air dried into the dark. Round cover slides were picked up and mounted on Histo-bound charged slides with 5 µl ProLong Gold antifade reagent (Life Technologies). After 30 minutes at RT into the dark, slides were stored at -20°C. Images were acquired by an Olympus FluoView1000 confocal microscope.

Rabbit anti-Nanog	Novus Biologicals	1:100
Rabbit anti-Sox2	Abcam	1:200
Rabbit anti-Oct4	Abcam	1:200
Mouse anti-SSEA-1	Cell signalling	1:200
Mouse anti-AFP	R&D	1:50
Rabbit anti-Brachyury	Abcam	1:100
Mouse anti-Nestin	Abcam	1:100
Goat anti-rabbit IgG (H^+L) AlexaFluor488 conjugated	Invitrogen	1:2000
Goat anti-mouse IgG (H^+L) AlexaFluor488 conjugated	Invitrogen	1:2000

Tab.1. Antibodies utilized for immunofluorescences.

3.2.9 *In vitro* differentiation assay

Following the hanging drop method, EBs were formed plating 1500 cells in each 20 µl drop. After 2 days EBs were collected and seeded on gelatin-coated coverslips in 24-well plates in ES medium without LIF. After 5 days of culture an immunofluorescence (§3.2.8) was performed on part of the cells using antibodies against Alphafetoprotein (AFP) and Brachyury. The remaining cells were treated with retinoic acid (Peprotech) to allow the differentiation towards ectoderm. After 19 day of culture an immunofluorescence was performed using an antibody against Nestin. The antibodies specifications are listed in Tab.1.

3.2.10 Teratoma formation assay

iPSc were trypsinized, separated from MEFs by magnetic beads (§3.2.14), and counted. For injection $5x10^6$ cells were resuspended in 100 µl PBS and loaded into a syringe. Each NSG mouse received 2 subcutaneous injections over the flanks. After about 4 weeks tumors grew up and were dissected. Mice were sacrificed by carbon dioxide inhalation. Nodules were separated from other tissues and put in PBS. They were fixed with 4% PFA and then embedded in paraffine for

hematoxylin and eosin staining by Dr. Scanziani's group (Pathology Department, University of Milan) (§3.2.27).

3.2.11 Gene Correction

The BAC contig RP24-241G10 belonging to the RPCI-24 C57BL/6J mouse BAC library was purchased from Children's Hospital Oakland Research Institute (CHORI) and engineered by Gene Bridges for the insertion of a neomycin resistance cassette. It was inserted in 241G10 BAC in intron 10 of *Tcirg1* gene, surrounded by FRT sites. $2x10^5$ iPS cells were plated into a gelatin-coated 6-well plate on a DR4 resistant MEFs (Applied StemCell) in 2 ml ES medium without P/S but supplemented with LIF and were incubated with 1 µg BAC overnight at 37°C, 5% CO_2 in presence of Lipofectamine-2000. The following day 200µg/ml G418 neomycin (Sigma-Aldrich) was added to select the resistant clones. After about 9 days neomycin resistant colonies were successfully isolated and expanded.

3.2.12 Elimination of the BAC resistance cassette

In order to excise neomycin resistance cassette, pCAG-Flpe plasmid (Addgene) was transfected overnight in the presence of Lipofectamine 2000. After a subcloning at a limiting dilution, clones were expanded in 2 different plates. In one G418 was added to identify the clones that had successfully lost the neomycin resistance cassette, while from the other plate the corresponding clones were isolated and further expanded.

3.2.13 FISH assay

Fluorescence in situ hybridization (FISH) is a cytogenetic technique able to localize the presence of specific DNA sequences or chromosomes. Briefly, the sample was prepared as for karyotype assay and a specific probe tagged with a fluorophore was applied to chromosomes. On iPSc metaphases the entire BAC was used as a probe, 20 to 30 images were analysed for each clone. The assay was performed by Dr. Paolo Vezzoni's group (Department of Human Genome, CNR).

3.2.14 iPSc purification from feeder cells

In order to avoid possible MEFs contamination in PCR analysis, all clones were purified with anti-SSEA-1 (stage-specific embryonic antigen-1) magnetic beads (Miltenyi Biotec) accordingly to kit instructions and passaged 3 times on gelatin-coated plates without feeder layer before collecting genomic DNA and RNA for analysis. In detail, cells were dissociated to single-cell suspension,

counted and centrifuged at 1500 rpm for 10 minutes. Cells were resuspended in 80 µl MACS buffer and 20 µl anti-SSEA-1 beads were added. Cells were mixed and incubated for 15 minutes at 4°C to allow specific binding. Cells were washed with 2 ml buffer, centrifuged at 1500 rpm for 10 minutes and resuspended in 500 µl buffer. MS column was placed in the magnetic field of a MACS Separator and rinsed with 500 µl buffer. Cells were applied onto the column and magnetically labeled cells were retained, while unlabeled cells run through. Cells were washed 3 times with 500 µl buffer and then column was removed from the separator and placed on a 15 ml collection tube. To elute SSEA-1 positive cells, 1 ml buffer was added and flushed out pushing a plunger into the column.

3.2.15 PCR reactions

3.2.15.1 Mouse colony genotyping

Mice were genotyped by PCR on genomic DNA from tail biopsies. Mice were enumerated with ear punches, or by toes tattoos in case of 1-3 days-old pups, using a Neo9 neonate Rodent tattooing system (Aims). Tail biopsies were digested by 15 µl Proteinase K enzyme in a 250 µl TLB solution at 56°C for about 2 hours. Upon dissolution of the tails, 250 µl isopropanol (Merk) was added and samples were centrifuged at 13200 rpm for 10 minutes. 250 µl of cold 70% ethanol was added to the pellet, and samples were centrifuged at 13200 rpm for 10 minutes. After air drying at 56°C, pellets were solubilized in TE buffer. DNA samples were stored at 4°C. PCR reaction to genotype the mouse colony was performed with Taq polymerase (Biotools) with thermal profile and primers listed in Tab.2.

Temperature	**Time**	**# cycles**
95°C	5’	1
95°C	30’’	40
60.5°C	30’’	
72°C	30’’	
72°C	5’	1
4°C	forever	

oc/oc	Forward	GGC CTG GCT CTT CTG AAG CC	600 nM
	Reverse	CCG CTG CAC TTC TTC CCG CA	600 nM
wt	Forward	TCA TGG GCT CTA TGT TCC GG	400 nM
	Reverse	GAA GGC GCT CAC GGA TTC GT	400 nM

Tab.2. Thermal profile, sequences and concentrations of primers of PCR reaction for mouse colony genotyping.

3.2.15.2 Correct BAC homologous recombination verification

PCR reactions were performed for detection of HIS3 and CM(R) sequences into the genome of iPSc. After the iPSc purification from feeder cells (§3.2.14), cells were collected into a 1.5 ml

microcentrifuge tube and centrifuged at 6000 rpm for 5 minutes. Pellet was washed in PBS and centrifuged at 6000 rpm for 5 minutes. Supernatant was discarded and pellet was stored at -20°C.
DNA was extracted with QIAamp DNA Mini kit (Qiagen) according to the manufacturer's instructions. Briefly, pellet was resuspended in 200 µl PBS, 20 µl Proteinase K and 200 µl buffer AL and cells were incubated for 10 minutes at 56°C. 200 µl 100% ethanol (Merck) was added and sample was transferred into a spin column. Column was washed with 500 µl buffer AW1 and buffer AW2. Sample was centrifuged at 13200 rpm for 3 minutes. DNA was eluted in 200 µl water and stored at -20°C. PCR reactions were performed with AccuTaq (Sigma-Aldrich) thermal profiles and primers listed in Tab.3.

Temperature	**Time**	**# cycles**
95°C	5'	1
95°C	30''	40
58°C	30''	
72°C	30''	
72°C	5'	1
4°C	forever	

HIS3	Forward	AGC ACT CGA TCT TCC CAG AA	800 nM
	Reverse	TTC AGT GGT GTG ATG GTC GT	800 nM
CM(R)	Forward	TCC GGC CTT TAT TCA CAT TC	600 nM
	Reverse	TCG TCG TGG TAT TCA CTC CA	600 nM

Tab.3. Thermal profile, sequences and concentrations of primers of PCR reactions for the verification of correct BAC homologous recombination.

3.2.15.3 Expression of *Tcirg1* gene

RNA was extracted from cell pellets with trizol method. 1 ml TRIzol Reagent (EUROzol, EuroClone) was added to a pellet, cells were lysed by pipetting up and down and incubated at RT for 5 minutes. 200 µl chloroform (AnalaR) was added and tube was shaked vigorously. After incubation at RT for 3 minutes, sample was centrifuged at 12000 g for 15 minutes at 4°C. Chloroform precipitated with protein and DNA, while RNA remained in the upper aqueous phase that was removed and placed into a new tube. 500 µl isopropanol (Merck) was added and tube was incubated at RT for 10 minutes. Sample was centrifuged at 12000 g for 15 minutes at 4°C. Supernatant was discarded and 1 ml 75% ethanol was added. Tube was vortexed to wash RNA and then centrifuged at 7500 g for 5 minutes at 4°C. Superrnatant was discarded and pellet was air dried without drying it completely. RNA pellet was resuspended in 50 µl RNase-free water and incubated at 55°C for 10 minutes. RNA was placed on ice and quantified by Nanodrop. 1 µg RNA was utilized for retrotranscription using QuantiTect Reverse Transcription Kit (Qiagen), according to manufacturer's procedure. cDNA was stored at -20°C. Reverse transcriptase PCR was performed with thermal profile previously indicated in Tab.2 with only wt forward and *oc/oc* reverse primers.

3.2.16 Differentiation to the hematopoietic lineage

To form EBs the hanging drop method was followed. 800 cells were placed in a 20 µl drop of culture medium without LIF. At day 2 plates were turned and EBs were transferred into plates adding cytokines to induce differentiation (50 ng/ml m-BMP4 (R&D), 50 ng/ml m-SCF (PeproTech), 50 ng/ml h-Flt3L (PeproTech), 10 ng/ml m-IL-3 (PeproTech), 10 ng/ml m-IL-6 (PeproTech), 10 ng/ml m-GM-CSF (PeproTech), 3 U/ml h-EPO (R&D)). At day 4 and 8 fresh medium was added with the same cytokine cocktail except for m-BMP4, since this protein was needed only for initial mesoderm induction. Fluorescence-activated cell sorter (FACS) analyses were performed every day from 8 to 12 of culture in most experiments.

3.2.17 Colony forming cell assay (CFC)

Cells from iPSc differentiation culture were seeded (40000 cells/ml) into semi-solid methylcellulose (MethoCult Media 3234, Stem Cell Technologies). They were centrifuged at 1200 rpm for 5 minutes. 1.85 ml methylcellulose was added to a round bottom tube. Methylcellulose was stored in aliquots at -20°C and thawed when needed. Cells resuspended in 150 µl IMDM and 5X cytokines (Tab.4) with 1X P/S resuspended in 500 µl IMDM were added to methylcellulose, to reach a final total volume of 2.5 ml containing 1X cytokines.

hEPO	3 U/ml	R&D
mSCF	20 ng/ml	PeproTech
mIL-6	10 ng/ml	PeproTech
mIL-3	10 ng/ml	PeproTech
mTPO	10 ng/ml	PeproTech
hFlt3L	20 ng/ml	PeproTech
mGM-CSF	10 ng/ml	PeproTech

Tab.4. Cytokines used for CFC assay.

Cells were resuspended slowly with a 2.5 ml syringe with a blunt end needle. 2.2 ml was taken with the syringe and plated dividing the volume into two 35-mm tissue culture dishes to obtain duplicates. Plates were incubated for 7-10 days, then colonies were observed and counted by optical microscope. Burst forming unit-erythroid colonies (BFU-E) derive from an immature progenitor of the erythroid lineage with high proliferative capacity, which gives rise to more than 200 erythoblasts in a single or multiple clusters. Colonies appears large, hemoglobinized (red or brown coloured) and single cells are difficult to distinguish. Colony forming unit-monocyte colonies (CFU-M) originate from a mature, myeloid-committed progenitor with limited proliferative capacity that give rise at least to 20 macrophage cells, typically more. Colonies are small, organized

in a single cluster and composed of colourless round cells. Colony forming unit-monocyte-granulocyte colonies (CFU-GM) arise from an earlier progenitor able to differentiate in both lineages. Colonies can contain thousand of cells in single or multiple clusters. Colony forming unit-granulocyte-erythrocyte-monocyte-megakaryocyte colonies (CFU-GEMM, also called mixed) derive from a multilineage immature progenitor and contain erythroblasts and cells of myeloid lineages. Colonies are large, with red clusters mixed with colourless cells.

3.2.18 FACS staining

Cells were collected, counted and centrifuged at 1200 rpm for 10 minutes. Cells were incubated for 30 minutes on ice with the chosen antibodies (Tab.5) diluted in 100 µl PBS FACS, then washed with 2 ml PBS FACS and centrifuged at 1500 rpm for 5 minutes. Cells were resuspended in 150 µl PBS FACS, transferred into a FACS tube and kept on ice. LSR Fortessa or FACSCanto II equipped with Diva software (BD) were used for data acquisition and FlowJo software (Tree Star) was employed to analyze data. Cell sorting was performed using a FACS Aria I, with a fluidic upgrade to the version III, (BD Biosciences) equipped with Diva software, and data were analyzed using FlowJo. Sorted cells were collected in FBS and centrifuged, and then resuspended in medium for culture.

anti-CD4	FITC conjugated	1:100	eBioscience
anti-CD8	FITC conjugated	1:100	eBioscience
anti-CD11b	FITC conjugated	1:100	eBioscience
anti-CD11b	AlexaFluor488 conjugated	1:100	eBioscience
anti-CD19	PE conjugated	1:100	eBioscience
anti-CD41	eFluor450 conjugated	1:50	eBioscience
anti-CD45	PerCP conjugated	1:1000	BD
anti-CD45	PE-Cy7 conjugated	1:500	eBioscience
anti-CD45.1	FITC conjugated	1:200	eBioscience
anti-CD45.2	eFluor450 conjugated	1:100	eBioscience
anti-cKit	PE conjugated	1:100	eBioscience
anti-cKit	eFluor780 conjugated	1:100	eBioscience
anti-Gr-1	eFluor780 conjugated	1:200	eBioscience
anti-Sca1	PE conjugated	1:100	eBioscience
anti-Sca1	APC conjugated	1:100	eBioscience
anti-SSEA1	AlexaFluor647 conjugated	1:50	eBioscience

Tab.5. Antibodies used for FACS staining. APC, allophycocyanin; Cy, cyanin dye; FITC, fluorescein isothiocyanate; PE, phycoerythrin; PerCP, peridinin chlorophyll protein.

3.2.19 Cytospin

From CFC assay, some colonies were individually picked with a micropipette and diluted into a PBS 10% FBS solution. Cells were centrifuged at 1800 rpm for 10 minutes and residual methylcellulose was removed by vacuum aspiration. Cells were resuspended in 150 µl PBS 2% FBS. Cytospin cassette was prepared with a Histo-bound charged slide and cellular resuspension

was loaded into it. Cells were centrifuged at 800 g for 5 minutes. Slide was then stained with May-Grunwald/Giemsa staining (§3.2.20).

3.2.20 May-Grunwald/Giemsa staining

May-Grunwald solution (Carlo Erba) was diluted 1:3 in water and added to slides for 7 minutes. Then it was discarded and added to slides a second time for 7 minutes. It was discarded and Giemsa solution (Carlo Erba) diluted 1:10 in water was added to slides for 18 minutes. It was discarded and slides were immerged in tap-water and then in distilled water to eliminate salts. Slides were air dried and mounted with Eukitt mounting medium (Sigma-Aldrich).

3.2.21 Osteoclast differentiation protocol

$CD45^+$ cells were purified from iPSc derived hematopoietic cells by magnetic beads as previously described (§3.2.14) and were cultured for a week in Minimal Essential Medium Alpha Modification (αMEM, Gibco), 10% FBS, 100 U/ml P/S, 2 mM L-glutamine in presence of 20 ng/ml m-SCF (Peprotech) and 100 ng/ml m-M-CSF (Peprotech). Then cells were transferred on plastic or on dentine slices (Osteosite, iDS, Pantec) and cultured in the same medium supplemented with 20 ng/ml m-M-CSF and 30 ng/ml m-RANKL (Peprotech). After 5-10 days osteoclasts on plastic were fixed and stained with TRAP assay (Sigma-Aldrich: acid phosphatase, Leukocyte) accordingly to kit instructions, while dentine slices were stained with 1% Toluidine Blue for 3 minutes and then washed in water. The same protocol was pursued with *oc/oc* or wt mice freshly-isolated splenocytes or BM cells, after purification of $CD11b^+$ (instead of $CD45^+$) cells by magnetic beads.

3.2.22 Actin ring staining

Cells were washed with warm PBS and then fixed with citrate solution (Sigma-Aldrich):acetone (Merk):37% formaldehyde (Merk) 2:4:1 30 seconds at RT. After a wash in water, DAPI, 1:50000 diluted in water, was added for 5 minutes at RT into the dark. Cells were washed twice in water and were permeabilized in Perm buffer 20 minutes at RT. Phalloidin TRITC conjugated (Sigma-Aldrich) 1:25 was added for 30 minutes at RT into the dark. Finally cells were washed 3 times in water.

3.2.23 Transplantation

In utero transplantation was performed as already described (Tondelli et al, 2005). Briefly, pregnant recipient heterozygous females were anesthetized with an intraperitoneal injection of 0.25 g/kg

body 2,2,2-Tribromoethanol (Avertin, Sigma-Aldrich) at 13.5 days p.c. An incision was performed through the skin and the peritoneum, and the uterine horns were exposed and kept wet with saline solution. The embryos were injected through the uterine wall and placenta in the direction of the liver with a glass capillary loaded with 10 µl of cells suspension. The uterus was reinserted in the peritoneal cavity and the incisions were sutured with absorbable sutures and staples.

For neonatal transplantation syringes loaded with 30 µl of cells suspension were used injecting mice with or without radiation (400 RAD, RADGIL radiator) in liver or in temporal vein, visualizing it through the skin with the help of optical fibres.

In both cases, donor cells were obtained from iPSc derived hematopoietic sorted cells or from wt CD45.1 bone marrow cells. The latter were collected by flushing of femurs and tibias using a 23-gauge needle. Bones were discarded and cells were filtered through a 30 µm filter (cell strainer, BD) and washed in PBS FACS by centrifuging at 1500 rpm for 10 minutes. Red blood cells were lysed by 2 ml Red Blood Lysis Buffer (Gibco) for 5 minutes at RT. Cells were washed in PBS FACS, refiltered and centrifuged at 1500 rpm 10 minutes.

3.2.24 Blood withdrawal

Mice were warmed under a heat lamp and local anesthesia was applied on tail. Through a cut in the tail using a blade, 2-3 blood drops were collected in 1X PBS 10 mM EDTA and blood flow was stopped by dabbing the tail. Blood was centrifuged at 1600 rpm for 5 minutes at RT and 200 µl-1 ml Red Blood Lysis Buffer was added to the pellet, accordingly to its dimension, for 10 minutes at RT. Ten v/v PBS FACS were added and cells were centrifuged at 1500 rpm for 10 minutes at RT.

3.2.25 Serum calcium level analyses

As terminal procedure, blood was collected in empty microcentrifuge tubes by a syringe from the heart of euthanized mice. Blood was allowed to clot and, after a centrifugation at 8000 rpm for 10 minutes, serum was collected. Blood total calcium levels were determined using a Ci16200 Architect Abbott instrument (Abbott Park).

3.2.26 Hematopoietic organs analyses

To evaluate engraftment level in the transplanted mice, they were euthanized and long bones, spines, spleens and thymi were dissected. Long bones were processed as described in §3.2.23.

Spleens and thymi were washed in PBS, smashed on a filter and centrifuged at 1500 rpm for 10 minutes. Obtained cells were used for FACS staining.

The spines were fixed in 4% PFA for 2 days, then 70% ethanol was added overnight and finally they were maintained in 100% ethanol. Spines were decalcified in Ion Exchange Decal Unit (Biocare Medical, Concord) and paraffin-embedded for hematoxylin and eosin staining (§3.2.27).

3.2.27 Hematoxylin and eosin staining

Sections were prepared from paraffin-embedded organs and were deparaffinized by 5 minutes in Xylene (Sigma-Aldrich). Then they were rehydrated by an inverse alcoholic scale: 5 minutes in 100% ethanol twice, 5 minutes in 90% ethanol, 5 minutes in 70% ethanol, 5 minutes in distilled water twice. They were stained 2 minutes in Hematoxylin (Sigma-Aldrich), washed in distilled water for 5 minutes and stained 10 minutes in Eosin (Sigma-Aldrich). After a wash in distilled water for 5 minutes, slides were dehydrated with an alcoholic scale: 5 minutes in 70% ethanol, 5 minutes in 90% ethanol, 5 minutes in 90% ethanol and finally 5 minutes in Xylene twice. Slides were mounted with Eukitt mounting medium.

4 Results

4.1 iPSc generation

To obtain iPSc from *oc/oc* mouse strain, a third generation self-inactivating polycistronic lentiviral vector was employed. The polycistronic cassette contains three out of the four Yamanaka's reprogramming factors: Oct4, Sox2, Klf4 under the control of the spleen focus-forming virus promoter (sffv) (Fig.9). c-Myc was not used to avoid problems related to tumorigenesis caused by its over-expression.

Fig.9. Scheme of lentiviral vector carrying the reprogramming genes. In the two LTRs are inserted loxP sites. The promoter sffv guides the transcription of the reprogramming genes Oct4, Sox2, Klf4, spaced by 2A peptides. The second peptide (2A*) is modified to avoid internal recombination. At the end, the WPRE element allows good expression levels and high virus titre during the production.

Fibroblasts isolated from a tail biopsy of an *oc/oc* female mouse expressing the CD45.1 isoform were transduced with the lentiviral vector using MOI =1 for reprogramming into pluripotent cells. Four weeks later, iPS colonies grew up and were picked on the basis of their ES cell-like morphology, with a reprogramming efficiency of 0.01%, estimated as the ratio of the number of iPS clones over the number of infected cells. Clones were analysed for the number of integrated vector copies, vector copy number (VCN), into the murine genome by real-time PCR analysis. The clones with the lowest VCN were selected and assessed for the chromosomal integrity by analysing the frequency of metaphases with normal distribution of chromosomes.

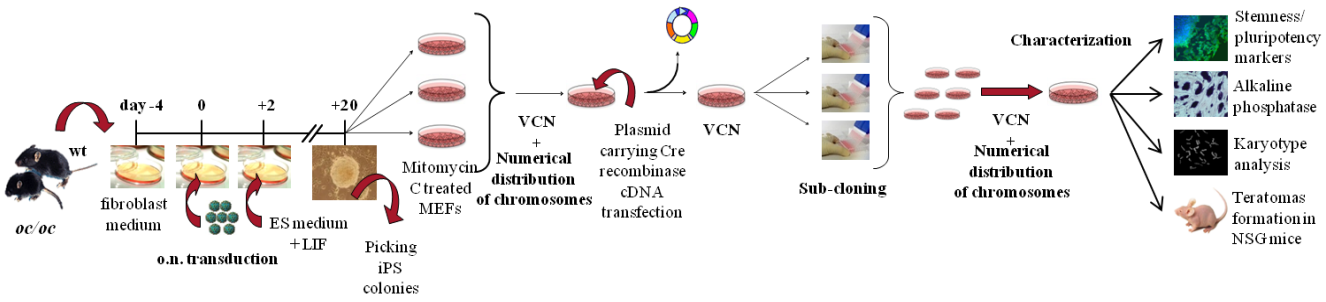

Fig.10. Scheme of the reprogramming and selecting procedure. Fibroblasts from wt and *oc/oc* mice were overnight transduced and subsequently cultured in a medium specific for pluripotent cells supplemented with LIF. After about 20 days iPS colonies grew up, were picked and transferred on mitotically inactive feeder cells. VCN and numerical distribution of chromosome analyses were performed to select clones to be transfected with a plasmid carrying Cre recombinase. This procedure excised the reprogramming vector from the iPSc genome. A VCN analysis was performed on bulk culture to evaluate the success of the excision and cells were subcloned at a limiting dilution. On the subclones, VCN and numerical distribution of chromosome analyses were performed to select iPSc with VCN=0 and optimal chromosomal setting. These subclones were then characterized for their stemness, pluripotent and safety profile.

Next, selected iPSc were transfected with a plasmid expressing Cre-recombinase to obtain the excision of lentiviral vector sequences. iPS clones showing a VCN near zero were subcloned. Subclones with VCN equal to zero showing a normal chromosomes content were selected and characterized: *oc/oc* iPSc #13.62 and #16.74 (Fig.10). The obtained iPS clones showed a normal karyotype (Fig.11A) and their stemness and pluripotency were assessed by various assays. They expressed the alkaline phosphatase, a marker of stemness (Fig.11B). Moreover, they expressed the typical pattern of genes important for the maintenance of self-renewal and pluripotency abilities: Oct4, Sox2, Nanog and SSEA-1 (Fig.11C). Next, the pluripotency of iPS clones was analysed by testing *in vitro* and *in vivo* their ability to differentiate towards the three germ layers. We pushed the *in vitro* differentiation towards mesoderm, endoderm and ectoderm, which were evaluated by immunofluorescence using antibodies against Brachyury, Alphafetoprotein and Nestin, respectively (Fig.11D). As for the *in vivo* differentiation, we used the teratoma formation assay in which, upon subcutaneous injection into NSG mice, iPS clones spontaneously formed a tumor solid mass comprising structures derived from the three germ layers (Fig.11E).

The same procedures of generation and characterization of iPSc were previously performed starting from MEFs obtained from a wt E13.5 male embryo (C57BL/6 CD45.1) giving rise to the wt iPSc #6.25.39 and #6.25.68 (data presented in the master degree thesis "Lentiviral-mediated induced pluripotent stem cells generation and differentiation to the hematopoietic lineage: towards a cellular therapy approach for infantile malignant osteopetrosis", Sharon Muggeo).

In conclusion, we were able to generate murine iPS clones from an osteopetrotic mouse model for the first time, with efficiency comparable to what we previously described for wt iPSc. Through various assays we demonstrated stemness and pluripotency of the obtained clones, which were vector free and showed a normal karyotype.

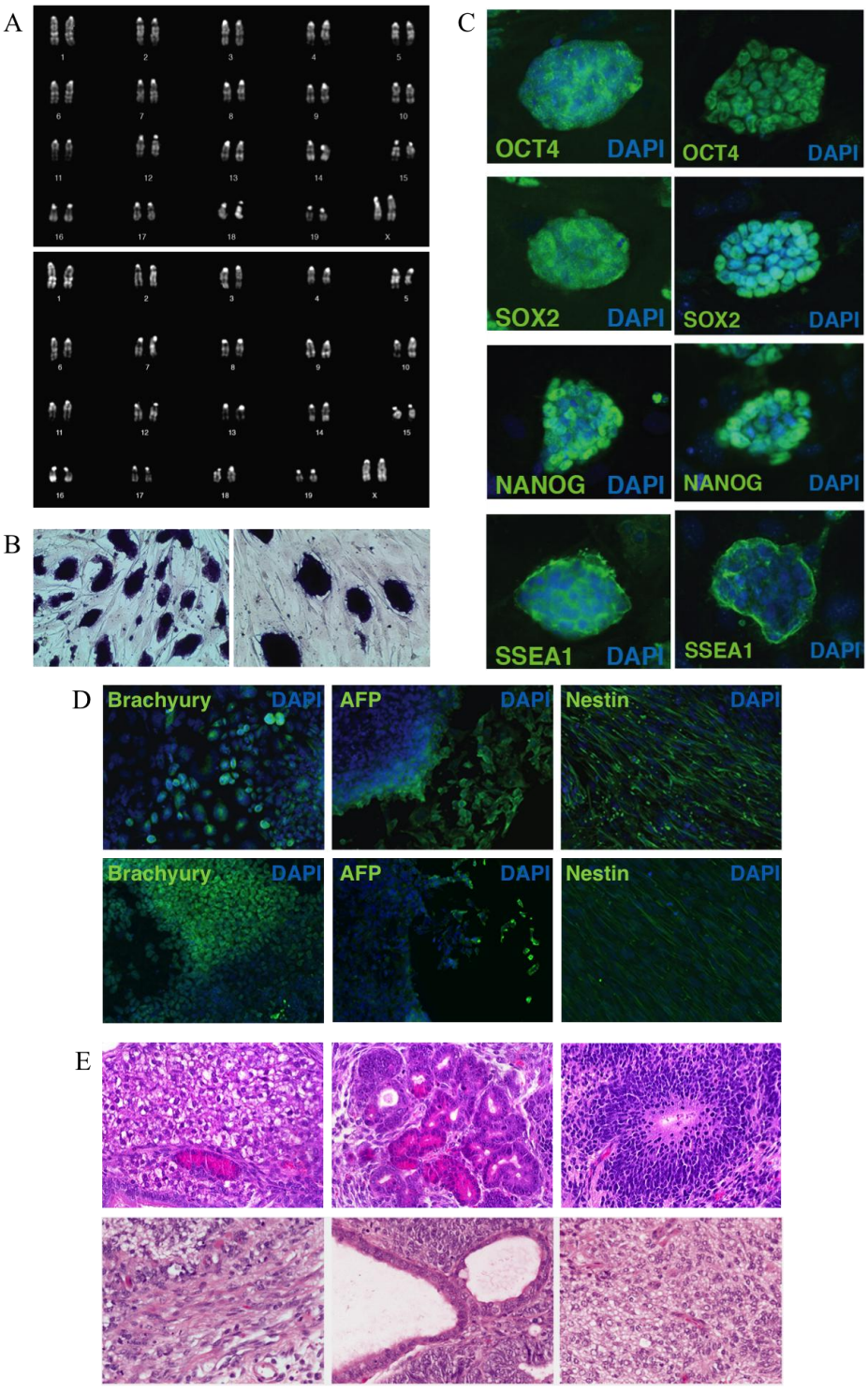

Fig.11. Characterization of selected *oc/oc* iPSc. (A) Karyotype of *oc/oc* iPSc #13.62 (upper panel) and *oc/oc* iPSc #16.74 (lower panel). (B) Alkaline phosphatase staining on *oc/oc* iPSc #13.62 (left panel) and *oc/oc* iPSc #16.74 (right panel). All images are at 10X magnification. (C) Immunofluorescence of indicated stemness markers on *oc/oc* iPSc #13.62 (left panel) and *oc/oc* iPSc #16.74 (right panel). Nuclei are stained with DAPI. All images are at 20X magnification. (D) Immunofluorescence of indicated pluripotency markers on *oc/oc* iPSc #13.62 (upper panel) and *oc/oc* iPSc #16.74 (lower panel). Nuclei are stained with DAPI. All images are at 20X magnification. (E) Hematoxylin and eosin staining on teratoma structures representing mesoderm (left panel), endoderm (middle panel) and ectoderm (right panel) tissues from *oc/oc* iPSc #13.62 (upper panel) and *oc/oc* iPSc #16.74 (lower panel). All images are at 40X magnification.

4.2 *oc/oc* iPSc correction

oc/oc iPSc #13.62 and #16.74 were transfected with a BAC containing the murine genomic region encompassing the entire *Tcirg1* gene coding sequence, including introns as well as 5' and 3' flanking regions, thus presumably maintaining most if not all of its regulatory sequences. To easily select the iPS clones integrating the donor sequences, we engineered the BAC by inserting a FRT-flanked neomycin resistance cassette into the intron 10 of the gene (Fig.12). The iPSc clones were cultured in the presence of neomycin on a neomycin-resistant DR4 feeder layer and only the resistant clones were analyzed for site-specific correction, after two rounds of selection.

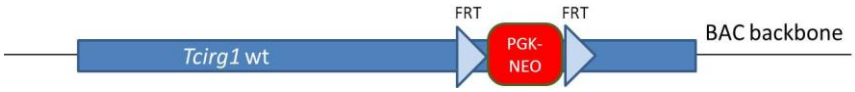

Fig.12. Scheme of BAC. Into the backbone of the bacterial artificial chromosome (BAC) is inserted the wt form of *Tcirg1* gene, with a neomycin resistance cassette under the control of the PGK promoter (PGK-NEO), flanked by FRT sites, included into the intron 10.

The presence and the expression of the correct sequence of *Tcirg1* were investigated by specific PCR analysis (Fig.13A and data not shown) and the iPS clones in which vector backbone sequences were still present due to occurrence of non-correct homologous recombination (off-targeting) were further excluded. As previously described (Howden et al, 2011), PCR reactions were performed with primers for Chloramphenicol resistance (CM(R)) and the yeast *Histidine3* (HIS3) gene, both present in the BAC backbone that should not be integrated into the genome (Fig.13B). The presence of *Tcirg1* gene in the chromosome 19, its endogenous murine position into the genome, was also confirmed by FISH assay (Fig.13C). Two clones were finally selected: iPSc #13.62.18-BAC and #16.74.32-BAC. After the genetic correction, the iPS clones maintained their pluripotency and showed a normal karyotype (data not shown). In conclusion, we were able to correct iPS osteopetrotic clones replacing the mutated gene by an engineered BAC system.

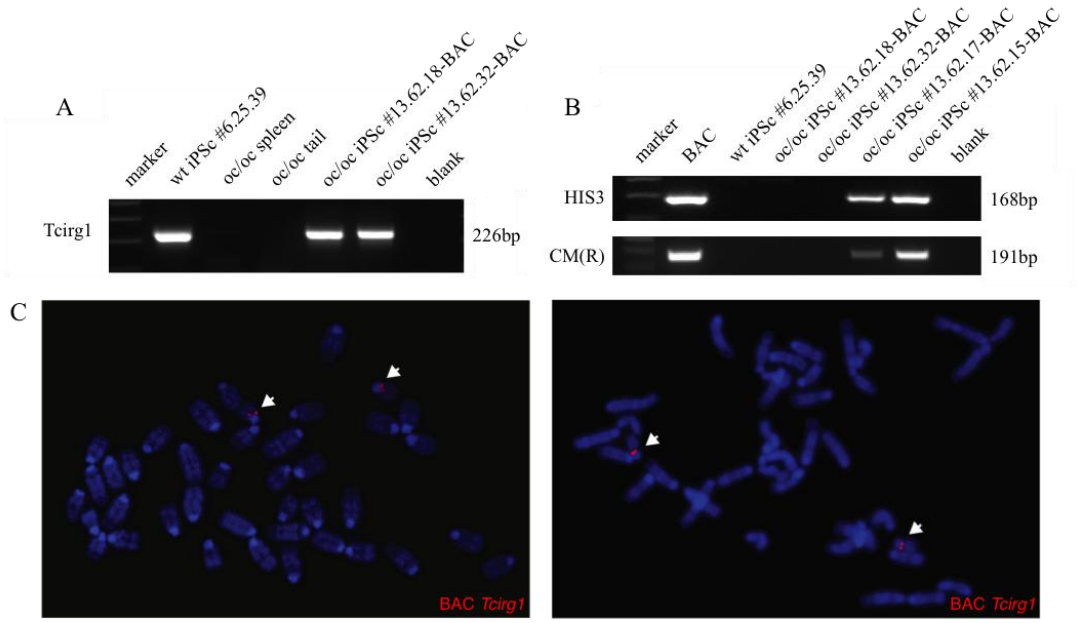

Fig.13. Successful correction of *oc/oc* iPS clones. (A) RT-PCR for detection of *Tcirg1* expression in wt iPSc #6.25.39 (used as a positive control), in two samples derived from spleen and tail of an *oc/oc* mouse (used as negative controls), in iPSc #13.62.18-BAC and #13.62.32-BAC. (B) PCR for detection of HIS3 and CM(R) sequences into the genome of wt iPSc #6.25.39 (used as negative control), iPSc #13.62.18-BAC, iPSc #13.62.32-BAC and two other clones previously discarded due to the insertion in another chromosome (#13.62.17-BAC) or to the presence of multiple BAC insertions (#13.62.15-BAC). The first lane is the internal positive control and shows the PCR product obtained from the BAC used for the transfection. (C) FISH assay on iPSc #13.62.18-BAC and #13.62.32-BAC. The arrows indicate the localization of the BAC probe on the chromosome 19 in a sub-centromeric localization.

4.3 Differentiation of iPS clones to the hematopoietic lineage

To obtain hematopoietic cells from corrected *oc/oc* iPSc, we took advantage of a differentiation protocol previously optimized on wt iPSc. EBs were first generated from iPSc, deprived of residual feeder cells and cultured in suspension in low attachment Petri dishes. However, this method was not efficient since only a minority of the cells expressed hematopoietic markers. Next, we tested the hanging drop method. In detail, iPSc were let grow in suspension concentrated at the lower of drops that hang from the lid of a plate. Two days later, EBs were cultured in a medium supplemented with cytokines inducing hematopoietic differentiation in tissue culture treated plates, to allow the formation of the hemogenic endothelium, from which HSCs arise at the early stage of embryo development (Fig.14).

From about 8 to 10 days of culture cardiomyocyte-like cells characterized by a rhythmic beat were observed, indicating that iPSc were able to differentiate into the mesodermal layer (data not shown). We obtained cells expressing the CD45 marker, specific for mature hematopoietic cells, and CD41 marker, the antigen present on primitive hematopoietic cells in E7 yolk sac and E11.5 fetal liver (§1.5.2, 1.5.3).

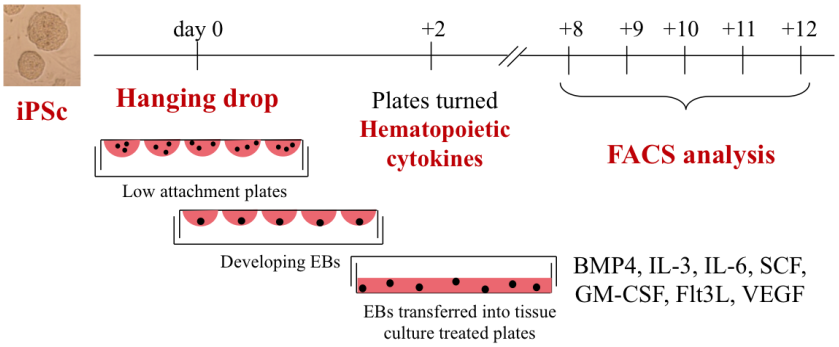

Fig.14. Scheme of the hematopoietic differentiation protocol. iPS clones were seeded in drops that hang from low attachment plates. At day 2 EBs were formed and transfected into tissue culture treated plates with hematopoietic cytokines (BMP4, IL-3, IL-6, SCF, GM-CSF, Flt3L, VEGF). From day 8 to 12 of culture cytofluorimetric analyses were performed.

In order to optimize the protocol and increase the number of hematopoietic cells, the effect of various hematopoietic cytokines was tested. For example, iPSc differentiation was performed in the presence or absence of the cytokine VEGF. The cell culture was analyzed at day 8 and 12. At day 8 of culture in the presence of VEGF we observed a significant increase in the total number of obtained cells and, in particular, a significant increase of the yield of $CD41^+$ cells (Fig.15).

We also evaluated the effect of TPO to the culture medium. The addition of this cytokine caused at day 8 a decrease of hematopoietic cells and immature progenitors expressing c-Kit and Sca1, indicating a detrimental effect on the differentiation (Fig.16). On this basis, we decided to modify the cytokine cocktail by adding VEGF.

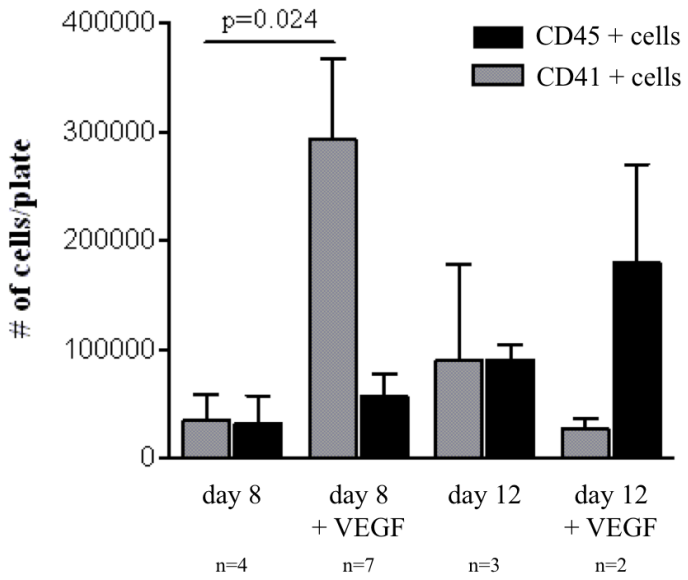

Fig.15. Effect of VEGF on hematopoietic differentiation. Histogram showing number of $CD41^+$ and $CD45^+$ cells obtained per culture plate from the specified days of culture, in presence or absence of VEGF. In each culture plate were seeded 75 EBs. Error bars indicate standard error.

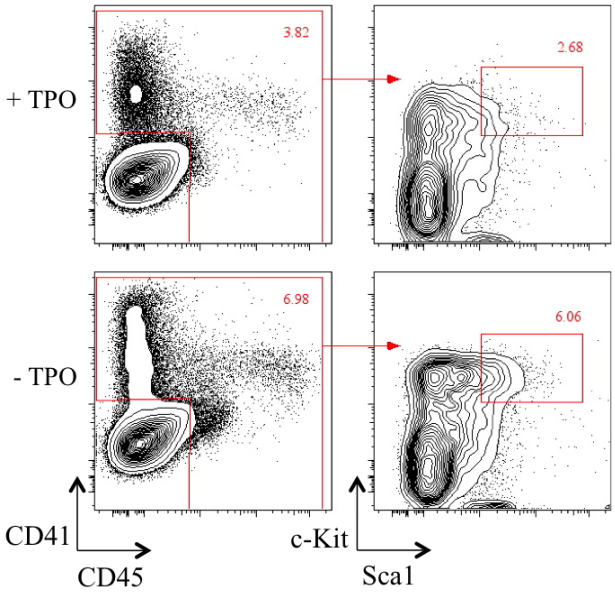

Fig.16. Effect of TPO on hematopoietic differentiation. FACS analysis representing day 8 of culture in presence (upper panel) or absence (lower panel) of TPO. The first columns show hematopoietic $CD41^+$ and/or $CD45^+$ cells and, gated on these, the second columns show immature progenitors expressing c-Kit and Sca1 markers. Numbers in the FACS plots indicate percentages among alive cells.

From day 8 to 12 of the culture we performed cytofluorimetric analyses to evaluate the generation of hematopoietic cells, with the aim to recognise the various subset of cellular populations and identify the day at which they emerged at the maximum frequency. FACS analyses consistently showed a population of $CD45^+$ cells, which reached the maximum at day 12. The vast majority of $CD45^+$ cells was also $CD11b^+$, indicating that they were committed to the myeloid lineage, whereas a minor but important part was composed of immature progenitors negative for CD11b and co-expressing c-Kit and Sca1 markers (Fig.17). As the $CD45^+$ fraction increased throughout time during culture, we observed a progressive decrease of the population expressing CD41, similarly to the physiologic fetal hematopoiesis (Fig.18).

The functionality of obtained differentiated cells was tested by the clonogenic CFC assay, which showed a great variety of hematopoietic colonies types at each tested time point. $c\text{-}Kit^+$ cells were purified by immunomagnetic beads and seeded into semi-solid methylcellulose medium supplemented with hematopoietic cytokines. After 7 to 10 days, the obtained individual colonies were scored and cytospin preparations were performed to identify cellular subpopulations (Fig.19). Erythroid, myeloid and mixed hematopoietic colonies were obtained, indicating the presence in the culture of clonogenic multipotent or oligopotent progenitors.

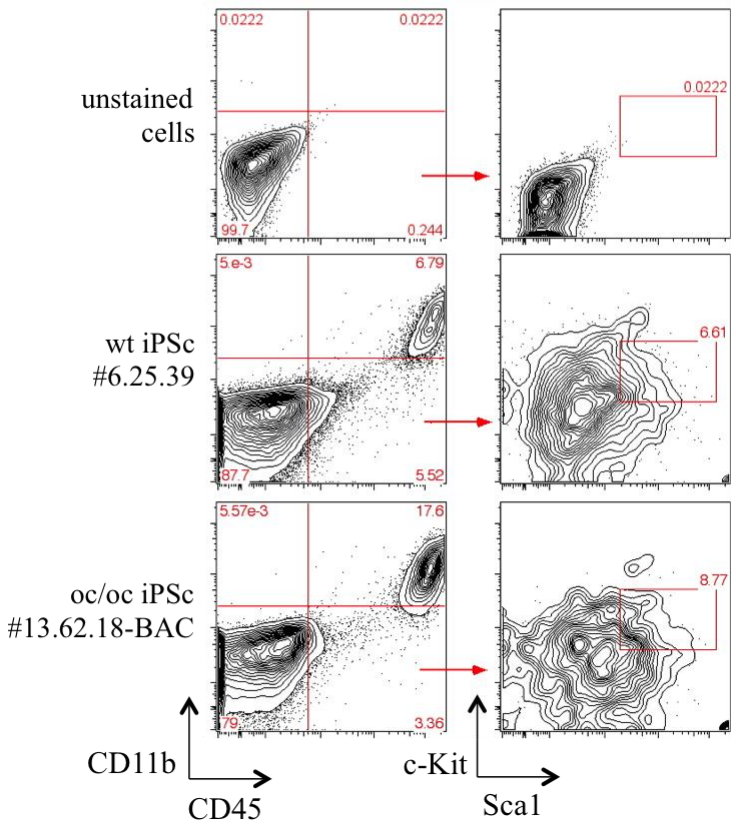

Fig.17. Presence of myeloid and progenitors cells in culture. Representative FACS plots showing the expression of CD45 pan-hematopoietic marker and of myeloid CD11b markers (left panels), and the expression of c-Kit and Sca1, progenitor cells markers, gated on the CD11b $^{low/-}$ CD45^{+} fraction (right panels), The contour plots referred to unstained cells (upper panel), wt iPSc #6.25.39 (middle panel), and iPSc #13.62.18-BAC (lower panel) at day 11 of culture. Numbers in the FACS plots indicate the percentages among alive cells.

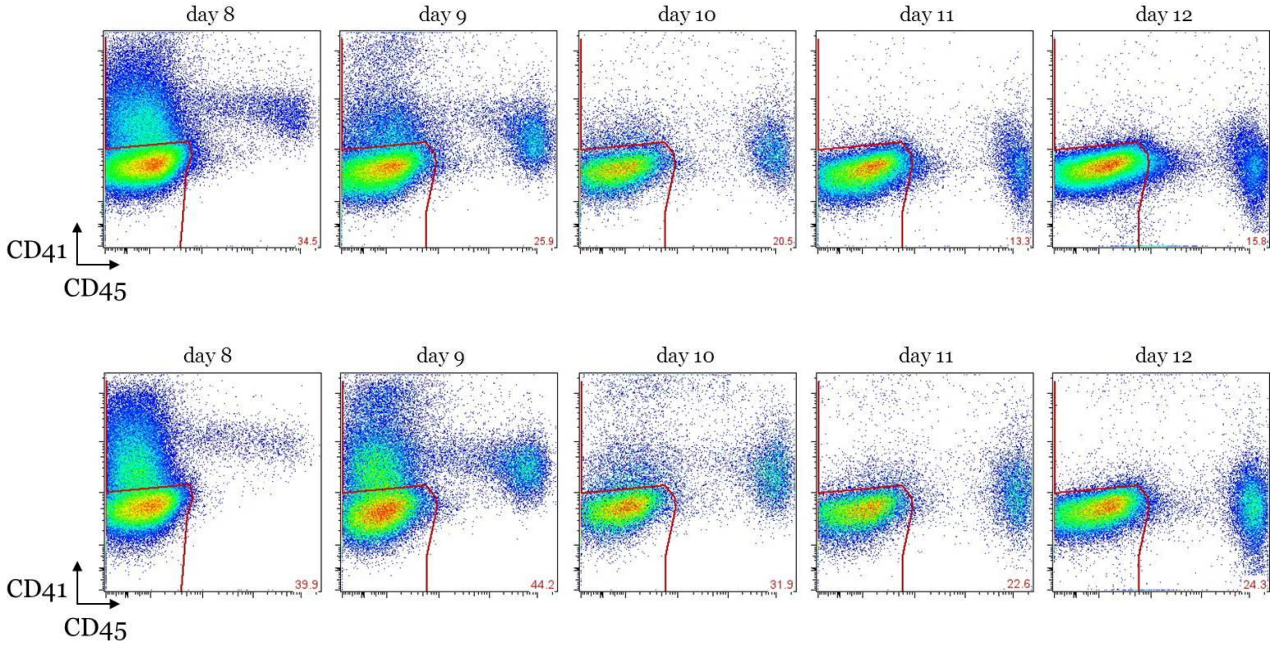

Fig.18. Time-course FACS analysis. Representative FACS plots showing the expression of CD41 and CD45 hematopoietic markers at different time points of the differentiation protocol (from day 8 to 12) of wt iPSc #6.25.39 (upper panel) and iPSc #13.62.18-BAC (lower panel). Numbers in the FACS plots indicate percentages among alive cells.

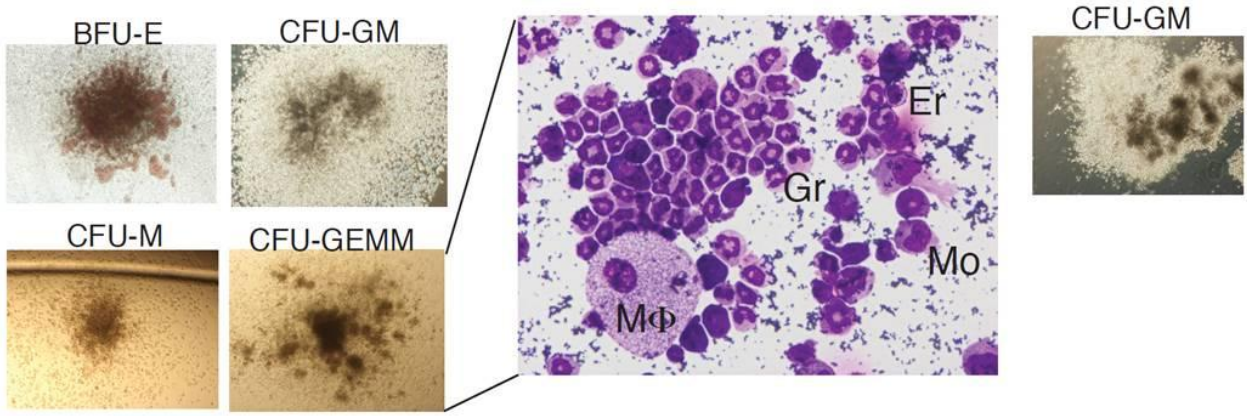

Fig.19. Hematopoietic colonies. Representative examples of an erythroid colony (BFU-E), a granulocyte-monocyte colony (CFU-GM), a monocyte colony (CFU-M) and a granulocyte-erythrocyte-monocyte-megakaryocyte colony (CFU-GEMM) from wt iPSc #6.25.39 (left panels). Middle insert shows a representative example of a cytospin preparation of a CFU-GEMM colony showing macrophages (MΦ), monocytes (Mo), granulocytes (Gr) and erythrocytes (Er). The right panel shows a representative example of a CFU-GM colony obtained from *oc/oc* iPSc #13.62.18-BAC. The colonies images are at 4X magnification while the cytospin image is at 40X magnification.

In conclusions, we succeeded in generating hematopoietic cells from wt and gene-corrected iPSc, including myeloid cells and early progenitors able to give rise to multipotent hematopoietic colonies.

4.4 Differentiation into osteoclasts

We next tested the ability of wt and gene-corrected iPSc to differentiate into osteoclasts, the relevant cells for the ARO treatment.

At the end of the hematopoietic differentiation period, $CD45^+$ cells were purified by immunomagnetic beads in order to enrich for the osteoclast precursors and eliminate non-hematopoietic cells that also developed during the process. Purified hematopoietic cells were cultured in presence of M-CSF and SCF to stimulate the proliferation of progenitor cells and push monocytes differentiation. Six days later RANKL was added, the cytokine necessary for the fusion of pre-osteoclasts and activation of mature osteoclasts (Fig.20).

Osteoclasts are giant multinucleated cells with a great number of vacuoles and lysosomes. The region of attachment, the sealing zone, is characterized by the presence of a ring composed of F-actin filaments (actin ring) (§1.6.1). At the appearance of osteoclast-like cells in culture, after careful observation under a phase-contrast inverted microscope (Fig.21A), their identity was confirmed by the count of the nuclei (>3), the presence of the actin ring and the expression of TRAP (Fig.21B, C), a lysosomal enzyme required for osteoclast functionality. These markers indicate the correct differentiation towards osteoclasts. As a control, iPSc derived cells were cultured in absence of RANKL and, as expected, they did not form osteoclasts (Fig.21D).

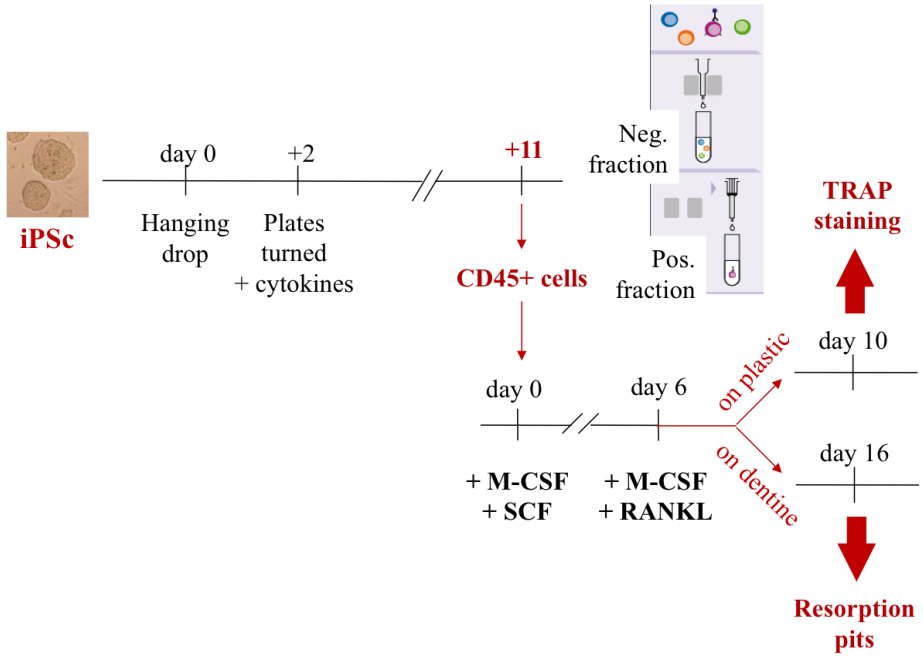

Fig.20. Scheme of the osteoclast differentiation protocol. At day 11 of the hematopoietic differentiation protocol, $CD45^+$ cells were purified by immunomagnetic beads and plated in presence of M-CSF and SCF. After six days, SCF was replaced by RANKL and cultures continued on plates or on dentine slides. In the first case, at day 10 from the purification of $CD45^+$ cells, cultured cells were stained to evaluate TRAP expression. In the second case, cells were cultured on dentine slides until day 16, when substrates were stained to verify the presence of resorption pits.

To test the resorption activity of obtained osteoclasts, a fraction of the cells was cultured on dentine discs, which were subsequently stained with toluidine blue to highlight the formation of resorption pits (Fig.21E).

All the tested iPS clones gave rise to osteoclasts in culture, which were comparable to those obtained starting from mouse bone marrow or spleen (Fig.21C). As expected, wt iPSc derived osteoclasts were able to resorb dentine, while *oc/oc* iPSc derived osteoclasts failed to form resorption pits due to the lack of the TCIRG1 protein into the acidification proton pump (Fig.21E). Our first attempt to generate corrected iPSc functionally able to resorb bone was unsuccessful (data not shown). Since it is known that the presence of the neomycin cassette may interfere with the transgene protein production (Scacheri et al, 2001), we decided to eliminate the antibiotic resistance from the corrected genomic region. Therefore, gene-corrected iPSc were transiently transfected with the Flp recombinase to excise the neomycin resistance cassette flanked by FRT sites. After subcloning, cellular clones that lost the resistance ability against the antibiotic were selected (iPSc #13.62.18.22). They were subsequently differentiated into osteoclasts and seeded on dentine slices, in which a fully restored capacity to resorb the substrate was observed, demonstrating the successful gene correction of *oc/oc* iPSc (Fig.21E).

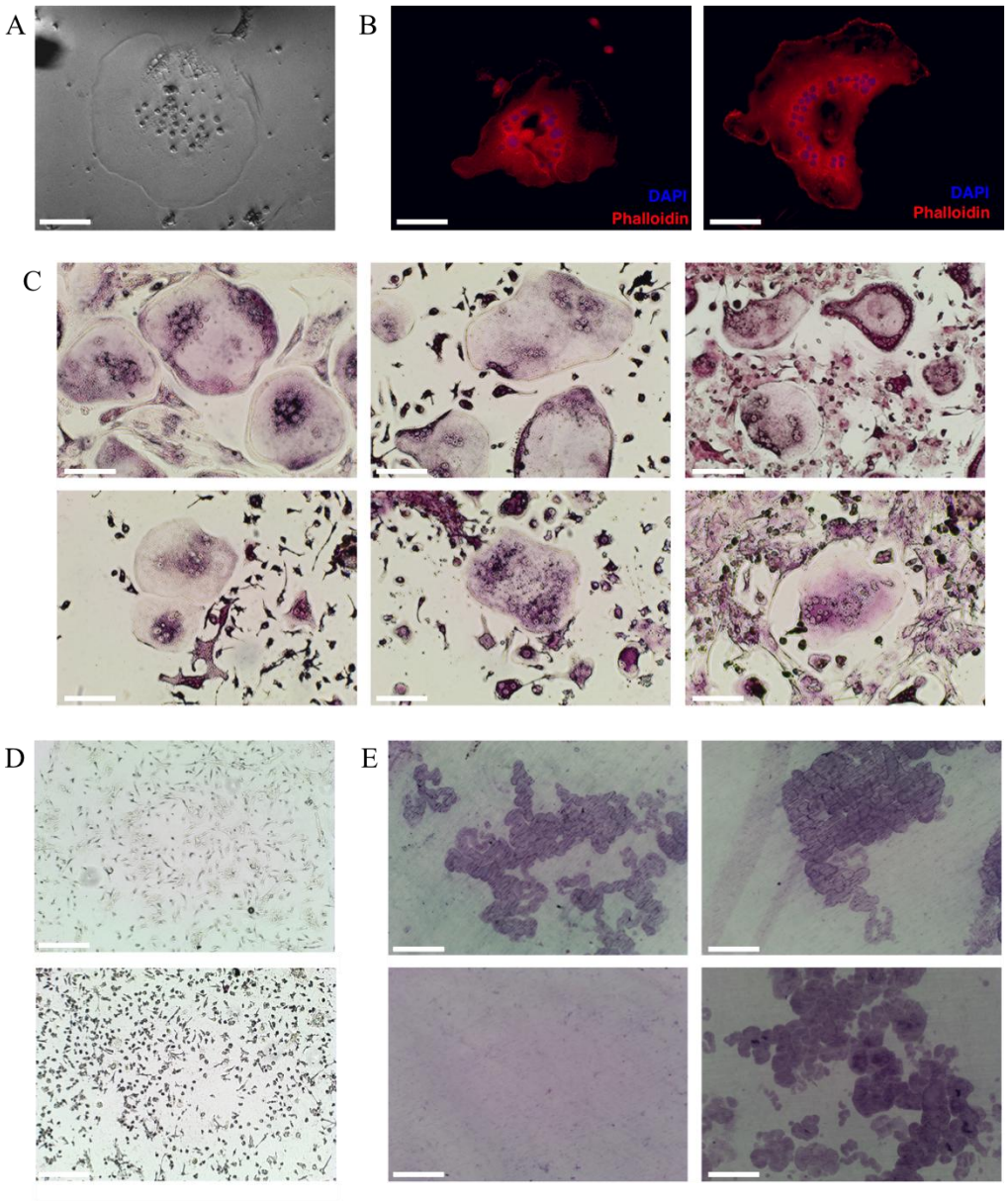

Fig.21. Osteoclasts formation and resorption pits from iPS clones. (A) Bright field representative image of an osteoclast in culture (20X magnification, scale bars = 50 μm). (B) Representative examples of immunofluorescence of phalloidin highlighting the actin ring (20X magnification, scale bars = 50 μm). (C) Representative TRAP staining of osteoclasts. In the first line they derive from wt iPSc #6.25.68 (left panel), wt spleen cells (middle panel), and wt bone marrow cells (right panel). In the second line they derive from *oc/oc* iPSc #13.62 (left panel), *oc/oc* spleen cells (middle panel), and iPSc #13.62.18-BAC after the flippase step (right panel). All the images are at 10X magnification, scale bars = 100 μm. (D) Representative images of TRAP staining of the cell culture without the presence of RANKL from wt bone marrow cells (upper panel) and wt iPSc #6.25.68 (lower panel). All the images are at 4X magnification, scale bars = 200 μm. (E) Representative images of resorption pits in dentine discs stained by toluidine blue. In the first line they derive from wt iPSc #6.25.68 (left panel) and wt bone marrow cells (right panel). In the second line they derive from *oc/oc* iPSc #13.62 (left panel) and iPSc #13.62.18-BAC after the flippase step (right panel). All the images are at 10X magnification, scale bars = 100 μm.

In conclusion, we were able to differentiate iPSc into very specialized cells such as osteoclasts, demonstrating also their functionality by the resorption pits assay. Moreover, *oc/oc* derived iPSc generated non-functional osteoclasts as cells derived from *oc/oc* mice. Upon gene-correction, *oc/oc*

iPSc become equally able to efficiently resorb dentine, demonstrating their fully functional correction.

4.5 *In vivo* experiments

We then moved from *in vitro* experiments to *in vivo* reconstitution assays, to test whether iPSc derived differentiated cells could give rise to HSCs able of life-long self-renewal and leading to rescue the *oc/oc* phenotype. To this end, we used the *oc/oc* strain as recipient of the transplant. This *in vivo* model allowed the evaluation of the engraftment capacity of *in vitro* iPS differentiated cells, their viability and persistence during the life, and their ability to differentiate *in vivo* into functional osteoclasts rescuing the bone phenotype.

To set up and optimize the *in vivo* transplantation experiments with iPSc, wt bone marrow cells were first used as positive control. We chose donor and recipient mice mismatched for CD45.1 and CD45.2 isoforms to track the donor derived hematopoietic cells. CD45.1 wt mice were chosen as donor and CD45.2 *oc/oc* strain was kept as recipient. Due to the very short life span of homozygous affected mice, we routinely maintain this strain by inter-crossing heterozygous mice.

Osteopetrotic defects occur early in life, even before birth. The transplantation can rescue only bone defects, while secondary neurological defects, such as hearing and visual loss due to cranial nerve compression, can only be prevented. Therefore the earliest the transplant, the best is the chance of recovery (§1.6.4). Previous studies have proposed an approach to prevent the onset of the disease before birth by performing HSC transplantation directly into the uterus (Frattini et al, 2005, Tondelli et al, 2009). These studies demonstrated the therapeutic efficacy and feasibility of this approach.

4.5.1 *In utero* transplantations

4.5.1.1 Set up of the technique with wt bone marrow cells

To test the *in utero* transplantation technique and evaluate the minimal amount of donor cells needed to obtain a rescue of the osteopetrotic phenotype, transplantations with an increasing number of wt bone marrow cells were performed. wt CD45.1 bone marrow cells were transplanted into the liver of embryos in anesthetized CD45.2 heterozygous pregnant females at 13.5 days *post coitum*, mated with heterozygous male mice. Animals did not receive any conditioning, as described in Frattini et al, 2005. At birth, newborns were genotyped and transplanted *oc/oc* mice were monitored for viability and health status. Starting from about 4 weeks after birth we checked the engraftment level by FACS analysis performed on peripheral blood. $1x10^6$ wt bone marrow cells

per embryo were initially transplanted, subsequently the number of transplanted cells was increased accordingly to Tab.6 until we obtained an *oc/oc* mouse with the rescue of the phenotype. The success of *in utero* transplantation depends on various factors: number and viability of the embryos, delivery of the cells to the fetal liver, outcome of the surgical operation, post-natal mother care, presence of *oc/oc* pups among the litter, reaching the sufficient number of transplanted cells to obtain a result. As highlighted by Tab.6, we faced all these issues. In case of wt and heterozygous mice, not showing any bone defect, we evaluated only the engraftment.

Pregnant females	Transplanted embryos	Transplanted cells/embryo	Born mice	Alive mice after P4	Engraftment/ phenotype rescue
3	15	$1x10^6$	6 (1 *oc/oc*)	3 (0 *oc/oc*)	0
4	33	$5x10^6$	20 (4 *oc/oc*)	2 (0 *oc/oc*)	1
2	15	$7x10^6$	7 (2 *oc/oc*)	7 (2 *oc/oc*)	0
1	8	$8x10^6$	4 (2 *oc/oc*)	4 (2 *oc/oc*)	1 *oc/oc*

Tab.6. Summary of *in utero* transplantations performed with wt bone marrow cells. Columns indicate the number of pregnant females operated, transplanted embryos, transplanted cells per embryo, resulting born mice, mice survived after 4 days from birth and mice which showed engraftment or rescue of the phenotype.

In the successful experiment, we transplanted $8x10^6$ cells. We observed the survival of an *oc/oc* mouse that was sacrificed at 8 months and analyzed for the engraftment. Any growth retardation was observed during its life. Periodical FACS analyses on peripheral blood were performed to evaluate the engraftment level. At 5 weeks after the transplantation, 29% of donor cells was found and the level gradually decreased until 7% at 26 weeks (Fig.22).

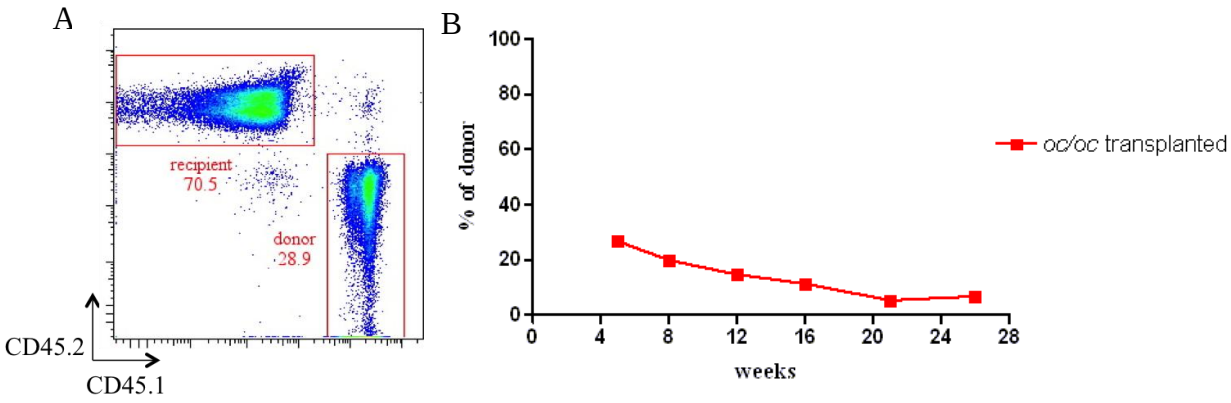

Fig.22. Evaluation of wt donor cells engraftment in transplanted *oc/oc* mouse. (A) Representative FACS plot showing the percentage of donor cells in the peripheral blood of the *oc/oc* recipient at 5 weeks. (B) Analysis of the percentage of wt donor cells in the transplanted *oc/oc* mouse evaluated by cytofluorimetric analyses from 5 to 26 weeks post-transplantation.

Eight months after birth the mouse was sacrificed to assess the engraftment level also in

hematopoietic organs and analyze the resorption activity of donor cells derived osteoclasts in the bone. By cytofluorimetric analyses the percentage of donor cells into the bone marrow, spleen and thymus was evaluated. Despite the low chimerism at the sacrifice, 7% in bone marrow, 5% in spleen and 2% in thymus (Fig.23), donor cells were sufficient to allow bone remodeling in the *oc/oc* mouse, which was more similar to those of a wild type than those of an osteopetrotic mouse (Fig.24).

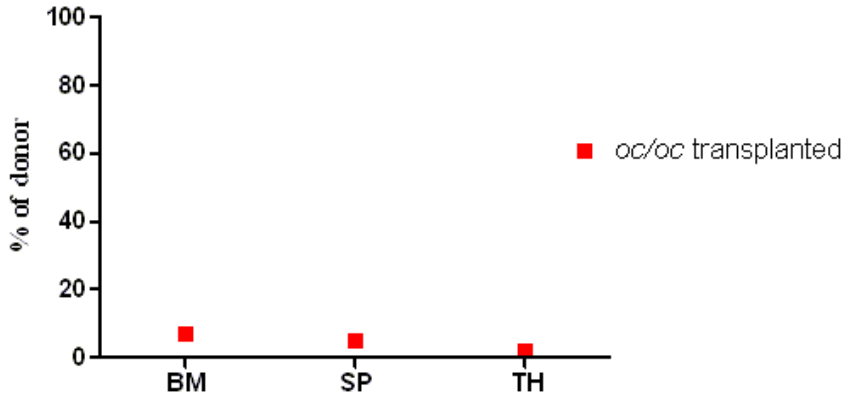

Fig.23. Engraftment of wt donor cells in the hematopoietic organs. Percentage of donor cells in bone marrow (BM), spleen (SP) and thymus (TH) at the sacrifice, evaluated by cytofluorimetric analyses.

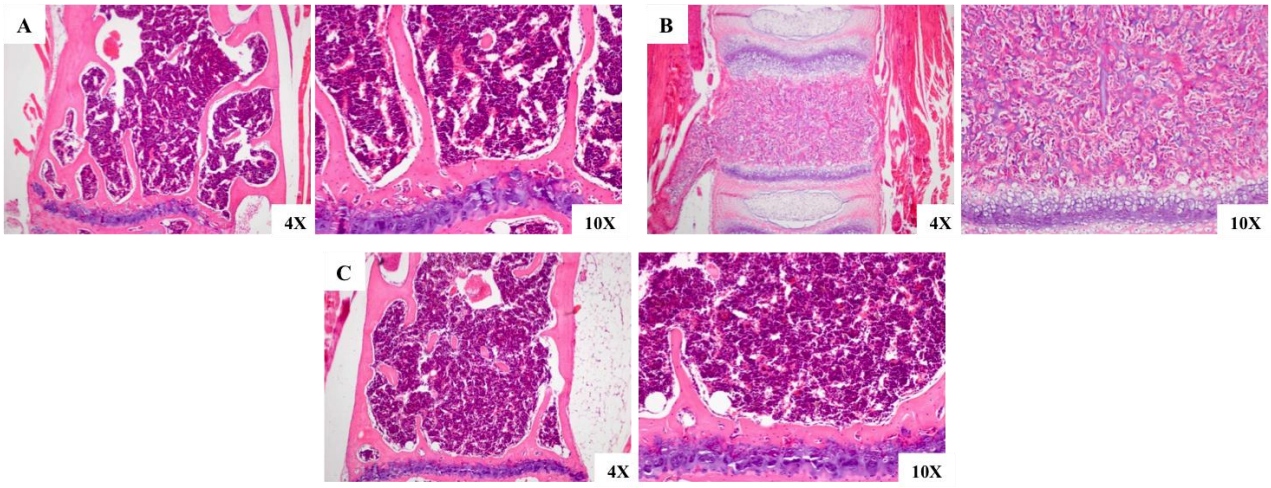

Fig.24. Morphological analyses of vertebrae. Hematoxylin and eosin staining of the vertebrae from (A) an untreated age-matched wt, (B) an untreated *oc/oc* mouse at 16 days, (C) the transplanted *oc/oc* at the sacrifice.

Moreover, the level of calcium in the serum of the *oc/oc* transplanted mouse was analyzed. This is a relevant parameter indicating osteoclasts resorption activity. In mice, values less than 2 mmol/L indicate ipocalcemia, typical condition of the *oc/oc* untreated mice. In our experiment, transplanted *oc/oc* showed a normal level of calcium at the sacrifice, indicating again the rescue of the bone phenotype (Fig.25).

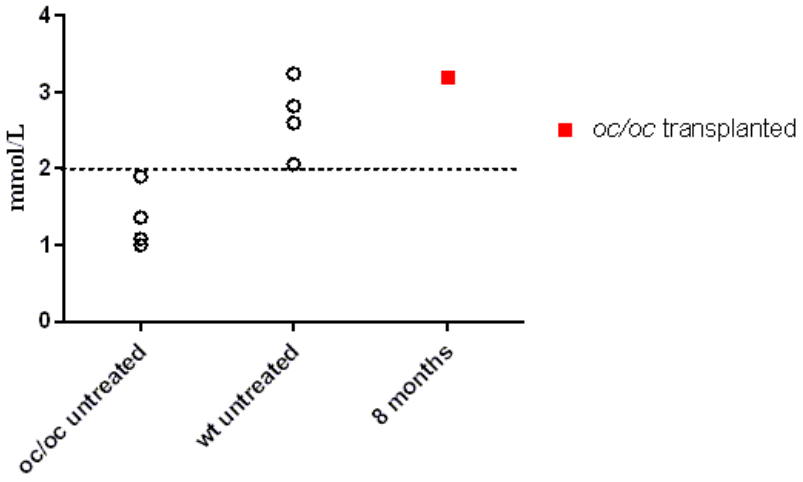

Fig.25. Serum calcium level. Analysis of calcium levels in the sera of different mice: *oc/oc* untreated (left column), wt untreated (middle column), and transplanted *oc/oc* mouse at the sacrifice (right column).

4.5.1.2 *In utero* transplantations using iPSc derived cells

For applying the tested protocol to iPSc derived cells, we started transplanting wt iPSc derived hematopoietic cells at the end of the differentiation period, synchronising the pregnancy of heterozygous females to reach 13.5 days *post coitum* on day 8 or 12 of the culture (Fig.26A). Differentiated hematopoietic cells were isolated by flow cytometry, sorting a population expressing the hematopoietic markers CD41 and/or CD45 and lacking SSEA1, the stemness marker expressed by undifferentiated iPSc (Fig.26B).

A

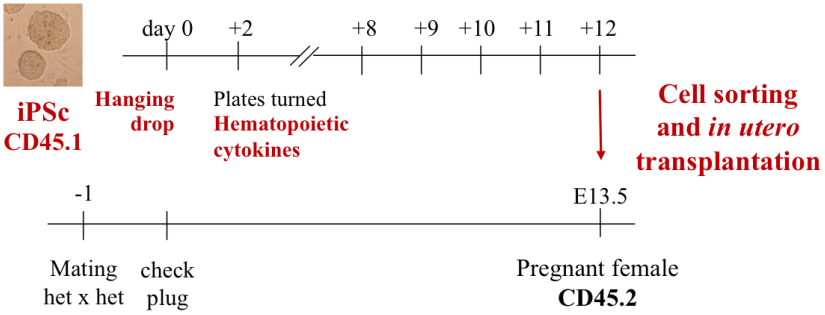

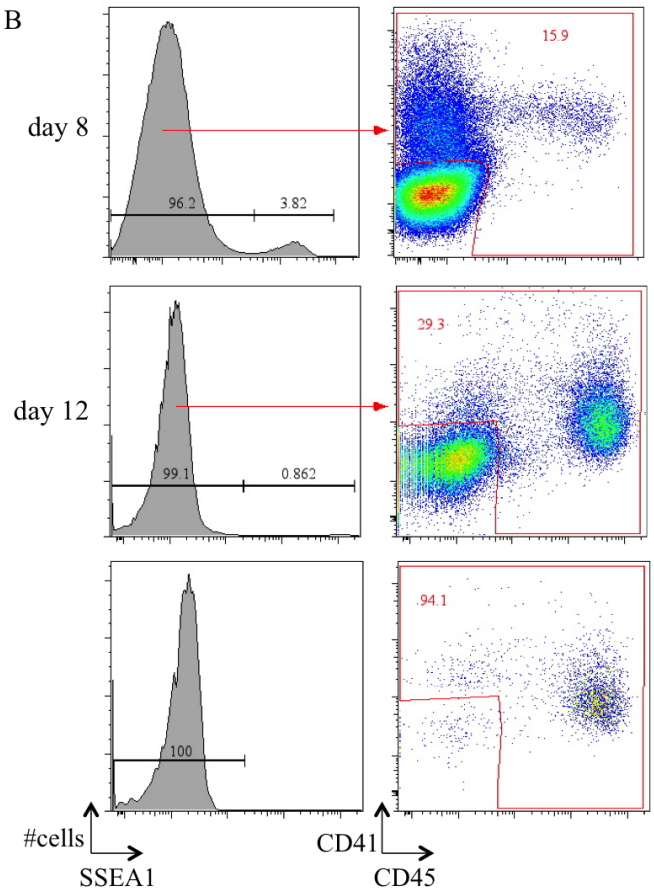

Fig.26. Scheme of the *in utero* transplantation protocol. (A) We synchronised the pregnancy of CD45.2 heterozygous females to reach 13.5 days *post coitum* on day 12 of the hematopoietic differentiation protocol. Then we collected CD45.1 hematopoietic cells from the *in vitro* culture, sorted and transplanted into the liver of the embryos, allowing the females to deliver pups after a week. In this scheme the transplantation is performed using cells obtained at day 12 of culture, similarly *in utero* transplantations were also performed with donor cells obtained at day 8 of the culture. (B) Flow sorting strategy to isolate hematopoietic cells used in the transplant. Gated on SSEA1$^-$ cells, CD41$^+$ and/or CD45$^+$ were selected. Representative plots indicating cells at day 8 of culture (upper panel) and day 12 of culture (middle panel). The last panel indicates a representative plot of the purity of the cells (lower panel).

Cells obtained either at day 8 or day 12 of culture were transplanted, since they may represent two different developmental stages, with more immature or more differentiated hematopoietic cells, respectively. Moreover, we tested the hypothesis that transplantation in fetal liver could allow the differentiation into hematopoietic cells directly *in vivo*, completing the specification started *in vitro*. We transplanted a number of cells ranging from $1x10^4$ cells up to $4.5x10^5$ cells per embryo, without knowing their genotype in advance (Tab.7). Despite we transplanted 101 embryos, our attempts were not successful, since we could analyze only 5 post-natal mice, of which only 1 *oc/oc*. In fact, unfortunately in all cases we had problems with the survival of either the females or the embryos (only 25 born mice), with high frequency of perinatal mortality (only 5 mice survived after P4) and also with the paucity of homozygous mutant mice in the progeny (Tab.7). In the few mice analyzed, we never observed engraftment of donor cells or rescue of the osteopetrotic phenotype.

Pregnant females	Transplanted embryos	Transplanted cells/embryo	Born mice	Alive mice after P4	Engraftment/ phenotype rescue
2	17	$1x10^4$	1 *oc/oc*	0	0
1	7	$2x10^4$	7 (4 *oc/oc*)	3 (1 *oc/oc*)	0
1	9	$5x10^4$	7	0	0
1	10	$9x10^4$	0	0	0
3	25	$1.5x10^5$	0	0	0
1	9	$2x10^5$	0	0	0
2	15	$3.5x10^5$	3	0	0
1	9	$4.5x10^5$	7	2	0

Tab.7. Summary of *in utero* transplantations performed with wt iPSc derived cells. Columns indicate the number of pregnant females operated, transplanted embryos, transplanted cells per embryo, resulting born mice, mice survived after 4 days from birth and mice which showed engraftment or rescue of the phenotype.

The positive control was represented by the transplant in which $8x10^6$ wt bone marrow cells were used. Based on these findings, we concluded that the number of wt iPSc derived hematopoietic cells was not sufficient to induce any effect in transplanted mice. We cannot draw any conclusions on the *in vivo* functionality of iPSc derived cells. As a result, we cannot compare the two methods and we cannot conclude the *in vivo* lack of functionality of iPSc derived cells. Due to technical limitations, we were unable to successfully scale-up the culture in order to obtain a higher number of cells. Based on this technical limitation, we decided to exploit another route for the transplantation.

4.5.2 Neonatal transplantations

4.5.2.1 Set up of the technique with wt bone marrow cells

As an alternative strategy post-natal transplantation was tested, to avoid critical issues of *in utero* transplantation technique, especially the need to distribute donor cells among all the embryos, since it is not possible knowing their genotype before.

Starting from wt bone marrow cells to set up a positive control, we decided to transplant 2-3 days old new-born *oc/oc* mice, performing the genotype on tail biopsies the day after birth, rather than 2-3 weeks old *oc/oc* mice because of the necessity to correct the defects as early as possible. The same amount of wt bone marrow cells used for the successful *in utero* transplantation was injected ($8x10^6$ cells). Injection directly into the liver was first tested, since it remains a hematopoietic site for few days after birth, with or without irradiating the neonates. However, the analysis of transplanted mice showed insufficient engraftment in the bone marrow (Tab.8 and data not shown). Then transplantation in the temporal vein was performed, allowing the cells to reach hematopoietic niches through the blood circulation. This technique gave the best rate of success. Treated mice receiving transplant in the absence of conditioning failed to engraft or did not reach long-term persistence, while irradiated mice showed high percentages of donor cells in the peripheral blood,

belonging to all different hematopoietic subpopulations (Fig.27A). Of note, three *oc/oc* mice showed rescue of the phenotype (Tab.8). The level of donor cells was monitored by periodical peripheral blood analysis. At 4 weeks after the transplantation, all the mice showed a range of donor cells from 79% to 92% apart from a heterozygous mouse showing 51% of engraftment and another control mouse without donor cells in the peripheral blood (Fig.27B). Importantly, the values remained stable until the sacrifice performed at 5 months and the presence of donor cells several weeks after transplant indicated that HSCs successfully engrafted.

Transplanted mice	Irradiation	Route of delivery	Alive mice after P4	Engraftment/ phenotype rescue
8	not performed	into the liver	8	0
7	400 RAD	into the liver	7	1
7	not performed	in temporal vein	7	4 short-term
7 (3 *oc/oc*)	400 RAD	in temporal vein	7 (3 *oc/oc*)	6 (3 *oc/oc*)

Tab.8. Summary of neonatal transplantations performed with wt bone marrow cells. Columns indicate the number of transplanted mice, conditioning regiment, route of delivery of the cells, number of mice survived after 4 days from birth and mice which showed engraftment or rescue of the phenotype.

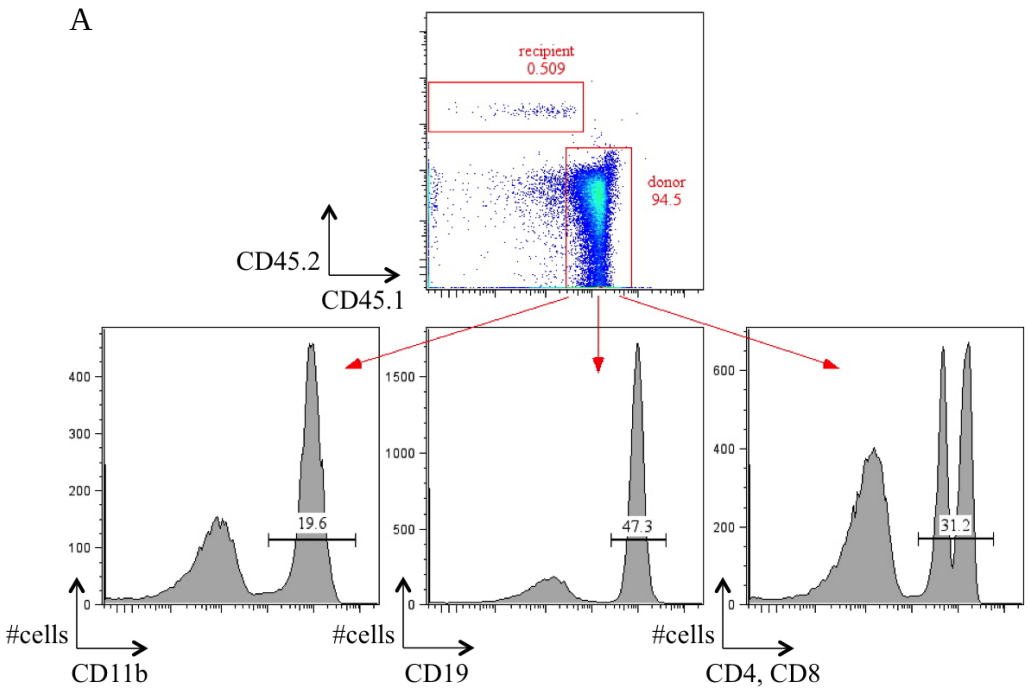

B

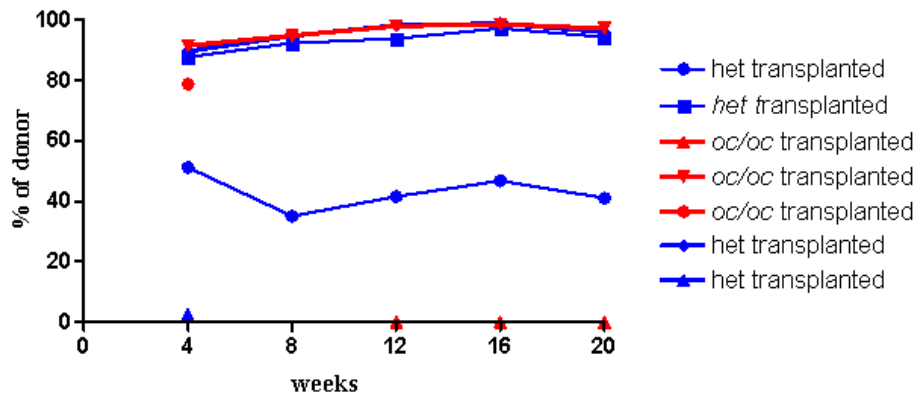

Fig.27. Evaluation of wt donor cells engraftment in transplanted mice. (A) Representative FACS plot showing the percentage of CD45.1^{+} cells in the peripheral blood of the *oc/oc* recipient at 20 weeks post-transplantation and contribution of these cells to all subpopulations: myeloid cells (left panel), B cells (middle panel), and T cells (right panel). (B) Analysis of the percentage of wt donor cells in transplanted mice evaluated by cytofluorimetric analyses from 4 to 20 weeks post-transplantation.

Interestingly, we observed an *oc/oc* mouse with neurological problems, hydrocephalus and visual impairment, which was sacrificed, together with a control mouse, at 47 days from the transplantation due to its poor health status. The engraftment level in hematopoietic organs (bone marrow, spleen, and thymus) was assessed by cytofluorimetric analysis. In the *oc/oc* mouse wt donor cells reached 97% in the bone marrow, 83% in spleen and 97% in thymus, while in the control mouse the transplantation did not worked and no donor cells were observed (Fig.28A). The resorption activity of osteoclasts in the bone was also analyzed, showing a complete rescue of the phenotype in the transplanted *oc/oc* (Fig.28B). This observation confirmed that, although the bone defect can be cured by the transplant, neurological alterations occurring during the first phases of the disease are not reversible.

Of note, we observed a long-term survival of a transplanted *oc/oc* mouse with no donor cells detectable in peripheral blood. The analysis in the peripheral blood started at week 12 after birth because of the very low body weight (<6gr) of the transplanted mouse. All the other time points did not reveal the presence of wt engrafted cells (Fig.27B). Nevertheless, the *oc/oc* mouse survived up to the sacrifice at 5 months indicating a rescue of the phenotype. Therefore we hypothesized the engraftment of short-term donor progenitor cells, which progressively exhausted during time, but were anyway enough to allow the rescue of the phenotype.

Five months after birth we sacrificed the mice to assess the engraftment level in hematopoietic organs and analyze the resorption activity of osteoclasts in the bone. The percentage of donor cells reached high values into the bone marrow (30-71%), spleen (26-96%) and thymus (27-100%). The *oc/oc* mouse previously mentioned was the exception, in fact it lacked donor cells in hematopoietic organs (Fig.29).

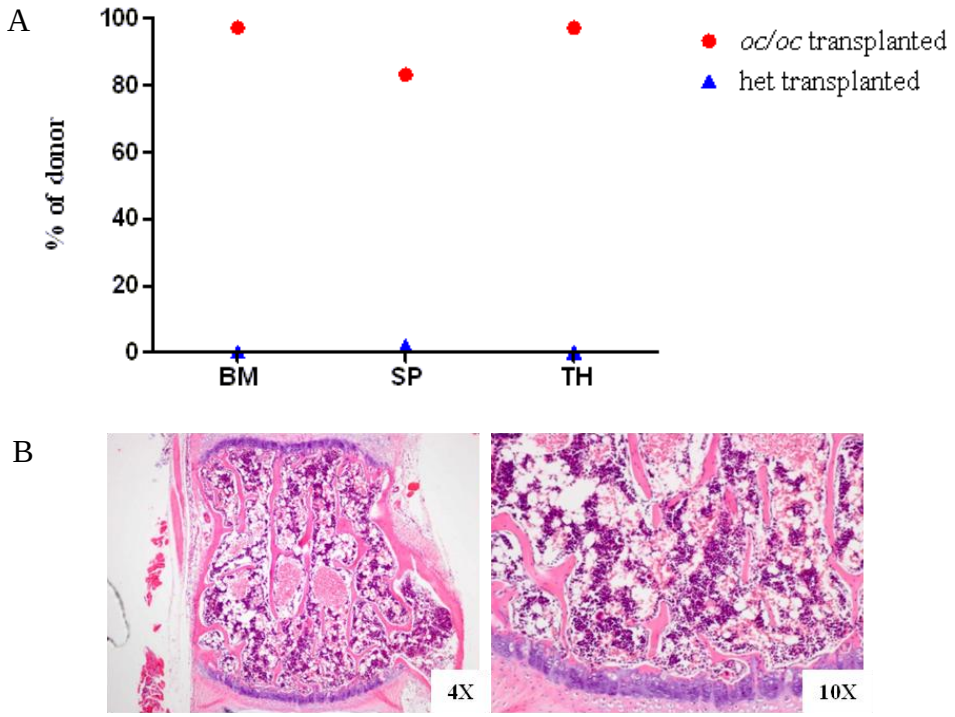

Fig.28. Analysis of transplanted mice organs at the sacrifice 47 days post-transplantation. (A) Percentage of donor cells in bone marrow (BM), spleen (SP) and thymus (TH) at the sacrifice, evaluated by cytofluorimetric analyses. (B) Hematoxylin and eosin staining of the vertebrae from the transplanted *oc/oc* at the sacrifice.

Donor cells differentiated *in vivo* into functional osteoclasts that remodeled *oc/oc* bones, resulting in a complete rescue of 1 *oc/oc* transplanted mouse and a partial rescue in the mutant mouse without long-term engraftment (Fig.30).

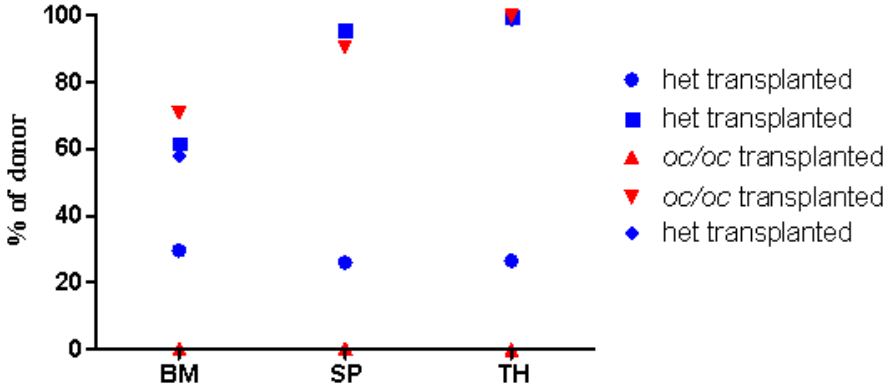

Fig.29. Presence of wt donor cells in the recipient organs. Percentage of donor cells in bone marrow (BM), spleen (SP) and thymus (TH) at the sacrifice evaluated by cytofluorimetric analyses.

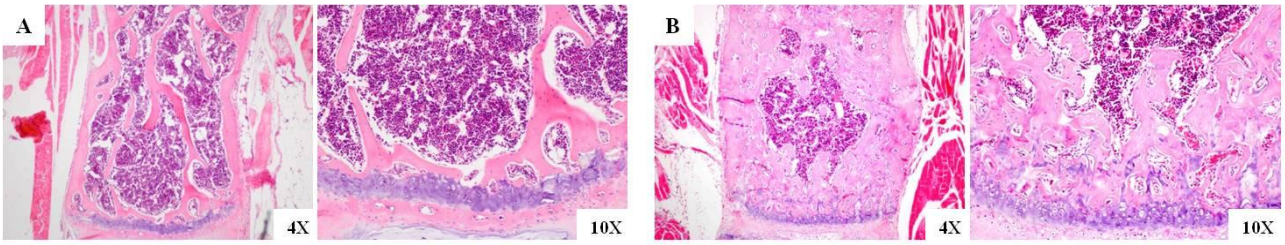

Fig.30. Morphological analyses of vertebrae. Hematoxylin and eosin staining of vertebrae from the transplanted *oc/oc* mice at the sacrifice showing a complete rescue of the phenotype (A) and only partial rescue for the *oc/oc* without long-term engraftment (B).

Furthermore, we analyzed the levels of calcium in the serum of transplanted *oc/oc* mice showing normal levels at the sacrifice, indicating once more the rescue of the phenotype (Fig.31).

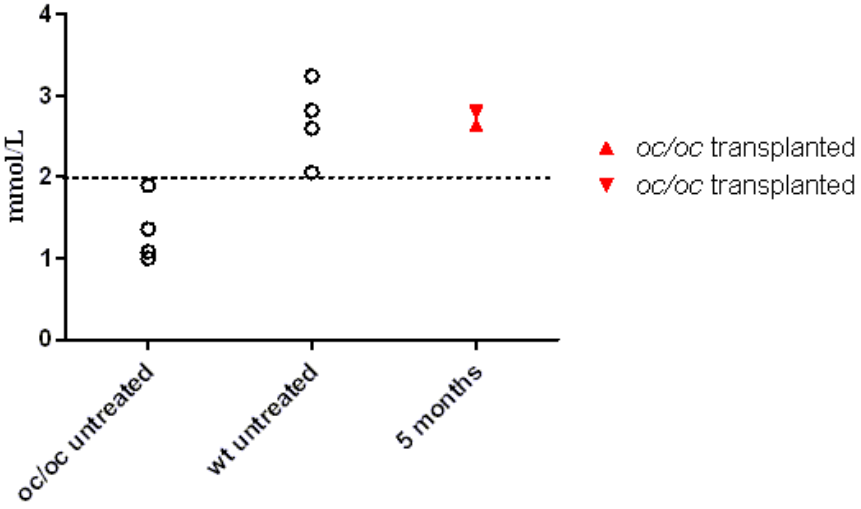

Fig.31. Serum calcium levels. Analysis of calcium levels in the sera of different mice: *oc/oc* untreated (first column), wt untreated (middle column) and transplanted *oc/oc* mice at the sacrifice (right column).

4.5.2.2. Neonatal transplantations using iPSc derived cells

As we demonstrated the feasibility and efficacy of the neonatal transplantation protocol in temporal vein using wt bone marrow cells, we evaluated the effect of the transplantation of iPSc derived hematopoietic cells in *oc/oc* new-born mice. We followed the neonatal transplantation protocol depicted in Fig.32. Donor cells were isolated following the flow sorting strategy indicated in Fig.26B.

We transplanted cells $1.6x10^5$ cells up to $3.7x10^6$ cells obtained at day 8 or day 12 of culture (Tab.9). Unfortunately, we did not detect donor cells in the recipients and indeed the *oc/oc* treated mice died soon indicating the failure of the transplantation. Since we could not transplant an amount of iPSc derived cells comparable to the number of wt positive control ($8x10^6$ cells), we could not compare these experiments to those performed with wt cells.

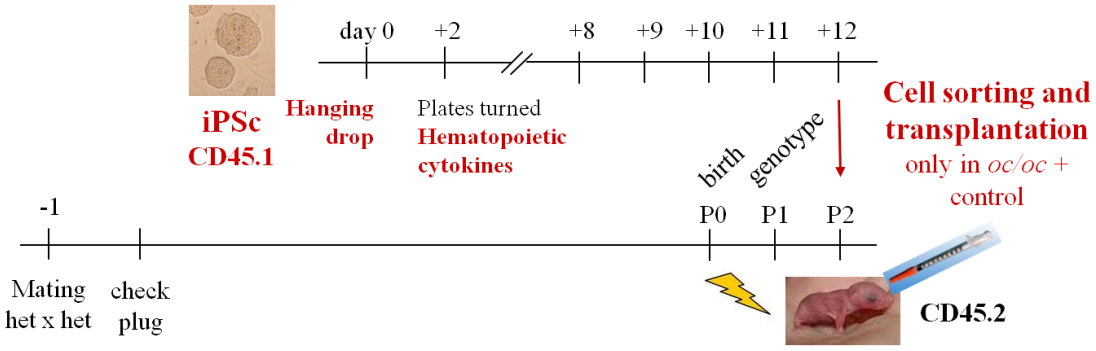

Fig.32. Scheme of the neonatal transplantation protocol. We synchronise the birth of pups with the achievement of differentiated cells obtained at day 12. Mice were genotyped the day after birth in order to select the mutant mice among the wild type and the heterozygous ones. Then we collected CD45.1 hematopoietic cells from the *in vitro* culture and transplanted only into affected and their control mice after radiation. In this scheme the transplantation was performed at day 12 of culture, a similar scheme was followed for transplantation at day 8 of culture.

We transplanted too few iPSc derived cells to exclude *a priori* the possibility that if present in an adequate number, they are able to rescue the osteopetrotic phenotype, but presently, with our settings, we are not able to increase this number. We speculate that the low number of iPSc derived cells, due to the technical limit to expand and obtain large amount of hematopoietic progenitors, is responsible of the lack of bone phenotype rescue.

Transplanted mice	Transplanted cells/embryo	Alive mice after P4	Engraftment/ phenotype rescue
7 (1 *oc/oc*)	$1.6x10^5$	6 (0 *oc/oc*)	0
1	$2x10^5$	1	0
10	$2.5x10^5$	9	0
2 (1 *oc/oc*)	$5x10^5$	2 (1 *oc/oc*)	0
4 (2 *oc/oc*)	$9x10^5$	1	0
1 *oc/oc*	$1x10^6$	1 *oc/oc*	0
1 *oc/oc*	$3.7x10^6$	1 *oc/oc*	0

Tab.9. Summary of neonatal transplantations performed with iPSc derived cells. Columns indicate the number of transplanted mice, number of mice survived after 4 days from birth and mice which showed engraftment or rescue of the phenotype.

Thus, the *in vivo* experiments indicate that despite the successful *in vitro* differentiation into the hematopoietic lineage including production of functional osteoclasts, further improvements of the culture conditions are needed to increase the number of cells necessary to test the *in vivo* functionality of differentiated iPSc.

5 Discussion

ARO is a rare life-threatening condition caused by a defect in the resorbing activity of osteoclasts. The most frequently mutated gene is TCIRG1, encoding for a subunit of the V-ATPase pump responsible for the acidification of the bone environment indispensable for the resorption activity of osteoclasts. The disease has as unique possible treatment HSC transplantation, since osteoclasts derive from myeloid precursors belonging to the hematopoietic lineage (Sobacchi et al, 2013). However, this treatment presents several difficulties, first of all the need for a matched donor. Only few patients have access to HLA-identical or HLA-matched unrelated donors, who ensure the best 5-year disease-free survival rate estimated at 88% and 80%, respectively (Schulz, 2013). On the other hand, this rate is evaluated only at 66% for patients transplanted with HLA-haploidentical donor cells. Engraftment complications are the most frequent cause of death and still patients treated after the age of 10 months frequently underwent serious complications (Schulz, 2013). During the years the outcome has greatly improved, since about a decade ago the success percentage was about 73% using HLA-identical donors, while with HLA-related donors was about 43% (Driessen et al, 2003). Moreover, secondary defects, such as hearing and visual loss due to cranial nerve compression can be prevented by transplantation, but not reversed once they have occurred.

Alternative strategies have been tested, such as T-cell depleted HSCs from HLA-haploidentical donors or cord blood from unrelated donors (Schulz et al, 2002), but severe problems were recurrently observed including rejection, delayed hematopoietic reconstitution, venous occlusive disease, pulmonary hypertension, and hypercalcemic crisis (Steward et al, 2004).

For these reasons, we have focused on corrected autologous HSCs as a novel approach to therapy. Autologous HSCs gene therapy represents an emerging therapeutic opportunity to avoid issues linked to the requirement of compatible donors and to the side effects caused by conditioning regimen, thus reducing the morbidity and mortality of the transplant. However, genetic manipulations of HSCs are difficult: they cannot be maintained in culture for long time, they are very slowly dividing cells and need cytokine pre-stimulation to induce cell proliferation with the risk to modify their characteristics (Baum et al, 2003). Moreover, they show low rate of homologous recombination and are difficult to be transfected (Waldman, 1992). As an alternative, iPSc represent an innovative source of donor cells. They are pluripotent stem cells derived from the reprogramming of somatic cells, so they have an easily accessible cell source, obtainable without invasive procedures. The feasibility to perform gene targeting is greater, for their tolerance to

homologous recombination, they are easily transfected, can be selected and expanded to obtain a homogeneous population in which 100% of the cells are genome edited.
Generation of iPSc from patients who do not have access to a HLA-identical donor could allow their site-specific genetic correction by homologous recombination, followed by differentiation towards hematopoietic progenitors and autologous transplantation.

In the present study, I have exploited iPSc as source of cells to treat ARO and to test the feasibility of gene-correction technology using as donor a BAC engineered vector. In particular, I show a step-by-step strategy by which gene-corrected osteopetrotic iPSc were used to generate hematopoietic progenitor cells able to give rise to functional osteoclasts, thus providing a proof of principle for an autologous cell therapy approach to treat ARO.

For the first time, iPSc from the osteopetrotic *oc/oc* mouse model were generated, together with iPSc from wt mouse. Their stemness and pluripotency were confirmed by immunofluorescence of expressed stemness markers (Oct4, Sox2, Nanog, SSEA1), and *in vitro* differentiated embryonic germ layers (mesoderm, endoderm and ectoderm) recognized by the expression of Brachyury, AFP and Nestin. Furthermore, we have demonstrated the *in vivo* generation of teratomas comprising the three germ layers by hematoxylin and eosin staining. The use of a self-inactivating lentiviral vector for reprogramming lowered the risk to influence the expression of genes adjacent to the viral insertion site, thus increasing safety. Furthermore, c-Myc was eliminated from the reprogramming factors list, to avoid problems related to its tumorigenic activity. The vector carries also two loxP sites in the LTRs to guide the recombination activity of the transiently expressed Cre recombinase, which mediates the excision of the vector sequences from the host genome. We selected only iPS clones in which the reprogramming vector was completely eliminated. Moreover, we chose iPSc with normal karyotype.

The next step was the correction of iPS osteopetrotic clones by replacing the mutated gene with an engineered BAC system. Taking advantage of the large genomic region carried by this vector, the entire correct form of *Tcirg1* gene was placed in, restoring the large mutation that causes the phenotype. Long arms up- and down-stream the gene, comprising the regulatory sequences, were added, to guarantee the correct expression of the gene and strongly support the homologous recombination process. In fact the larger homology sequences are included in the vector, the best efficiency of homologous recombination is reached. It was necessary to select the clones in which insertion of the full *Tcirg1* gene had occurred, by specific PCR and RT-PCR analysis that assess the

presence and the expression of the gene. Moreover, specific analysis was performed in order to detect potential backbone sequences (HIS3 and CM(R)) left into the genome, signs of non-homologous recombination. FISH assays were conducted to verify the correct position of the inserted gene into the genome in a sub-centromeric position of the chromosome 19. The correction likely happens in heterozygosis due to the rare occurrence of the homologous recombination event. Anyhow, this should be sufficient to correct the cellular phenotype, since heterozygous mice and humans are not affected by the disease.

As the aim was to evaluate the ability of wt and *oc/oc* corrected iPSc to form functional osteoclasts, a protocol for the hematopoietic differentiation was first set up, to obtain myeloid precursors of osteoclasts. Various differentiation protocols have been described to obtain *in vitro* the hematopoietic lineage, but the only ones which provide long-term stem cells utilize the over-expression of additional transcription factors, such as Hoxb4, Lhx2, or the combination of Gata2, Gfi1b, cFos, and Etv6 (Kyba et al, 2002, Kitajima et al, 2011, Pereira et al, 2013). This represents an additional manipulation and requires the use of integrating vectors for the stable expression of transgenes, while several efforts have been made during time to circumvent non-targeted, potentially dangerous genetic manipulations. We decided to avoid the over-expression of supplementary transgenes, to induce differentiation in more physiological conditions. The EBs method was chosen, in conjugation of a hematopoietic cytokines cocktail that first induces the mesoderm development at the expense of the other two germ layers, and then pushes towards the hematopoietic specification, likely through a hemogenic endothelium intermediate, in order to obtain a robust stem/progenitor fraction.

After about a week of culture we obtained cardiomyocyte-like cells characterized by a rhythmic beat, demonstrating the presence of mesodermal cells derived from iPSc. At the end of the differentiation period we succeeded in generating hematopoietic cells expressing the pan-hematopoietic marker CD45 and/or the CD41 antigen, present on primitive hematopoietic cells. Time-course experiments were performed to identify the day of the culture in which hematopoietic cells reach the highest possible proportion. They revealed a kinetics resembling the physiological one, with $CD41^+$ cells decreasing throughout time, gradually giving rise to mature $CD45^+$ cells. This trend was shown also by BAC-corrected iPSc. Among the mature cells, myeloid cells were predominantly obtained, the ones we need to test the functionality of corrected *oc/oc* derived iPSc, since osteoclasts derive from myeloid progenitors. Early progenitors were also obtained, negative for the myeloid marker CD11b and expressing c-Kit and Sca1, markers of immature cells.

Moreover, c-Kit$^+$ cells were able to give rise to erythroid, myeloid and mixed hematopoietic colonies, indicating the presence in culture of clonogenic multipotent or oligopotent progenitors.
At the end of the hematopoietic differentiation period a selective specification towards osteoclasts was induced adding to the culture medium the cytokines M-CSF, SCF and finally RANKL. Osteoclasts similar to the ones produced from wt bone marrow and spleen cells were obtained and they demonstrated their functionality by the resorption pits assay. *oc/oc* derived iPSc generated non-functional osteoclasts, as cells derived from *oc/oc* mice. Upon gene-correction, *oc/oc* iPSc become able to efficiently resorb dentine, demonstrating their fully functional correction. Interestingly, the cells became functional only after the excision of the neomycin resistance cassette inserted into the BAC to facilitate the selection of transfected clones. The excision was possible through the transient expression of the Flp recombinase, thanks to the presence of FRT sites flanking the cassette. Probably this sequence, even if placed in an intron, interfered with the correct expression of the *Tcirg1* gene (Scacheri et al, 2001).

We tried also to test the *in vivo* functionality of iPSc derived hematopoietic cells, to assess their capacity to engraft and rescue the osteopetrotic phenotype. The *oc/oc* mouse model was used as recipient of the transplantation. In this model the earliest the transplant, the best is the chance of recovery, because of irreversible damages occur early in life, even before birth. For this reason, the transplantation can rescue only bone defects, while neurological and secondary defects, such as hearing and visual loss due to cranial nerve compression, can only be prevented. On this basis, *in utero* transplantation represents the earliest time-point in which the administration of hematopoietic cells can prevent the onset of osteopetrotic signs (Frattini et al, 2005, Tondelli et al, 2009). However this technique, although feasible in humans, has several critical issues: operator's manual skills, number and viability of the embryos, delivery of the cells to the organ of injection (embryonic liver), outcome of the surgical operation, post-natal mother care, the presence of a limited number of *oc/oc* pups among the litter in which evaluate the rescue of the phenotype.
To set up and optimize the *in vivo* transplantation experiments with iPSc, wt bone marrow cells were first used as positive control. We gradually increased the number of transplanted cells until the achievement of a positive result. $8x10^6$ cells were necessary to observe the survival of an *oc/oc* mouse without any growth retardation and resulting in 26% of donor cells in the peripheral blood, which were maintained during its entire life, until the sacrifice at 8 months. Despite the low chimerism at the sacrifice (7% in bone marrow, 5% in spleen and 2% in thymus), wt donor cells were sufficient to allow the rescue of the phenotype of the *oc/oc* mouse, with long-term survival instead of 2-3 weeks of life span. In addition, the bones were successfully remodeled, showing

normal trabeculae with normal bone marrow cells inside, a very different situation respect to the osteopetrotic bone characterized by a "bone-in-bone" appearance without any bone marrow cells inside. The transplanted *oc/oc* mouse showed also a normal level of calcium at the sacrifice, indicating again the rescue of the bone remodeling activity by wt osteoclasts.

Unfortunately we did not reach the same results with iPSc derived hematopoietic cells. Cells obtained either at day 8 or day 12 of the hematopoietic differentiation protocol were transplanted, since they may represent two different developmental stages, with more immature or more differentiated hematopoietic cells, respectively. All stages of maturation were tested, since transplantation in fetal liver might allow the differentiation into hematopoietic cells directly *in vivo*, completing the specification started *in vitro* providing the correct microenvironment for the survival and differentiation. We isolated by cell sorting hematopoietic cells lacking the SSEA1, a marker of undifferentiated cells and expressing CD41 and/or CD45 antigens. We transplanted all the available cells, ranging from $1x10^4$ cells up to $4.5x10^5$ cells per embryo. In the few analyzable mice, we never observed engraftment of donor cells. Furthermore in the only evaluable *oc/oc* mouse we did not have rescue of the osteopetrotic phenotype. We had to face several issues related to the technique. We first had problems with the survival of either the pregnant females undergoing *in utero* procedures or the embryos. We also observed a high frequency of perinatal mortality and a scarcity of *oc/oc* mice in the progeny. Importantly, we transplanted too few iPSc derived cells for technical limit, thus not achieving the number of hematopoietic cells obtained from the wt bone marrow, preventing us to draw conclusions on the *in vivo* functionality of iPSc derived cells. We were unable to successfully scale-up the culture in order to obtain a higher number of cells. Moreover, because of the technical limitation of this technique we decided to test another method for the transplantation.

To circumvent the problems related to *in utero* transplantation and in particular to increase the number of transplanted cells without dividing the amount among all the embryos of a pregnant female, transplantations in post-natal mice were performed. In this way we could determine the mice genotype before the transplant and injected all the iPSc derived differentiated cells into the *oc/oc* host. In order to perform the transplant the earlier possible moment, we injected 2-3 days old new-born mice. Transplantations with wt bone marrow cells were first performed, to test the optimal route of delivery in mice. The same amount of wt bone marrow cells used for the successful *in utero* transplantation was injected. Injection directly into the liver was first tested with or without irradiation, since this organ remains a hematopoietic site for few days after birth. However, the analysis of transplanted mice showed insufficient engraftment. Probably liver traps the cells and do

not support enough their survival and homing to the other hematopoietic sites. Then transplantation in the temporal vein was performed, allowing the cells to reach hematopoietic niches through the blood circulation. Without irradiating recipient mice, transplanted cells failed at all the engraftment or did not reach long-term persistence. Hence, mice were sub-lethally irradiated before the transplant, based on the literature indications (Johansson et al, 2006). In one of the *oc/oc* mice transplanted in temporal vein post-irradiation we observed rescue of the phenotype with long-term survival, up to the sacrifice at 5 months post-transplantation, normal growth and high percentages of donor cells in the peripheral blood reaching 99%, even several weeks after transplant, belonging to all different hematopoietic subpopulations. It showed high levels of donor cells also at the sacrifice (71% in bone marrow, 91% in spleen and 100% in thymus) and normalization of the bone remodeling activity.

Interestingly, we observed an *oc/oc* transplanted mouse with a prolonged life span showing 79% of donor cells in the peripheral blood. Despite the engraftment, it showed neurological problems, hydrocephalus and visual impairment. So it was sacrificed at 47 days from the transplantation due to its poor health status. The high engraftment level was confirmed at the sacrifice in hematopoietic organs (97% in bone marrow, 83% in spleen and 97% in thymus), together with a complete rescue of the bone phenotype. This confirmed the possibility that neurological defects occurring early at the onset of the disease, cannot be rescued by the transplant, which can cure the bone defect.

We observed also long-term survival, up to 5 months, of a transplanted *oc/oc* mouse with no donor cells detectable in peripheral blood. Before week 12 it was not possible to analyze the peripheral blood because the body weight was too low and in all the other time points, comprised the sacrifice at 5 months, wt donor cells were not present. Nevertheless, the prolonged survival indicates that probably a short-term engraftment of donor progenitor cells had occurred, instead of HSCs. They initiated a bone remodeling activity that persisted also until the sacrifice, in which a partial rescue of the bone phenotype was evident, but they progressively exhausted during time. We can conclude that for the treatment of this disease transplant of HSCs is not strictly required, and that hematopoietic progenitors might be enough to produce a partial rescue, sufficient for a long-term result. Also in this case we did not reproduce these results with iPSc derived cells. We followed the previously applied flow sorting strategy to purify hematopoietic cells from the culture. Even if we tried to increase the number of transplanted cells, ranging from $1.6x10^5$ to $3.7x10^6$ cells, because of technical reasons we did not reach the amount of $8x10^6$ cells necessary to be curative. Thus, we hypothesize to have transplanted too few iPSc derived cells to exclude the possibility that they have the capacity to rescue the osteopetrotic phenotype. Unfortunately, the current laboratory technology does not allow to obtain such a high number of iPSc, unless using bioreactor technology. Although

we obtained successful differentiation *in vitro* into the hematopoietic lineage including production of functional osteoclasts, further improvements of the culture conditions to increase the number of obtained cells and their percentages in the culture are necessary to test the *in vivo* functionality of differentiated iPSc.

At the present day we were not able to reach *in vivo* results, however in literature there are no data showing the possibility to obtain transplantable HSCs from an iPSc culture without adding supplemental transgenes. In addition, for human cells, also the use of HoxB4 was not sufficient to obtain fully functional HSCs able to reconstitute a hematopoietic system. Despite all the efforts, the scientific community has not yet reached the goal to *in vitro* reproduce the complex microenvironment made of cells, cytokines and signals that sustains the correct HSCs development.

6 Bibliography

Adolfsson, J., O. J. Borge, D. Bryder, K. Theilgaard-Monch, I. Astrand-Grundstrom, E. Sitnicka, Y. Sasaki and S. E. Jacobsen (2001). "Upregulation of Flt3 expression within the bone marrow Lin(-)Sca1($^{+}$)c-kit($^{+}$) stem cell compartment is accompanied by loss of self-renewal capacity." Immunity 15(4): 659-669.

Aker, M., A. Rouvinski, S. Hashavia, A. Ta-Shma, A. Shaag, S. Zenvirt, S. Israel, M. Weintraub, A. Taraboulos, Z. Bar-Shavit and O. Elpeleg (2012). "An SNX10 mutation causes malignant osteopetrosis of infancy." J Med Genet 49(4): 221-226.

Alipio, Z., W. Liao, E. J. Roemer, M. Waner, L. M. Fink, D. C. Ward and Y. Ma (2010). "Reversal of hyperglycemia in diabetic mouse models using induced-pluripotent stem (iPS)-derived pancreatic beta-like cells." Proc Natl Acad Sci U S A 107(30): 13426-13431.

Anokye-Danso, F., C. M. Trivedi, D. Juhr, M. Gupta, Z. Cui, Y. Tian, Y. Zhang, W. Yang, P. J. Gruber, J. A. Epstein and E. E. Morrisey (2011). "Highly efficient miRNA-mediated reprogramming of mouse and human somatic cells to pluripotency." Cell Stem Cell 8(4): 376-388.

Antas, V. I., M. A. Al-Drees, A. J. Prudence, D. Sugiyama and S. T. Fraser (2013). "Hemogenic endothelium: a vessel for blood production." Int J Biochem Cell Biol 45(3): 692-695.

Ban, H., N. Nishishita, N. Fusaki, T. Tabata, K. Saeki, M. Shikamura, N. Takada, M. Inoue, M. Hasegawa, S. Kawamata and S. Nishikawa (2011). "Efficient generation of transgene-free human induced pluripotent stem cells (iPSCs) by temperature-sensitive Sendai virus vectors." Proc Natl Acad Sci U S A 108(34): 14234-14239.

Bar-Nur, O., J. Brumbaugh, C. Verheul, E. Apostolou, I. Pruteanu-Malinici, R. M. Walsh, S. Ramaswamy and K. Hochedlinger (2014). "Small molecules facilitate rapid and synchronous iPSC generation." Nat Methods 11(11): 1170-1176.

Baum, C., J. Dullmann, Z. Li, B. Fehse, J. Meyer, D. A. Williams and C. von Kalle (2003). "Side effects of retroviral gene transfer into hematopoietic stem cells." Blood 101(6): 2099-2114.

Bertrand, J. Y., S. Giroux, R. Golub, M. Klaine, A. Jalil, L. Boucontet, I. Godin and A. Cumano (2005). "Characterization of purified intraembryonic hematopoietic stem cells as a tool to define their site of origin." Proc Natl Acad Sci U S A 102(1): 134-139.

Blin-Wakkach, C., A. Wakkach, P. M. Sexton, N. Rochet and G. F. Carle (2004). "Hematological defects in the *oc/oc* mouse, a model of infantile malignant osteopetrosis." Leukemia 18(9): 1505-1511.

Boskey, A. L. (1989). "Noncollagenous matrix proteins and their role in mineralization." Bone Miner 6(2): 111-123.

Bradley, A., M. Evans, M. H. Kaufman and E. Robertson (1984). "Formation of germ-line chimeras from embryo-derived teratocarcinoma cell lines." Nature 309(5965): 255-256.

Burt, R. K., L. Verda, D. A. Kim, Y. Oyama, K. Luo and C. Link (2004). "Embryonic stem cells as an alternate marrow donor source: engraftment without graft-versus-host disease." J Exp Med 199(7): 895-904.

Calvi, L. M., G. B. Adams, K. W. Weibrecht, J. M. Weber, D. P. Olson, M. C. Knight, R. P. Martin, E. Schipani, P. Divieti, F. R. Bringhurst, L. A. Milner, H. M. Kronenberg and D. T. Scadden (2003). "Osteoblastic cells regulate the hematopoietic stem cell niche." Nature 425(6960): 841-846.

Capecchi, M. R. (1989). "Altering the genome by homologous recombination." Science 244(4910): 1288-1292.

Chadwick, K., L. Wang, L. Li, P. Menendez, B. Murdoch, A. Rouleau and M. Bhatia (2003). "Cytokines and BMP-4 promote hematopoietic differentiation of human embryonic stem cells." Blood 102(3): 906-915.

Chalhoub, N., N. Benachenhou, V. Rajapurohitam, M. Pata, M. Ferron, A. Frattini, A. Villa and J. Vacher (2003). "Grey-lethal mutation induces severe malignant autosomal recessive osteopetrosis in mouse and human." Nat Med 9(4): 399-406.

Chen, Y., B. Wu, L. Xu, H. Li, J. Xia, W. Yin, Z. Li, D. Shi, S. Li, S. Lin, X. Shu and D. Pei (2012). "A SNX10/V-ATPase pathway regulates ciliogenesis *in vitro* and *in vivo*." Cell Res 22(2): 333-345.

Cho, S. K., T. D. Webber, J. R. Carlyle, T. Nakano, S. M. Lewis and J. C. Zuniga-Pflucker (1999). "Functional characterization of B lymphocytes generated *in vitro* from embryonic stem cells." Proc Natl Acad Sci U S A 96(17): 9797-9802.

Choi, K. D., M. Vodyanik and Slukvin, II (2008). Hematopoietic differentiation. StemBook. Cambridge (MA), Harvard Stem Cell Institute. Copyright: (c) 2012 Kyung-Dal Choi, Maxim Vodyanik, and Igor I Slukvin.

Coccia, P. F., W. Krivit, J. Cervenka, C. Clawson, J. H. Kersey, T. H. Kim, M. E. Nesbit, N. K. Ramsay, P. I. Warkentin, S. L. Teitelbaum, A. J. Kahn and D. M. Brown (1980). "Successful bone-marrow transplantation for infantile malignant osteopetrosis." N Engl J Med 302(13): 701-708.

Coulombel, L. (2004). "Identification of hematopoietic stem/progenitor cells: strength and drawbacks of functional assays." Oncogene 23(43): 7210-7222.

Cowan, C. A., I. Klimanskaya, J. McMahon, J. Atienza, J. Witmyer, J. P. Zucker, S. Wang, C. C. Morton, A. P. McMahon, D. Powers and D. A. Melton (2004). "Derivation of embryonic stem-cell lines from human blastocysts." N Engl J Med 350(13): 1353-1356.

Cumano, A., F. Dieterlen-Lievre and I. Godin (1996). "Lymphoid potential, probed before circulation in mouse, is restricted to caudal intraembryonic splanchnopleura." Cell 86(6): 907-916.

Cumano, A. and I. Godin (2007). "Ontogeny of the hematopoietic system." Annu Rev Immunol 25: 745-785.

Cyranoski, D. (2013). Stem cells cruise to clinic. Nature. England. 494: 413.

Czechowicz, A., D. Kraft, I. L. Weissman and D. Bhattacharya (2007). "Efficient transplantation via antibody-based clearance of hematopoietic stem cell niches." Science 318(5854): 1296-1299.

da Silva Santos, P. S., A. P. Esperidiao and R. R. de Freitas (2009). "Maxillofacial aspects in malignant osteopetrosis." Cleft Palate Craniofac J 46(4): 388-390.

Damert, A., L. Miquerol, M. Gertsenstein, W. Risau and A. Nagy (2002). "Insufficient VEGFA activity in yolk sac endoderm compromises hematopoietic and endothelial differentiation." Development 129(8): 1881-1892.

de Bruijn, M. F., X. Ma, C. Robin, K. Ottersbach, M. J. Sanchez and E. Dzierzak (2002). "Hematopoietic stem cells localize to the endothelial cell layer in the midgestation mouse aorta." Immunity 16(5): 673-683.

de Bruijn, S. F., M. Budde, S. Teunisse, R. J. de Haan and J. Stam (2000). "Long-term outcome of cognition and functional health after cerebral venous sinus thrombosis." Neurology 54(8): 1687-1689.

Dimos, J. T., K. T. Rodolfa, K. K. Niakan, L. M. Weisenthal, H. Mitsumoto, W. Chung, G. F. Croft, G. Saphier, R. Leibel, R. Goland, H. Wichterle, C. E. Henderson and K. Eggan (2008). "Induced pluripotent

stem cells generated from patients with ALS can be differentiated into motor neurons." Science 321(5893): 1218-1221.

Doetschman, T. C., H. Eistetter, M. Katz, W. Schmidt and R. Kemler (1985). "The *in vitro* development of blastocyst-derived embryonic stem cell lines: formation of visceral yolk sac, blood islands and myocardium." J Embryol Exp Morphol 87: 27-45.

Douni, E., V. Rinotas, E. Makrinou, J. Zwerina, J. M. Penninger, E. Eliopoulos, G. Schett and G. Kollias (2012). "A RANKL G278R mutation causing osteopetrosis identifies a functional amino acid essential for trimer assembly in RANKL and TNF." Hum Mol Genet 21(4): 784-798.

Drake, F. H., R. A. Dodds, I. E. James, J. R. Connor, C. Debouck, S. Richardson, E. Lee-Rykaczewski, L. Coleman, D. Rieman, R. Barthlow, G. Hastings and M. Gowen (1996). "Cathepsin K, but not cathepsins B, L, or S, is abundantly expressed in human osteoclasts." J Biol Chem 271(21): 12511-12516.

Driessen, G. J., E. J. Gerritsen, A. Fischer, A. Fasth, W. C. Hop, P. Veys, F. Porta, A. Cant, C. G. Steward, J. M. Vossen, D. Uckan and W. Friedrich (2003). "Long-term outcome of hematopoietic stem cell transplantation in autosomal recessive osteopetrosis: an EBMT report." Bone Marrow Transplant 32(7): 657-663.

Ducy, P., T. Schinke and G. Karsenty (2000). "The osteoblast: a sophisticated fibroblast under central surveillance." Science 289(5484): 1501-1504.

Dull, T., R. Zufferey, M. Kelly, R. J. Mandel, M. Nguyen, D. Trono and L. Naldini (1998). "A third-generation lentivirus vector with a conditional packaging system." J Virol 72(11): 8463-8471.

Dzierzak, E. and N. A. Speck (2008). "Of lineage and legacy: the development of mammalian hematopoietic stem cells." Nat Immunol 9(2): 129-136.

Ebert, A. D., J. Yu, F. F. Rose, Jr., V. B. Mattis, C. L. Lorson, J. A. Thomson and C. N. Svendsen (2009). "Induced pluripotent stem cells from a spinal muscular atrophy patient." Nature 457(7227): 277-280.

Egawa, N., S. Kitaoka, K. Tsukita, M. Naitoh, K. Takahashi, T. Yamamoto, F. Adachi, T. Kondo, K. Okita, I. Asaka, T. Aoi, A. Watanabe, Y. Yamada, A. Morizane, J. Takahashi, T. Ayaki, H. Ito, K. Yoshikawa, S. Yamawaki, S. Suzuki, D. Watanabe, H. Hioki, T. Kaneko, K. Makioka, K. Okamoto, H. Takuma, A. Tamaoka, K. Hasegawa, T. Nonaka, M. Hasegawa, A. Kawata, M. Yoshida, T. Nakahata, R. Takahashi, M. C. Marchetto, F. H. Gage, S. Yamanaka and H. Inoue (2012). "Drug screening for ALS using patient-specific induced pluripotent stem cells." Sci Transl Med 4(145): 145ra104.

Evans, M. J. and M. H. Kaufman (1981). "Establishment in culture of pluripotential cells from mouse embryos." Nature 292(5819): 154-156.

Fandrich, F., X. Lin, G. X. Chai, M. Schulze, D. Ganten, M. Bader, J. Holle, D. S. Huang, R. Parwaresch, N. Zavazava and B. Binas (2002). "Preimplantation-stage stem cells induce long-term allogeneic graft acceptance without supplementary host conditioning." Nat Med 8(2): 171-178.

Fasth, A. (2009). "Osteopetrosis--more than only a disease of the bone." Am J Hematol 84(8): 469-470.

Ferrara, J. L. (1995). "Cytokine inhibitors and graft-versus-host disease." Ann N Y Acad Sci 770: 227-236.

Frattini, A., P. J. Orchard, C. Sobacchi, S. Giliani, M. Abinun, J. P. Mattsson, D. J. Keeling, A. K. Andersson, P. Wallbrandt, L. Zecca, L. D. Notarangelo, P. Vezzoni and A. Villa (2000). "Defects in TCIRG1 subunit of the vacuolar proton pump are responsible for a subset of human autosomal recessive osteopetrosis." Nat Genet 25(3): 343-346.

Frattini, A., H. C. Blair, M. G. Sacco, F. Cerisoli, F. Faggioli, E. M. Cato, A. Pangrazio, A. Musio, F. Rucci, C. Sobacchi, A. C. Sharrow, S. E. Kalla, M. G. Bruzzone, R. Colombo, M. C. Magli, P. Vezzoni and A. Villa (2005). "Rescue of ATPa3-deficient murine malignant osteopetrosis by hematopoietic stem cell transplantation *in utero*." Proc Natl Acad Sci U S A 102(41): 14629-14634.

Freedman, B. S., A. Q. Lam, J. L. Sundsbak, R. Iatrino, X. Su, S. J. Koon, M. Wu, L. Daheron, P. C. Harris, J. Zhou and J. V. Bonventre (2013). "Reduced ciliary polycystin-2 in induced pluripotent stem cells from polycystic kidney disease patients with PKD1 mutations." J Am Soc Nephrol 24(10): 1571-1586.

Fuller, K., J. M. Owens, C. J. Jagger, A. Wilson, R. Moss and T. J. Chambers (1993). "Macrophage colony-stimulating factor stimulates survival and chemotactic behavior in isolated osteoclasts." J Exp Med 178(5): 1733-1744.

Gerritsen, E. J., J. M. Vossen, I. H. van Loo, J. Hermans, M. H. Helfrich, C. Griscelli and A. Fischer (1994). "Autosomal recessive osteopetrosis: variability of findings at diagnosis and during the natural course." Pediatrics 93(2): 247-253.

Gordon-Keylock, S., M. Sobiesiak, S. Rybtsov, K. Moore and A. Medvinsky (2013). "Mouse extra-embryonic arterial vessels harbor precursors capable of maturing into definitive HSCs." Blood 122(14): 2338-2345.

Graves, A. R., P. K. Curran, C. L. Smith and J. A. Mindell (2008). "The Cl-/H^+ antiporter ClC-7 is the primary chloride permeation pathway in lysosomes." Nature 453(7196): 788-792.

Guerrini, M. M., C. Sobacchi, B. Cassani, M. Abinun, S. S. Kilic, A. Pangrazio, D. Moratto, E. Mazzolari, J. Clayton-Smith, P. Orchard, F. P. Coxon, M. H. Helfrich, J. C. Crockett, D. Mellis, A. Vellodi, I. Tezcan, L. D. Notarangelo, M. J. Rogers, P. Vezzoni, A. Villa and A. Frattini (2008). "Human osteoclast-poor osteopetrosis with hypogammaglobulinemia due to TNFRSF11A (RANK) mutations." Am J Hum Genet 83(1): 64-76.

Guo, L., R. M. Abrams, J. E. Babiarz, J. D. Cohen, S. Kameoka, M. J. Sanders, E. Chiao and K. L. Kolaja (2011). "Estimating the risk of drug-induced proarrhythmia using human induced pluripotent stem cell-derived cardiomyocytes." Toxicol Sci 123(1): 281-289.

Gurdon, J. B. (1962). "The developmental capacity of nuclei taken from intestinal epithelium cells of feeding tadpoles." J Embryol Exp Morphol 10: 622-640.

Hanna, J., M. Wernig, S. Markoulaki, C. W. Sun, A. Meissner, J. P. Cassady, C. Beard, T. Brambrink, L. C. Wu, T. M. Townes and R. Jaenisch (2007). "Treatment of sickle cell anemia mouse model with iPS cells generated from autologous skin." Science 318(5858): 1920-1923.

Hochman, E., S. Kinston, A. Harmelin, B. Gottgens and S. Izraeli (2006). "The SCL 3' enhancer responds to Hedgehog signaling during hemangioblast specification." Exp Hematol 34(12): 1643-1650.

Horii, T., S. Morita, M. Kimura, R. Kobayashi, D. Tamura, R. U. Takahashi, H. Kimura, I. Suetake, H. Ohata, K. Okamoto, S. Tajima, T. Ochiya, Y. Abe and I. Hatada (2013). "Genome engineering of mammalian haploid embryonic stem cells using the Cas9/RNA system." PeerJ 1: e230.

Howden, S. E., A. Gore, Z. Li, H. L. Fung, B. S. Nisler, J. Nie, G. Chen, B. E. McIntosh, D. R. Gulbranson, N. R. Diol, S. M. Taapken, D. T. Vereide, K. D. Montgomery, K. Zhang, D. M. Gamm and J. A. Thomson (2011). "Genetic correction and analysis of induced pluripotent stem cells from a patient with gyrate atrophy." Proc Natl Acad Sci U S A 108(16): 6537-6542.

Huangfu, D., K. Osafune, R. Maehr, W. Guo, A. Eijkelenboom, S. Chen, W. Muhlestein and D. A. Melton (2008). "Induction of pluripotent stem cells from primary human fibroblasts with only Oct4 and Sox2." Nat Biotechnol 26(11): 1269-1275.

Inoue, K., N. Ogonuki, Y. Yamamoto, K. Takano, H. Miki, K. Mochida and A. Ogura (2004). "Tissue-specific distribution of donor mitochondrial DNA in cloned mice produced by somatic cell nuclear transfer." Genesis 39(2): 79-83.

Johansson, M., L. Jansson, M. Ehinger, A. Fasth, S. Karlsson and J. Richter (2006). "Neonatal hematopoietic stem cell transplantation cures *oc/oc* mice from osteopetrosis." Exp Hematol 34(2): 242-249.

Kamps, W. A. and M. D. Cooper (1982). "Microenvironmental studies of pre-B and B cell development in human and mouse fetuses." J Immunol 129(2): 526-531.

Kenny, A. D. (1985). "Role of carbonic anhydrase in bone: partial inhibition of disuse atrophy of bone by parenteral acetazolamide." Calcif Tissue Int 37(2): 126-133.

Kiel, M. J., T. Iwashita, O. H. Yilmaz and S. J. Morrison (2005). "Spatial differences in hematopoiesis but not in stem cells indicate a lack of regional patterning in definitive hematopoietic stem cells." Dev Biol 283(1): 29-39.

Kiel, M. J., O. H. Yilmaz, T. Iwashita, C. Terhorst and S. J. Morrison (2005). "SLAM family receptors distinguish hematopoietic stem and progenitor cells and reveal endothelial niches for stem cells." Cell 121(7): 1109-1121.

Kim, J. B., V. Sebastiano, G. Wu, M. J. Arauzo-Bravo, P. Sasse, L. Gentile, K. Ko, D. Ruau, M. Ehrich, D. van den Boom, J. Meyer, K. Hubner, C. Bernemann, C. Ortmeier, M. Zenke, B. K. Fleischmann, H. Zaehres and H. R. Scholer (2009). "Oct4-induced pluripotency in adult neural stem cells." Cell 136(3): 411-419.

Kim, J. J., J. S. Lee, B. H. Moon, M. O. Lee, S. H. Song, H. Li, A. J. Fornace and H. J. Cha (2010). "Wip1-expressing feeder cells retain pluripotency of co-cultured mouse embryonic stem cells under leukemia inhibitory factor-deprivated condition." Arch Pharm Res 33(8): 1253-1260.

Kinder, S. J., T. E. Tsang, G. A. Quinlan, A. K. Hadjantonakis, A. Nagy and P. P. Tam (1999). "The orderly allocation of mesodermal cells to the extra-embryonic structures and the anteroposterior axis during gastrulation of the mouse embryo." Development 126(21): 4691-4701.

Kitajima, K., K. Minehata, K. Sakimura, T. Nakano and T. Hara (2011). "*In vitro* generation of HSC-like cells from murine ESCs/iPSCs by enforced expression of LIM-homeobox transcription factor Lhx2." Blood 117(14): 3748-3758.

Kong, Y. Y., H. Yoshida, I. Sarosi, H. L. Tan, E. Timms, C. Capparelli, S. Morony, A. J. Oliveira-dos-Santos, G. Van, A. Itie, W. Khoo, A. Wakeham, C. R. Dunstan, D. L. Lacey, T. W. Mak, W. J. Boyle and J. M. Penninger (1999). "OPGL is a key regulator of osteoclastogenesis, lymphocyte development and lymph-node organogenesis." Nature 397(6717): 315-323.

Kornak, U., D. Kasper, M. R. Bosl, E. Kaiser, M. Schweizer, A. Schulz, W. Friedrich, G. Delling and T. J. Jentsch (2001). "Loss of the ClC-7 chloride channel leads to osteopetrosis in mice and man." Cell 104(2): 205-215.

Kusadasi, N., R. A. Oostendorp, W. J. Koevoet, E. A. Dzierzak and R. E. Ploemacher (2002). "Stromal cells from murine embryonic aorta-gonad-mesonephros region, liver and gut mesentery expand human umbilical cord blood-derived CAFC(week6) in extended long-term cultures." Leukemia 16(9): 1782-1790.

Kyba, M., R. C. Perlingeiro and G. Q. Daley (2002). "HoxB4 confers definitive lymphoid-myeloid engraftment potential on embryonic stem cell and yolk sac hematopoietic progenitors." Cell 109(1): 29-37.

Lacey, D. L., E. Timms, H. L. Tan, M. J. Kelley, C. R. Dunstan, T. Burgess, R. Elliott, A. Colombero, G. Elliott, S. Scully, H. Hsu, J. Sullivan, N. Hawkins, E. Davy, C. Capparelli, A. Eli, Y. X. Qian, S. Kaufman, I. Sarosi, V. Shalhoub, G. Senaldi, J. Guo, J. Delaney and W. J. Boyle (1998). "Osteoprotegerin ligand is a cytokine that regulates osteoclast differentiation and activation." Cell 93(2): 165-176.

Lee, B. S., S. L. Gluck and L. S. Holliday (1999). "Interaction between vacuolar H($^{+}$)-ATPase and microfilaments during osteoclast activation." J Biol Chem 274(41): 29164-29171.

Leisle, L., C. F. Ludwig, F. A. Wagner, T. J. Jentsch and T. Stauber (2011). "ClC-7 is a slowly voltage-gated 2Cl(-)/1H($^{+}$)-exchanger and requires Ostm1 for transport activity." Embo j 30(11): 2140-2152.

Lessard, J., A. Faubert and G. Sauvageau (2004). "Genetic programs regulating HSC specification, maintenance and expansion." Oncogene 23(43): 7199-7209.

Li, Y. P., W. Chen, Y. Liang, E. Li and P. Stashenko (1999). "Atp6i-deficient mice exhibit severe osteopetrosis due to loss of osteoclast-mediated extracellular acidification." Nat Genet 23(4): 447-451.

Li, J., I. Sarosi, X. Q. Yan, S. Morony, C. Capparelli, H. L. Tan, S. McCabe, R. Elliott, S. Scully, G. Van, S. Kaufman, S. C. Juan, Y. Sun, J. Tarpley, L. Martin, K. Christensen, J. McCabe, P. Kostenuik, H. Hsu, F. Fletcher, C. R. Dunstan, D. L. Lacey and W. J. Boyle (2000). "RANK is the intrinsic hematopoietic cell

surface receptor that controls osteoclastogenesis and regulation of bone mass and calcium metabolism." Proc Natl Acad Sci U S A 97(4): 1566-1571.

Lo Iacono, N., H. C. Blair, P. L. Poliani, V. Marrella, F. Ficara, B. Cassani, F. Facchetti, E. Fontana, M. M. Guerrini, E. Traggiai, F. Schena, M. Paulis, S. Mantero, A. Inforzato, S. Valaperta, A. Pangrazio, L. Crisafulli, V. Maina, P. Kostenuik, P. Vezzoni, A. Villa and C. Sobacchi (2012). "Osteopetrosis rescue upon RANKL administration to Rankl(-/-) mice: a new therapy for human RANKL-dependent ARO." J Bone Miner Res 27(12): 2501-2510.

Ludwig, D. L., J. R. Stringer, D. C. Wight, H. C. Doetschman and J. J. Duffy (1996). "FLP-mediated site-specific recombination in microinjected murine zygotes." Transgenic Res 5(6): 385-395.

Maekawa, M., K. Yamaguchi, T. Nakamura, R. Shibukawa, I. Kodanaka, T. Ichisaka, Y. Kawamura, H. Mochizuki, N. Goshima and S. Yamanaka (2011). "Direct reprogramming of somatic cells is promoted by maternal transcription factor Glis1." Nature 474(7350): 225-229.

Manolagas, S. C. (2000). "Birth and death of bone cells: basic regulatory mechanisms and implications for the pathogenesis and treatment of osteoporosis." Endocr Rev 21(2): 115-137.

Martin, T. J. and N. A. Sims (2005). "Osteoclast-derived activity in the coupling of bone formation to resorption." Trends Mol Med 11(2): 76-81.

Matsa, E., D. Rajamohan, E. Dick, L. Young, I. Mellor, A. Staniforth and C. Denning (2011). "Drug evaluation in cardiomyocytes derived from human induced pluripotent stem cells carrying a long QT syndrome type 2 mutation." Eur Heart J 32(8): 952-962.

Matsuoka, S., Y. Ebihara, M. Xu, T. Ishii, D. Sugiyama, H. Yoshino, T. Ueda, A. Manabe, R. Tanaka, Y. Ikeda, T. Nakahata and K. Tsuji (2001). "CD34 expression on long-term repopulating hematopoietic stem cells changes during developmental stages." Blood 97(2): 419-425.

McGrath, K. E., A. D. Koniski, J. Malik and J. Palis (2003). "Circulation is established in a stepwise pattern in the mammalian embryo." Blood 101(5): 1669-1676.

Medvinsky, A. L., N. L. Samoylina, A. M. Muller and E. A. Dzierzak (1993). "An early pre-liver intraembryonic source of CFU-S in the developing mouse." Nature 364(6432): 64-67.

Medvinsky, A. and E. Dzierzak (1996). "Definitive hematopoiesis is autonomously initiated by the AGM region." Cell 86(6): 897-906.

Medvinsky, A., S. Rybtsov and S. Taoudi (2011). "Embryonic origin of the adult hematopoietic system: advances and questions." Development 138(6): 1017-1031.

Mikkola, H. K., Y. Fujiwara, T. M. Schlaeger, D. Traver and S. H. Orkin (2003). "Expression of CD41 marks the initiation of definitive hematopoiesis in the mouse embryo." Blood 101(2): 508-516.

Mitjavila-Garcia, M. T., M. Cailleret, I. Godin, M. M. Nogueira, K. Cohen-Solal, V. Schiavon, Y. Lecluse, F. Le Pesteur, A. H. Lagrue and W. Vainchenker (2002). "Expression of CD41 on hematopoietic progenitors derived from embryonic hematopoietic cells." Development 129(8): 2003-2013.

Montini, E., D. Cesana, M. Schmidt, F. Sanvito, M. Ponzoni, C. Bartholomae, L. Sergi Sergi, F. Benedicenti, A. Ambrosi, C. Di Serio, C. Doglioni, C. von Kalle and L. Naldini (2006). "Hematopoietic stem cell gene transfer in a tumor-prone mouse model uncovers low genotoxicity of lentiviral vector integration." Nat Biotechnol 24(6): 687-696.

Moon, J. H., J. S. Heo, J. S. Kim, E. K. Jun, J. H. Lee, A. Kim, J. Kim, K. Y. Whang, Y. K. Kang, S. Yeo, H. J. Lim, D. W. Han, D. W. Kim, S. Oh, B. S. Yoon, H. R. Scholer and S. You (2011). "Reprogramming fibroblasts into induced pluripotent stem cells with Bmi1." Cell Res 21(9): 1305-1315.

Moore, M. A. and D. Metcalf (1970). "Ontogeny of the haemopoietic system: yolk sac origin of *in vivo* and *in vitro* colony forming cells in the developing mouse embryo." Br J Hematol 18(3): 279-296.

Moore, T., S. Huang, L. W. Terstappen, M. Bennett and V. Kumar (1994). "Expression of CD43 on murine and human pluripotent hematopoietic stem cells." J Immunol 153(11): 4978-4987.

Nagamatsu, G., T. Kosaka, S. Saito, H. Honda, K. Takubo, T. Kinoshita, H. Akiyama, T. Sudo, K. Horimoto, M. Oya and T. Suda (2013). "Induction of pluripotent stem cells from primordial germ cells by single reprogramming factors." Stem Cells 31(3): 479-487.

Nakagawa, N., M. Kinosaki, K. Yamaguchi, N. Shima, H. Yasuda, K. Yano, T. Morinaga and K. Higashio (1998). "RANK is the essential signaling receptor for osteoclast differentiation factor in osteoclastogenesis." Biochem Biophys Res Commun 253(2): 395-400.

Nakagawa, M., M. Koyanagi, K. Tanabe, K. Takahashi, T. Ichisaka, T. Aoi, K. Okita, Y. Mochiduki, N. Takizawa and S. Yamanaka (2008). "Generation of induced pluripotent stem cells without Myc from mouse and human fibroblasts." Nat Biotechnol 26(1): 101-106.

Nakano, T., H. Kodama and T. Honjo (1994). "Generation of lymphohematopoietic cells from embryonic stem cells in culture." Science 265(5175): 1098-1101.

Narsinh, K., K. H. Narsinh and J. C. Wu (2011). "Derivation of human induced pluripotent stem cells for cardiovascular disease modeling." Circ Res 108(9): 1146-1156.

Nienhuis, A. W., C. E. Dunbar and B. P. Sorrentino (2006). "Genotoxicity of retroviral integration in hematopoietic cells." Mol Ther 13(6): 1031-1049.

North, T. E., W. Goessling, M. Peeters, P. Li, C. Ceol, A. M. Lord, G. J. Weber, J. Harris, C. C. Cutting, P. Huang, E. Dzierzak and L. I. Zon (2009). "Hematopoietic stem cell development is dependent on blood flow." Cell 137(4): 736-748.

Okita, K., T. Ichisaka and S. Yamanaka (2007). "Generation of germline-competent induced pluripotent stem cells." Nature 448(7151): 313-317.

Okita, K., M. Nakagawa, H. Hyenjong, T. Ichisaka and S. Yamanaka (2008). "Generation of mouse induced pluripotent stem cells without viral vectors." Science 322(5903): 949-953.

Orkin, S. H. and L. I. Zon (2008). "Hematopoiesis: an evolving paradigm for stem cell biology." Cell 132(4): 631-644.

Osawa, M., K. Hanada, H. Hamada and H. Nakauchi (1996). "Long-term lymphohematopoietic reconstitution by a single CD34-low/negative hematopoietic stem cell." Science 273(5272): 242-245.

Ottersbach, K. and E. Dzierzak (2005). "The murine placenta contains hematopoietic stem cells within the vascular labyrinth region." Dev Cell 8(3): 377-387.

Palis, J., S. Robertson, M. Kennedy, C. Wall and G. Keller (1999). "Development of erythroid and myeloid progenitors in the yolk sac and embryo proper of the mouse." Development 126(22): 5073-5084.

Pangrazio, A., P. L. Poliani, A. Megarbane, G. Lefranc, E. Lanino, M. Di Rocco, F. Rucci, F. Lucchini, M. Ravanini, F. Facchetti, M. Abinun, P. Vezzoni, A. Villa and A. Frattini (2006). "Mutations in OSTM1 (grey

lethal) define a particularly severe form of autosomal recessive osteopetrosis with neural involvement." J Bone Miner Res 21(7): 1098-1105.

Pangrazio, A., M. E. Caldana, N. Lo Iacono, S. Mantero, P. Vezzoni, A. Villa and C. Sobacchi (2012). "Autosomal recessive osteopetrosis: report of 41 novel mutations in the TCIRG1 gene and diagnostic implications." Osteoporos Int 23(11): 2713-2718.

Pangrazio, A., C. Sobacchi, P. Vezzoni and A.Villa (2011). "Osteopetrosi autosomica recessiva: ripartiamo dalla diagnosi molecolare." Prospettive in Pediatria 41(164): 214-220.

Park, I. H., N. Arora, H. Huo, N. Maherali, T. Ahfeldt, A. Shimamura, M. W. Lensch, C. Cowan, K. Hochedlinger and G. Q. Daley (2008). "Disease-specific induced pluripotent stem cells." Cell 134(5): 877-886.

Park, I. H., R. Zhao, J. A. West, A. Yabuuchi, H. Huo, T. A. Ince, P. H. Lerou, M. W. Lensch and G. Q. Daley (2008). "Reprogramming of human somatic cells to pluripotency with defined factors." Nature 451(7175): 141-146.

Pereira, C. F., B. Chang, J. Qiu, X. Niu, D. Papatsenko, C. E. Hendry, N. R. Clark, A. Nomura-Kitabayashi, J. C. Kovacic, A. Ma'ayan, C. Schaniel, I. R. Lemischka and K. Moore (2013). "Induction of a hemogenic program in mouse fibroblasts." Cell Stem Cell 13(2): 205-218.

Pirovano, S., L. D. Notarangelo, F. Malacarne, E. Mazzolari, F. Porta, A. Lanfranchi, S. Giliani, S. Zucca, S. Pecorelli, A. Albertini, A. G. Ugazio and L. Imberti (2004). "Reconstitution of T-cell compartment after *in utero* stem cell transplantation: analysis of T-cell repertoire and thymic output." Hematologica 89(4): 450-461.

Pressey, S. N., K. J. O'Donnell, T. Stauber, J. C. Fuhrmann, J. Tyynela, T. J. Jentsch and J. D. Cooper (2010). "Distinct neuropathologic phenotypes after disrupting the chloride transport proteins ClC-6 or ClC-7/Ostm1." J Neuropathol Exp Neurol 69(12): 1228-1246.

Purton, L. E. and D. T. Scadden (2007). "Limiting factors in murine hematopoietic stem cell assays." Cell Stem Cell 1(3): 263-270.

Qin, A., T. S. Cheng, N. J. Pavlos, Z. Lin, K. R. Dai and M. H. Zheng (2012). "V-ATPases in osteoclasts: structure, function and potential inhibitors of bone resorption." Int J Biochem Cell Biol 44(9): 1422-1435.

Qiu, C., E. Hanson, E. Olivier, M. Inada, D. S. Kaufman, S. Gupta and E. E. Bouhassira (2005). "Differentiation of human embryonic stem cells into hematopoietic cells by coculture with human fetal liver cells recapitulates the globin switch that occurs early in development." Exp Hematol 33(12): 1450-1458.

Rafii, S., D. Lyden, R. Benezra, K. Hattori and B. Heissig (2002). "Vascular and hematopoietic stem cells: novel targets for anti-angiogenesis therapy?" Nat Rev Cancer 2(11): 826-835.

Rafii, S., C. C. Kloss, J. M. Butler, M. Ginsberg, E. Gars, R. Lis, Q. Zhan, P. Josipovic, B. S. Ding, J. Xiang, O. Elemento, N. Zaninovic, Z. Rosenwaks, M. Sadelain, J. A. Rafii and D. James (2013). "Human ESC-derived hemogenic endothelial cells undergo distinct waves of endothelial to hematopoietic transition." Blood 121(5): 770-780.

Robin, C., K. Ottersbach, J. C. Boisset, A. Oziemlak and E. Dzierzak (2011). "CD41 is developmentally regulated and differentially expressed on mouse hematopoietic stem cells." Blood 117(19): 5088-5091.

Rodan, G. A. and T. J. Martin (1981). "Role of osteoblasts in hormonal control of bone resorption--a hypothesis." Calcif Tissue Int 33(4): 349-351.

Roodman, G. D. (1991). "Osteoclast differentiation." Crit Rev Oral Biol Med 2(3): 389-409.

Rossant, J. and J. C. Cross (2001). "Placental development: lessons from mouse mutants." Nat Rev Genet 2(7): 538-548.

Russ, A. P., C. Friedel, M. Grez and H. von Melchner (1996). "Self-deleting retrovirus vectors for gene therapy." J Virol 70(8): 4927-4932.

Rybtsov, S., M. Sobiesiak, S. Taoudi, C. Souilhol, J. Senserrich, A. Liakhovitskaia, A. Ivanovs, J. Frampton, S. Zhao and A. Medvinsky (2011). "Hierarchical organization and early hematopoietic specification of the developing HSC lineage in the AGM region." J Exp Med 208(6): 1305-1315.

Sakuma, T., S. Hosoi, K. Woltjen, K. Suzuki, K. Kashiwagi, H. Wada, H. Ochiai, T. Miyamoto, N. Kawai, Y. Sasakura, S. Matsuura, Y. Okada, A. Kawahara, S. Hayashi and T. Yamamoto (2013). "Efficient TALEN construction and evaluation methods for human cell and animal applications." Genes Cells 18(4): 315-326.

Sanchez, M. J., A. Holmes, C. Miles and E. Dzierzak (1996). "Characterization of the first definitive hematopoietic stem cells in the AGM and liver of the mouse embryo." Immunity 5(6): 513-525.

Scacheri, P. C., J. S. Crabtree, E. A. Novotny, L. Garrett-Beal, A. Chen, K. A. Edgemon, S. J. Marx, A. M. Spiegel, S. C. Chandrasekharappa and F. S. Collins (2001). "Bidirectional transcriptional activity of PGK-neomycin and unexpected embryonic lethality in heterozygote chimeric knockout mice." Genesis 30(4): 259-263.

Schlesinger, P. H., H. C. Blair, S. L. Teitelbaum and J. C. Edwards (1997). "Characterization of the osteoclast ruffled border chloride channel and its role in bone resorption." J Biol Chem 272(30): 18636-18643.

Schmitt, T. M., R. F. de Pooter, M. A. Gronski, S. K. Cho, P. S. Ohashi and J. C. Zuniga-Pflucker (2004). "Induction of T cell development and establishment of T cell competence from embryonic stem cells differentiated *in vitro*." Nat Immunol 5(4): 410-417.

Schulz, A. S., C. F. Classen, W. A. Mihatsch, M. Sigl-Kraetzig, M. Wiesneth, K. M. Debatin, W. Friedrich and S. M. Muller (2002). "HLA-haploidentical blood progenitor cell transplantation in osteopetrosis." Blood 99(9): 3458-3460.

Schulz, A. S., D. Moshous, C. Steward, M. Hoenig, C. Schuetz, C. Sobacchi, A. Fischer, K. M. Debatin and A. Villa (2013). "Osteopetrosis: a heterogeneous group of dieases requiring individualized therapeutic strategies - results of the osteopetrosis registry on behalf of ESID and EBMT." 39th Annual Meeting of the European Group for Blood and Marrow Transplantation.

Schwartz, S. D., J. P. Hubschman, G. Heilwell, V. Franco-Cardenas, C. K. Pan, R. M. Ostrick, E. Mickunas, R. Gay, I. Klimanskaya and R. Lanza (2012). "Embryonic stem cell trials for macular degeneration: a preliminary report." Lancet 379(9817): 713-720.

Scimeca, J. C., A. Franchi, C. Trojani, H. Parrinello, J. Grosgeorge, C. Robert, O. Jaillon, C. Poirier, P. Gaudray and G. F. Carle (2000). "The gene encoding the mouse homologue of the human osteoclast-specific 116-kDa V-ATPase subunit bears a deletion in osteosclerotic (*oc/oc*) mutants." Bone 26(3): 207-213.

Sebastiano, V., M. L. Maeder, J. F. Angstman, B. Haddad, C. Khayter, D. T. Yeo, M. J. Goodwin, J. S. Hawkins, C. L. Ramirez, L. F. Batista, S. E. Artandi, M. Wernig and J. K. Joung (2011). "In situ genetic correction of the sickle cell anemia mutation in human induced pluripotent stem cells using engineered zinc finger nucleases." Stem Cells 29(11): 1717-1726.

Seita, J. and I. L. Weissman (2010). "Hematopoietic stem cell: self-renewal versus differentiation." Wiley Interdiscip Rev Syst Biol Med 2(6): 640-653.

Shi, Y., C. Desponts, J. T. Do, H. S. Hahm, H. R. Scholer and S. Ding (2008). "Induction of pluripotent stem cells from mouse embryonic fibroblasts by Oct4 and Klf4 with small-molecule compounds." Cell Stem Cell 3(5): 568-574.

Shizuya, H., B. Birren, U. J. Kim, V. Mancino, T. Slepak, Y. Tachiiri and M. Simon (1992). "Cloning and stable maintenance of 300-kilobase-pair fragments of human DNA in Escherichia coli using an F-factor-based vector." Proc Natl Acad Sci U S A 89(18): 8794-8797.

Sobacchi, C., A. Frattini, P. Orchard, O. Porras, I. Tezcan, M. Andolina, R. Babul-Hirji, I. Baric, N. Canham, D. Chitayat, S. Dupuis-Girod, I. Ellis, A. Etzioni, A. Fasth, A. Fisher, B. Gerritsen, V. Gulino, E. Horwitz, V. Klamroth, E. Lanino, M. Mirolo, A. Musio, G. Matthijs, S. Nonomaya, L. D. Notarangelo, H. D. Ochs, A. Superti Furga, J. Valiaho, J. L. van Hove, M. Vihinen, D. Vujic, P. Vezzoni and A. Villa (2001). "The mutational spectrum of human malignant autosomal recessive osteopetrosis." Hum Mol Genet 10(17): 1767-1773.

Sobacchi, C., A. Frattini, M. M. Guerrini, M. Abinun, A. Pangrazio, L. Susani, R. Bredius, G. Mancini, A. Cant, N. Bishop, P. Grabowski, A. Del Fattore, C. Messina, G. Errigo, F. P. Coxon, D. I. Scott, A. Teti, M. J. Rogers, P. Vezzoni, A. Villa and M. H. Helfrich (2007). "Osteoclast-poor human osteopetrosis due to mutations in the gene encoding RANKL." Nat Genet 39(8): 960-962.

Sobacchi, C., A. Schulz, F. P. Coxon, A. Villa and M. H. Helfrich (2013). "Osteopetrosis: genetics, treatment and new insights into osteoclast function." Nat Rev Endocrinol 9(9): 522-536.

Soldner, F., D. Hockemeyer, C. Beard, Q. Gao, G. W. Bell, E. G. Cook, G. Hargus, A. Blak, O. Cooper, M. Mitalipova, O. Isacson and R. Jaenisch (2009). "Parkinson's disease patient-derived induced pluripotent stem cells free of viral reprogramming factors." Cell 136(5): 964-977.

Spangrude, G. J., S. Heimfeld and I. L. Weissman (1988). "Purification and characterization of mouse hematopoietic stem cells." Science 241(4861): 58-62.

Stadtfeld, M., M. Nagaya, J. Utikal, G. Weir and K. Hochedlinger (2008). "Induced pluripotent stem cells generated without viral integration." Science 322(5903): 945-949.

Stark, Z. and R. Savarirayan (2009). "Osteopetrosis." Orphanet J Rare Dis 4: 5.

Steward, C. G. (2003). "Neurological aspects of osteopetrosis." Neuropathol Appl Neurobiol 29(2): 87-97.

Steward, C. G., I. Pellier, A. Mahajan, M. T. Ashworth, A. G. Stuart, A. Fasth, D. Lang, A. Fischer, W. Friedrich and A. S. Schulz (2004). "Severe pulmonary hypertension: a frequent complication of stem cell transplantation for malignant infantile osteopetrosis." Br J Hematol 124(1): 63-71.

Suda, T., N. Takahashi and T. J. Martin (1992). "Modulation of osteoclast differentiation." Endocr Rev 13(1): 66-80.

Sugarman, J. (2008). "Human stem cell ethics: beyond the embryo." Cell Stem Cell 2(6): 529-533.

Swijnenburg, R. J., S. Schrepfer, F. Cao, J. I. Pearl, X. Xie, A. J. Connolly, R. C. Robbins and J. C. Wu (2008). "*In vivo* imaging of embryonic stem cells reveals patterns of survival and immune rejection following transplantation." Stem Cells Dev 17(6): 1023-1029.

Takahashi, K., K. Tanabe, M. Ohnuki, M. Narita, T. Ichisaka, K. Tomoda and S. Yamanaka (2007). "Induction of pluripotent stem cells from adult human fibroblasts by defined factors." Cell 131(5): 861-872.

Takahashi, K. and S. Yamanaka (2006). "Induction of pluripotent stem cells from mouse embryonic and adult fibroblast cultures by defined factors." Cell 126(4): 663-676.

Takayama, N., S. Nishimura, S. Nakamura, T. Shimizu, R. Ohnishi, H. Endo, T. Yamaguchi, M. Otsu, K. Nishimura, M. Nakanishi, A. Sawaguchi, R. Nagai, K. Takahashi, S. Yamanaka, H. Nakauchi and K. Eto (2010). "Transient activation of c-MYC expression is critical for efficient platelet generation from human induced pluripotent stem cells." J Exp Med 207(13): 2817-2830.

Takayanagi, H. (2012). "New developments in osteoimmunology." Nat Rev Rheumatol 8(11): 684-689.

Takeuchi, M., T. Sekiguchi, T. Hara, T. Kinoshita and A. Miyajima (2002). "Cultivation of aorta-gonad-mesonephros-derived hematopoietic stem cells in the fetal liver microenvironment amplifies long-term repopulating activity and enhances engraftment to the bone marrow." Blood 99(4): 1190-1196.

Taoudi, S., A. M. Morrison, H. Inoue, R. Gribi, J. Ure and A. Medvinsky (2005). "Progressive divergence of definitive hematopoietic stem cells from the endothelial compartment does not depend on contact with the fetal liver." Development 132(18): 4179-4191.

Tavian, M. and B. Peault (2005). "Embryonic development of the human hematopoietic system." Int J Dev Biol 49(2-3): 243-250.

Teitelbaum, S. L. and F. P. Ross (2003). "Genetic regulation of osteoclast development and function." Nat Rev Genet 4(8):638-649.

Thomson, J. A., J. Itskovitz-Eldor, S. S. Shapiro, M. A. Waknitz, J. J. Swiergiel, V. S. Marshall and J. M. Jones (1998). "Embryonic stem cell lines derived from human blastocysts." Science 282(5391): 1145-1147.

Thoren, L. A., K. Liuba, D. Bryder, J. M. Nygren, C. T. Jensen, H. Qian, J. Antonchuk and S. E. Jacobsen (2008). "Kit regulates maintenance of quiescent hematopoietic stem cells." J Immunol 180(4): 2045-2053.

Tondelli, B., H. C. Blair, M. Guerrini, K. D. Patrene, B. Cassani, P. Vezzoni and F. Lucchini (2009). "Fetal liver cells transplanted *in utero* rescue the osteopetrotic phenotype in the *oc/oc* mouse." Am J Pathol 174(3): 727-735.

Toyomura, T., Y. Murata, A. Yamamoto, T. Oka, G. H. Sun-Wada, Y. Wada and M. Futai (2003). "From lysosomes to the plasma membrane: localization of vacuolar-type H^+ -ATPase with the a3 isoform during osteoclast differentiation." J Biol Chem 278(24): 22023-22030.

Tsai, S., S. G. Emerson, C. A. Sieff and D. G. Nathan (1986). "Isolation of a human stromal cell strain secreting hemopoietic growth factors." J Cell Physiol 127(1): 137-145.

Tsuji, O., K. Miura, Y. Okada, K. Fujiyoshi, M. Mukaino, N. Nagoshi, K. Kitamura, G. Kumagai, M. Nishino, S. Tomisato, H. Higashi, T. Nagai, H. Katoh, K. Kohda, Y. Matsuzaki, M. Yuzaki, E. Ikeda, Y. Toyama, M. Nakamura, S. Yamanaka and H. Okano (2010). "Therapeutic potential of appropriately evaluated safe-induced pluripotent stem cells for spinal cord injury." Proc Natl Acad Sci U S A 107(28): 12704-12709.

Twomey, C. "Understanding Stem Cells: An Overview of the Science and Issues." National Academies http://www.nationalacademies.org/stemcells

Van Wesenbeeck, L., P. R. Odgren, F. P. Coxon, A. Frattini, P. Moens, B. Perdu, C. A. MacKay, E. Van Hul, J. P. Timmermans, F. Vanhoenacker, R. Jacobs, B. Peruzzi, A. Teti, M. H. Helfrich, M. J. Rogers, A. Villa and W. Van Hul (2007). "Involvement of PLEKHM1 in osteoclastic vesicular transport and osteopetrosis in incisors absent rats and humans." J Clin Invest 117(4): 919-930.

Vandekerckhove, B., S. Vanhee, S. Van Coppernolle, S. Snauwaert, I. Velghe, T. Taghon, G. Leclercq, T. Kerre and J. Plum (2011). "*In vitro* generation of immune cells from pluripotent stem cells." Front Biosci (Landmark Ed) 16: 1488-1504.

Venta, P. J., R. J. Welty, T. M. Johnson, W. S. Sly and R. E. Tashian (1991). "Carbonic anhydrase II deficiency syndrome in a Belgian family is caused by a point mutation at an invariant histidine residue (107 His----Tyr): complete structure of the normal human CA II gene." Am J Hum Genet 49(5): 1082-1090.

Villa, A., M. M. Guerrini, B. Cassani, A. Pangrazio and C. Sobacchi (2009). "Infantile malignant, autosomal recessive osteopetrosis: the rich and the poor." Calcif Tissue Int 84(1): 1-12.

Waldman, A. S. (1992). "Targeted homologous recombination in mammalian cells." Crit Rev Oncol Hematol 12(1): 49-64.

Walmsley, M., D. Cleaver and R. Patient (2008). "Fibroblast growth factor controls the timing of Scl, Lmo2, and Runx1 expression during embryonic blood development." Blood 111(3): 1157-1166.

Wang, Y., F. Yates, O. Naveiras, P. Ernst and G. Q. Daley (2005). "Embryonic stem cell-derived hematopoietic stem cells." Proc Natl Acad Sci U S A 102(52): 19081-19086.

Warren, L., P. D. Manos, T. Ahfeldt, Y. H. Loh, H. Li, F. Lau, W. Ebina, P. K. Mandal, Z. D. Smith, A. Meissner, G. Q. Daley, A. S. Brack, J. J. Collins, C. Cowan, T. M. Schlaeger and D. J. Rossi (2010). "Highly efficient reprogramming to pluripotency and directed differentiation of human cells with synthetic modified mRNA." Cell Stem Cell 7(5): 618-630.

Weissman, I. L. and J. A. Shizuru (2008). "The origins of the identification and isolation of hematopoietic stem cells, and their capability to induce donor-specific transplantation tolerance and treat autoimmune diseases." Blood 112(9): 3543-3553.

Wengler, G. S., A. Lanfranchi, T. Frusca, R. Verardi, A. Neva, D. Brugnoni, S. Giliani, M. Fiorini, P. Mella, F. Guandalini, E. Mazzolari, S. Pecorelli, L. D. Notarangelo, F. Porta and A. G. Ugazio (1996). "In-utero transplantation of parental CD34 hematopoietic progenitor cells in a patient with X-linked severe combined immunodeficiency (SCIDXI)." Lancet 348(9040): 1484-1487.

Wernig, M., A. Meissner, J. P. Cassady and R. Jaenisch (2008). c-Myc is dispensable for direct reprogramming of mouse fibroblasts. Cell Stem Cell. United States. 2: 10-12.

Wernig, M., J. P. Zhao, J. Pruszak, E. Hedlund, D. Fu, F. Soldner, V. Broccoli, M. Constantine-Paton, O. Isacson and R. Jaenisch (2008). "Neurons derived from reprogrammed fibroblasts functionally integrate into the fetal brain and improve symptoms of rats with Parkinson's disease." Proc Natl Acad Sci U S A 105(15): 5856-5861.

Wiles, M. V. and G. Keller (1991). "Multiple hematopoietic lineages develop from embryonic stem (ES) cells in culture." Development 111(2): 259-267.

Wilmut, I., A. E. Schnieke, J. McWhir, A. J. Kind and K. H. Campbell (1997). "Viable offspring derived from fetal and adult mammalian cells." Nature 385(6619): 810-813.

Woltjen, K., I. P. Michael, P. Mohseni, R. Desai, M. Mileikovsky, R. Hamalainen, R. Cowling, W. Wang, P. Liu, M. Gertsenstein, K. Kaji, H. K. Sung and A. Nagy (2009). "piggyBac transposition reprograms fibroblasts to induced pluripotent stem cells." Nature 458(7239): 766-770.

Woo, J. T., M. Kato, M. Takami and K. Nagai (2000). "Receptor activator of NF-kappaB ligand induces the fusion of mononuclear preosteoclasts into multinucleated osteoclasts." Cytotechnology 33(1-3): 203-211.

Yamanaka, S. (2009). "A fresh look at iPS cells." Cell 137(1): 13-17.

Yang, L., D. Bryder, J. Adolfsson, J. Nygren, R. Mansson, M. Sigvardsson and S. E. Jacobsen (2005). "Identification of Lin(-)Sca1($^{+}$)kit($^{+}$)CD34($^{+}$)Flt3- short-term hematopoietic stem cells capable of rapidly reconstituting and rescuing myeloablated transplant recipients." Blood 105(7): 2717-2723.

Yoder, M. C., K. Hiatt and P. Mukherjee (1997). "*In vivo* repopulating hematopoietic stem cells are present in the murine yolk sac at day 9.0 postcoitus." Proc Natl Acad Sci U S A 94(13): 6776-6780.

Yu, J., M. A. Vodyanik, K. Smuga-Otto, J. Antosiewicz-Bourget, J. L. Frane, S. Tian, J. Nie, G. A. Jonsdottir, V. Ruotti, R. Stewart, Slukvin, II and J. A. Thomson (2007). "Induced pluripotent stem cell lines derived from human somatic cells." Science 318(5858): 1917-1920.

Zhang, J., C. Niu, L. Ye, H. Huang, X. He, W. G. Tong, J. Ross, J. Haug, T. Johnson, J. Q. Feng, S. Harris, L. M. Wiedemann, Y. Mishina and L. Li (2003). "Identification of the hematopoietic stem cell niche and control of the niche size." Nature 425(6960): 836-841.

Zhang, X., J. Zhang, T. Wang, M. A. Esteban and D. Pei (2008). "Esrrb activates Oct4 transcription and sustains self-renewal and pluripotency in embryonic stem cells." J Biol Chem 283(51): 35825-35833.

Zhao, R. and G. Q. Daley (2008). "From fibroblasts to iPS cells: induced pluripotency by defined factors." J Cell Biochem 105(4): 949-955.

Zhou, H., S. Wu, J. Y. Joo, S. Zhu, D. W. Han, T. Lin, S. Trauger, G. Bien, S. Yao, Y. Zhu, G. Siuzdak, H. R. Scholer, L. Duan and S. Ding (2009). "Generation of induced pluripotent stem cells using recombinant proteins." Cell Stem Cell 4(5): 381-384.

Zufferey, R., T. Dull, R. J. Mandel, A. Bukovsky, D. Quiroz, L. Naldini and D. Trono (1998). "Self-inactivating lentivirus vector for safe and efficient *in vivo* gene delivery." J Virol 72(12): 9873-9880.